CHAPTER 4

RESULTS AND DISCUSSION

4.1 Fibre Volume Fraction, V_f

Fibre volume fraction, V_f of composite specimen were calculated using the Equation 4.1. The fibre volume fractions (V_f) were evaluated for each composite from the matrix and fibre weight fractions (W_f) assuming the densities of glass fibres and PA6 of 2,540 and 1,140 kgm^{-3}, respectively. However, there is always a strong possibility that the resin has been modified by the presence of the fibres and the density of the matrix might be different from the pure resin because of fibre nucleating effect, molecular conformation effects of polymer chains at an interface, dissolutions effects and reaction of the sizing.

$$V_f = \frac{\frac{M_f}{\delta_f}}{\frac{M_f}{\delta_f} + \frac{M_m}{\delta_m}} \qquad (4.1)$$

where M and δ are weight and density respectively; and subscript f and m referred to the fibre and matrix respectively

Table 4.1 shows the experimental value of V_f and the values obtained are expected, although physical blending approach had been adopted in mixing the compounded materials with the virgin matrix in order to reduce V_f of final composite. As reported by Hassan *et al.* [63], a precaution should be taken in preparing the materials before feeding into injection moulding machine. At the same fibre loading, the blends were prepared in batches with a total weight of 500 g each. If a large quantity of blend is used, the compounded materials tend to settle down in the feed hopper of the injection moulding machine and leaving the polymer matrix at the top. The same phenomenon was observed when mixing the glass fibre composites and carbon fibre composites to form hybrid composites. This is believed due to low density of carbon fibre. Thus, the volume fraction of moulded specimen was found to be inconsistent [66].

Table 4.1: Determination of fibre volume fraction.

Sample	Intended fibre weight fraction, W_f (%)	Experimental fibre weight fraction, W_f (%)	Average V_f
SG2	5	4.97 5.01 4.95	0.02
SG5	10	10.82 11.41 10.62	0.05
SG8	15	16.17 16.18 16.15	0.08
SG10	20	20.28 21.68 20.00	0.10
SG16	30	29.53 29.53 29.98	0.16

4.2 Fibre Length Distribution (FLD)

It is generally known that the mechanical properties of injection moulded short glass fibre reinforced polymer (SFRP) such as strength, stiffness and modulus is strongly depend on the fibre length distribution (FLD) and fibre orientation distribution (FOD) of final composites. It is also highly dependent on the critical fibre length and the shear strength at the fibre matrix interface. Therefore, it is greatly importance to study the effects of the FLD and FOD due to the fact that both parameters depend on the fibre volume fraction, the gate geometry and the processing conditions [26, 67].

SGF/PA6 composites having V_f of 2%, 5%, 10% and 16% were analyzed for FLD. FLD histograms of these composites is given in Figure 4.1. From this figure, it can be seen that all fibre volume fraction show quite normal distribution with most of the fibres have lengths between 0.15 mm to 0.45 mm. This indicates that more fibre population with higher length occurred in composites at higher V_f. In SGF/PA6 composites, up to the fibre length of 0.25 mm, composites with lower V_f of 2% and 5% has more population of fibres compared to the composite at 10% and 16% V_f. This suggest that the composites with higher V_f will have more fibre population with shorter length, indicating more fibre degradation takes place during compounding and moulding, probably due to fibre-fibre, fibre-matrix and fibre-machinery surface friction. The same trend was reported by Hassan *et al.* [63] where fibre length up to 0.25 mm, composites with higher V_f has more population of fibres compared to the composites with lower V_f.

Figure 4.2 represents the cumulative FLD for SGF/PA6 composites for 2%, 5%, 10% and 16% V_f. Instead of more fibre degradation occurring during the processing of composite with higher V_f, it is interesting to note that cumulative FLD of 16% V_f is better than that of SGF/PA6 composites with lower V_f of 2%. This behaviour suggests that as the fibre volume fraction increase, most of the fibres tend to degrade during processing. This type of behaviour can also be seen from the calculated values of percentage of fibre with length, L less than 0.2 mm, 0.4 mm and 0.6 mm (Table 4.2). It can be seen that at any L below 0.6 mm, the composites have less percentage of fibres indicating that there are more fibres with L longer than 0.6 mm.

Table 4.2: The fibre characteristic of injection moulded SGF/PA6 composites.

V_f (%)	Percentage of fibre with length, L		
	L<0.2 mm	L<0.4 mm	L<0.6 mm
2	27.0	89.6	99.9
5	45.8	86.9	98.5
10	52.0	86.8	98.4
16	63.2	92.7	99.1

Fibre length distribution data can also be explained from the statistical point of view by the number average fibre length, L_n that gives a measure of fibre ends density and weight average fibre length, L_w. These terms are given by equation (4.3) and (4.4) respectively:

$$L_n = \frac{\Sigma(f_i L_i)}{\Sigma f_i} \tag{4.3}$$

Whereas the weight-average fibre-length, is expressed by (this expression is valid only if fibres of equal diameter are assumed)

$$L_w = \frac{\sum f_i L_i^2}{f_i L_i} \tag{4.4}$$

where f_i is the number of fibre count (frequency) of fibres of species i with length L_i. A midpoint of fibre length ranges each at 0.1 mm interval was taken as an average value of fibre length, L_i in the calculation [63].

The average number, L_n reflects the level of fibre damage during processing, whereas, the weight average, L_w corresponding to the volume fraction of fibres having at that length and therefore useful in represent the composite mechanical properties which are mainly related to volume fractions [63].

The effect of fibre volume fractions on both L_n and L_w are presented in Figure 4.3. As the glass fibre content increased, both L_n and L_w were substantially reduce. Generally, the increase of fibre volume fraction would lead to lower average fibre length due to higher viscous forces exerting on fibres. Additionally as fibre volume fraction increases, fibre-fibre interaction would also cause more damage to fibre length [28, 33]. Shiao & Nair [20] believed that increased fibre breakdown was most likely due to increasing geometric constraint imposed by nearby glass fibres during the flow process of injection moulding. Fibre breakdown due to geometric constraint by nearby glass fibres was most substantial for composites when the glass fibre content passed through 20% wt.

It is well known that the processing of glass fibres into injection moulded composites leads to large reductions in the fibre length due to fibre/fibre interactions, which are logically higher at higher initial fibre fractions. This is in line with the study by Thomason [68] and Ozkoc *et al.* [69] where they found that fibre length reduction occurred by the compounding and moulding process. The lower residual fibre length actually increases their mobility and their aptitude to orient. The strong interactions between fibres and with the surrounding molten polymer or the mould have decreased the fibre mobility and increased the fibre breakage and the structural heterogeneities [70].

On the other hand, Fua *et al.* [71] shows that the mean glass fibre length decreases almost linearly with increase of the glass fibre volume fraction. The increased damage to the fibre length for a greater fibre volume fraction is attributed to the greater fibre-fibre interaction. In addition, the mean glass and carbon fibre lengths increase with increases of the glass fibre volume fraction, whilst they decrease with increases of the carbon fibres volume fraction. This indicates that the interaction between the glass fibres and the carbon fibres (glass-carbon interaction) brings about more damage to the glass fibres than the glass-glass interaction, whilst the glass carbon interaction leads to less damage to the carbon fibres than the carbon-carbon interaction. Furthermore, the fibre-related fracture energy would also increase as the mean fibre length increases since there would be more fibres active in the fibre-related mechanisms as mean fibre length increases.

Thomason [68, 72] also claim that the glass content plays a role in determining the residual composite fibre length. Below 10 % wt fibre content the final average fibre length appears to be independent of the fibre concentration. In the range of 10-40 % wt. of fibres there is little significant difference due to the fact that increased fibre loadings leads to increased probability of fibre-fibre and fibre-machine interaction and an increased apparent melt viscosity resulting in higher bending forces on the fibres during compounding and moulding. This decrease in residual fibre length with increasing fibre loading is an important factor in the explanation of why the strength based properties of these composites show a decreasing reinforcing effect as the fibre concentration is increased. In addition, during the injection moulding of composite materials, fibre attrition occurs resulting in lower average fibre length. Average fibre orientation parameter also appears to decrease with increasing fibre content.

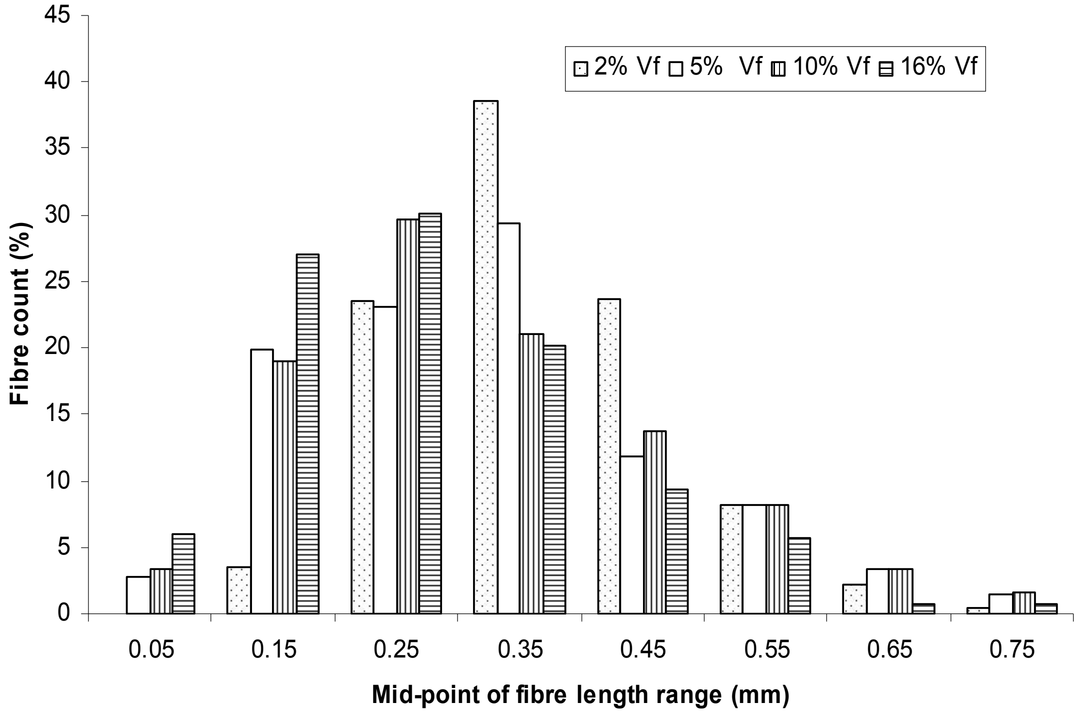

Figure 4.1: Fibre length distribution of injection moulded SGF/PA6 composites.

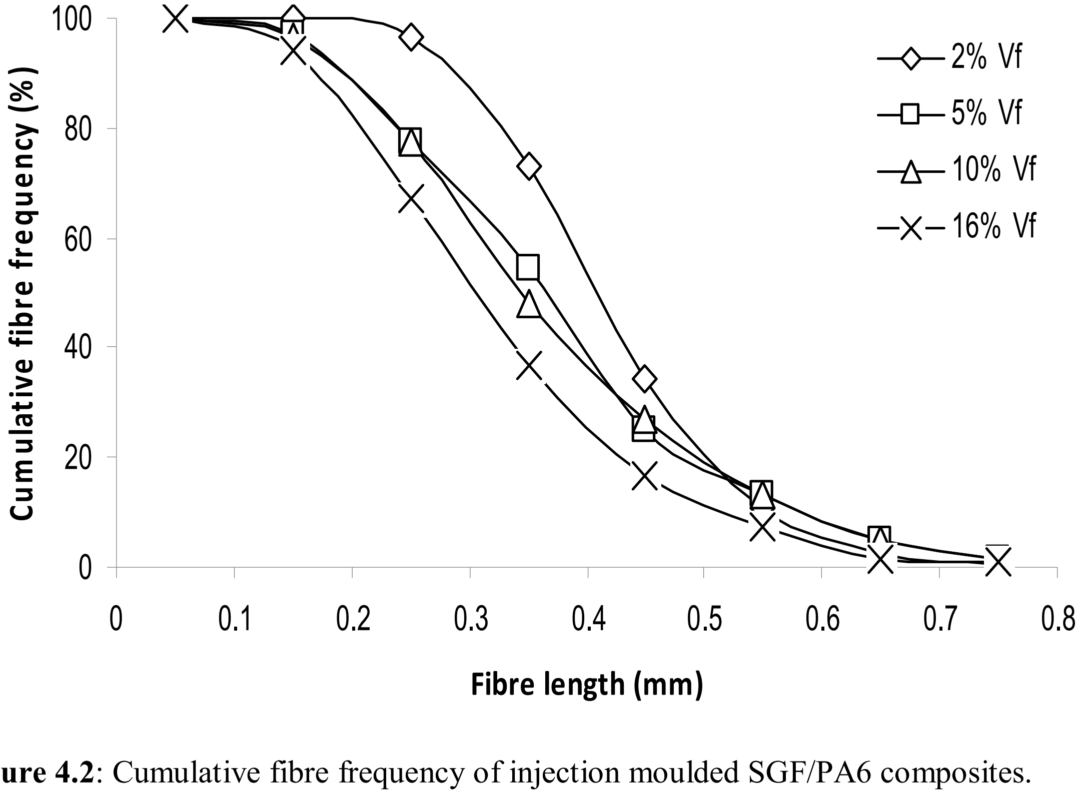

Figure 4.2: Cumulative fibre frequency of injection moulded SGF/PA6 composites.

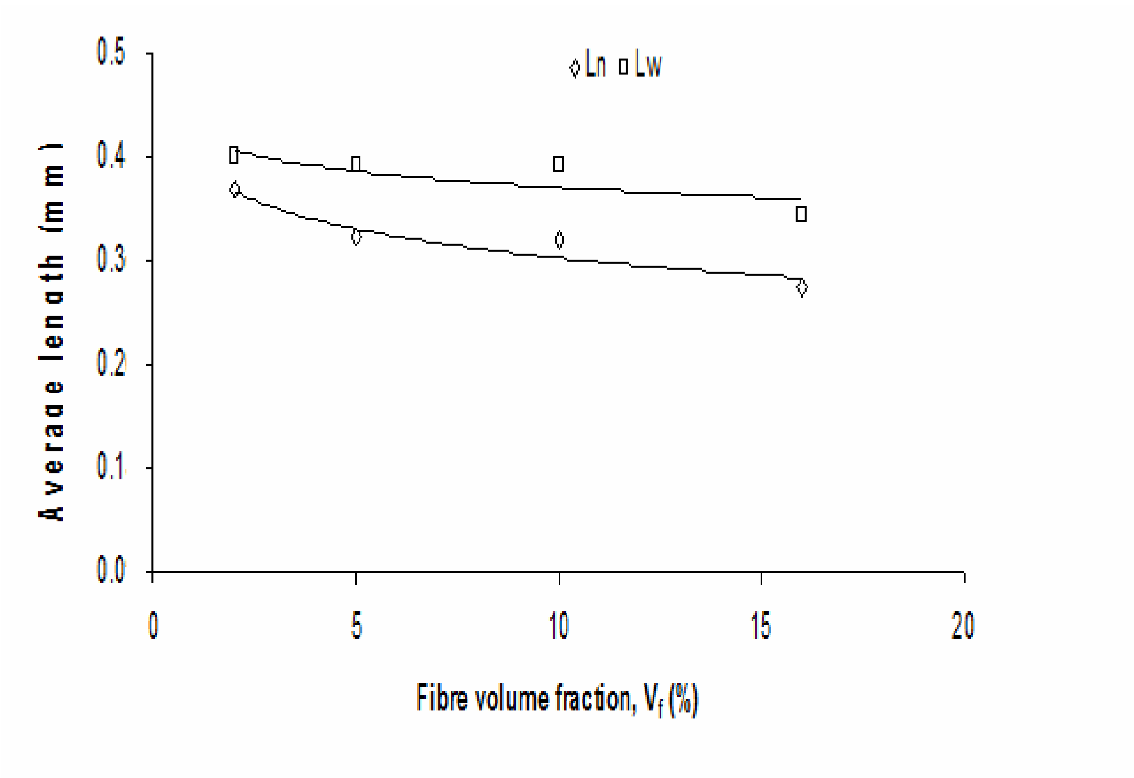

Figure 4.3: Average residual fibre length against fibre volume fraction of injection moulded SGF/PA6 composites.

4.3 Thermal Properties

4.3.1 Thermogravimetric Analysis (TGA)

4.3.1.1 The Effect of Fibre Volume Fraction, V_f

One of the important properties of polymeric materials is its thermal behaviour. TGA is a thermo analytical method used to study the thermal properties of polymer. In this method, the weight of sample is continuously monitored as the sample temperature increases. When a sample decomposes or degrades, normally the decomposition components volatile off, result in a change in weight. Although polyamide has good thermal stability, they tend to degrade in the melt when held for long periods of time or at high temperatures [7].

Details of the thermal degradation of neat PA6 and SGF/PA6 composites at various V_f is given in Table 4.3. According to these data, the introduction of SGF to PA6 matrix increased the degradation temperature of the composites in DAM specimens. The same trend was also observed for specimen subjected to 50% RH and wet condition. This might be due to the heat absorption capacity of glass fibre is higher than that of PA6. As the content of fibres increased, the fibres in the composites absorbed more heat, thus higher temperature was therefore required to achieve the threshold energy for commencement of the degradation process resulting in a shift upward of the degradation temperature. This is in line with the study by Rezaei *et al.* [73] that states the introduction of carbon fibre and increasing fibre length in polypropylene matrix leading to an increase of the thermal stability of the polymer. They also claim that incorporated fillers reduced the chain mobility in the absorption and boundary layers. This led to a decreased in the tension induced to the carbon - carbon chain by the thermal excitation and since majority of bond breaking is via this mode, less degradation occurs eventually improved the thermal stability. In addition, the increase in thermal stability of SGF/PA6 composites is attributed to the organic/inorganic interaction between the polymer and fibres [74]. The increase in decomposition temperature is also attributed to the hindered diffusion (i.e., barrier effect) of volatile decomposition products caused by the dispersed clay particles in the polypropylene matrix as reported by Lee *et al.* [75].

Table 4.3: TGA thermogravimetric data of injection moulded SGF/PA6 composites.

Sample	Condition	Fibre weight fraction, W_f	Range of decomposition temperature (°C)	$T_{50\%}$ (˚C)	Moisture uptake (%)
SGD00	DAM	-	326 - 494 (168)	442	-
SGD02		5	330 - 495 (165)	444	
SGD05		10	345 - 496 (151)	438	
SGD10		20	328 - 499 (171)	447	
SGD16		30	316 - 502 (186)	454	
SGR00	50% RH	-	358 - 494 (136)	435	2.48
SGR02		5	343 - 494 (151)	437	2.99
SGR05		10	345 - 493 (148)	441	2.51
SGR10		20	343 - 492 (149)	445	2.29
SGR16		30	329 - 492 (163)	453	1.76
SGW00	Wet	-	358 - 494 (136)	437	8.80
SGW02		5	343 - 494 (151)	433	7.99
SGW05		10	345 - 493 (148)	437	7.64
SGW10		20	343 - 492 (149)	446	5.88
SGW16		30	328 - 492 (164)	454	5.37

Keynotes:
$T_{50\%}$ (˚C): temperatures at 50% weight loss

It is often stated that, the presence of glass fibre in a polymer enhances its thermal stability and this is attributed to the improved barrier properties and the tortuous path for volatile decomposition products which hinder the diffusion out of the material. Generally, for all condition tested, it was found that neat PA6 degrades a little faster than SGF/PA6 composites, that is, the SGF/PA6 are stable up to 300˚C.

In addition, the initial weight loss decreasing as fibre loading increase. This is because incorporation of glass fibre reduced the chain mobility in the absorption and boundary layers. This led to a decreased in the tension induced to the carbon-carbon chain by the thermal excitation and since majority of bond breaking is via this mode, less degradation occurs. Hence, the grafting of macromolecules onto the filler surface and the formation of spatial chemical structures in the filled polymer improved the thermal stability [73].

On the other hand, it is a common practice to consider 50% weight loss as an indicator for structural destabilization as given in this reference [76]. In this study, 50% of the total weight loss is considered as the structural destabilization point of the system. Results showed that, (Table 4.3) as fibre content increase, temperatures at 50% weight loss also increased. The same trend was also observed in wet condition and 50% RH specimens. These results suggested that the incorporation of glass fibre into the system has improved the structural destabilization point of the composites.

4.3.1.2 The Effect of Moisture

The effect of moisture on the thermal degradation of SGF/PA6 composites was investigated. A TGA curve for SGF/PA6 composites at DAM is given in Figure 4.4. PA6 is considered as dry when the water absorption is less than 0.2% and saturated at 7.2% [77]. The unfilled PA6 sample loses about 1.76-2.48% and 5.37-8.80% for 50% RH and wet condition respectively due to the loss of moisture (Table 4.3). Between 400˚C and 500˚C the sample decomposes almost completely, as it undergoes almost 100% degradation. A sudden drop in the mass of the sample indicated the thermal degradation of the material. As seen in the Figure 4.4, all fibre volume fractions show two weight losses. The first weight loss is around 330˚C due to the PA6 matrix decomposition. The PA6 shows one more weight loss at around 500˚C due to degradation of organic matter. The same behaviour was also observed to polyimide as reported by Ajit [78]. No further weight drop was observed till 900˚C which shows the thermal stability of glass fibre to high temperatures.

At 50% RH and wet condition, as seen in the Figures 4.5 and 4.6, all V_f investigated show three weight loss. The first weight loss is at around 100˚C with a weight loss of around 1.76-2.48% and 5.37-8.80% by weight for 50% RH and wet condition respectively. This initial weight loss in SGF/PA6 composites is due to the water evaporation. Both figures show one more weight drop at around 310°C due to matrix decomposition. The third weight loss was observed at 510°C. This is results from degradation of organic matter or additives. No further weight drop was observed till 900°C, which shows the thermal stability of glass fibre to high temperatures.

Figure 4.7 - 4.11 shows TGA curves at different condition. For all fibre volume fraction investigated, results found that SGF/PA6 composites subjected to DAM presents thermal stability slightly superior than specimen subjected to 50% RH and wet condition. For neat PA6, the onset temperature was found to be 326°C. Addition of V_f 2% and 5%, the onset temperature was found to be 330°C and 345°C respectively. Further increase in the glass fibre loading (10% and 16% V_f), the onset temperature drop to 327°C and 316°C. However, reverse observation was observed when subjected to 50% RH. The onset temperature was found to be 252°C for neat PA6. Addition of 2, 5, 10 and 16% V_f, the onset temperature was found to be 302°C, 303°C, 304°C and 339°C respectively. By contrast, SGF/PA6 subjected to wet condition showed decrement in the onset temperature from 358°C for neat PA6 to 343°C, 345°C, 343°C and 328°C for 2, 5, 10 and 16% V_f respectively. This suggests that the thermal degradation is highly influence by the moisture absorption.

For all condition studied, the materials started to thermally degrade at around 330°C and decompose at 500°C where substantial loss in their weight was observed. The degradation curve also shows that thermal degradation began to occur only after the materials have absorbed certain amounts of heat energy. The heat initiated the degradation processes and the breaking down of the fibres and matrix structure by causing molecular chain ruptures.

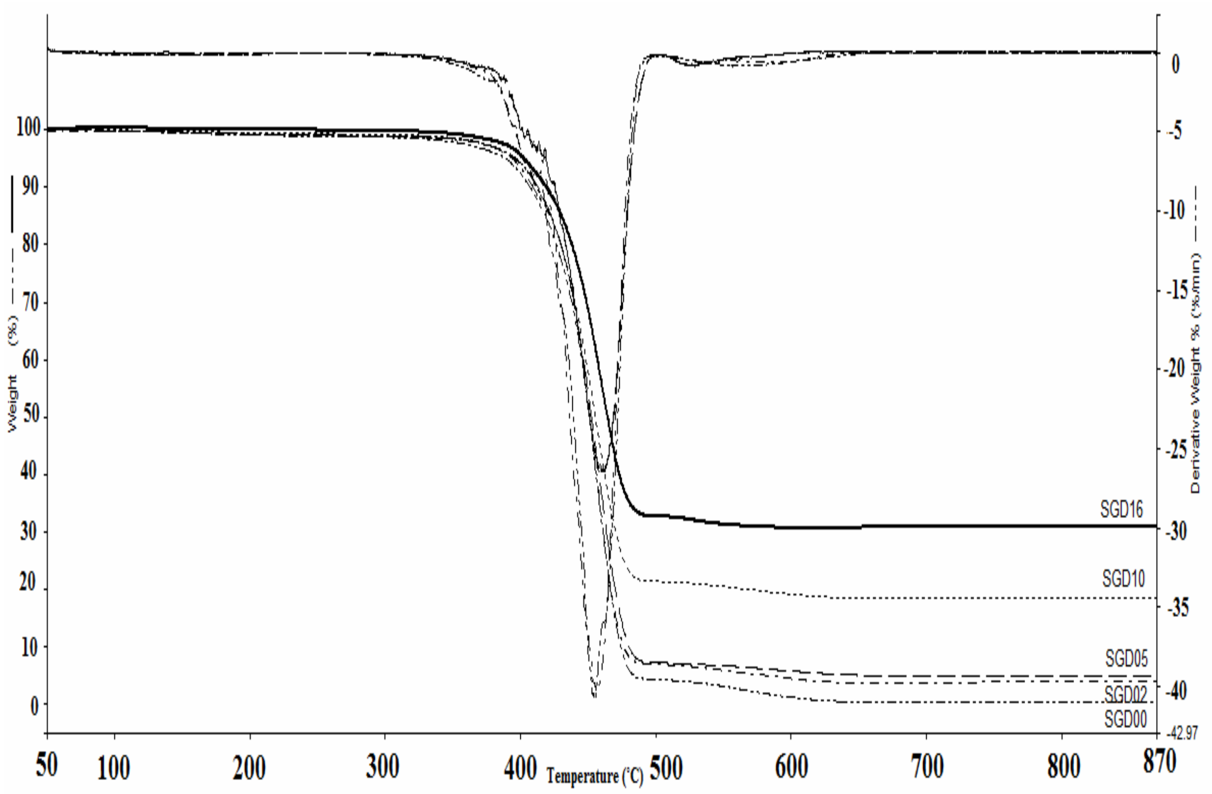

Figure 4.4: TGA curves of injection moulded SGF/PA6 composites at DAM.

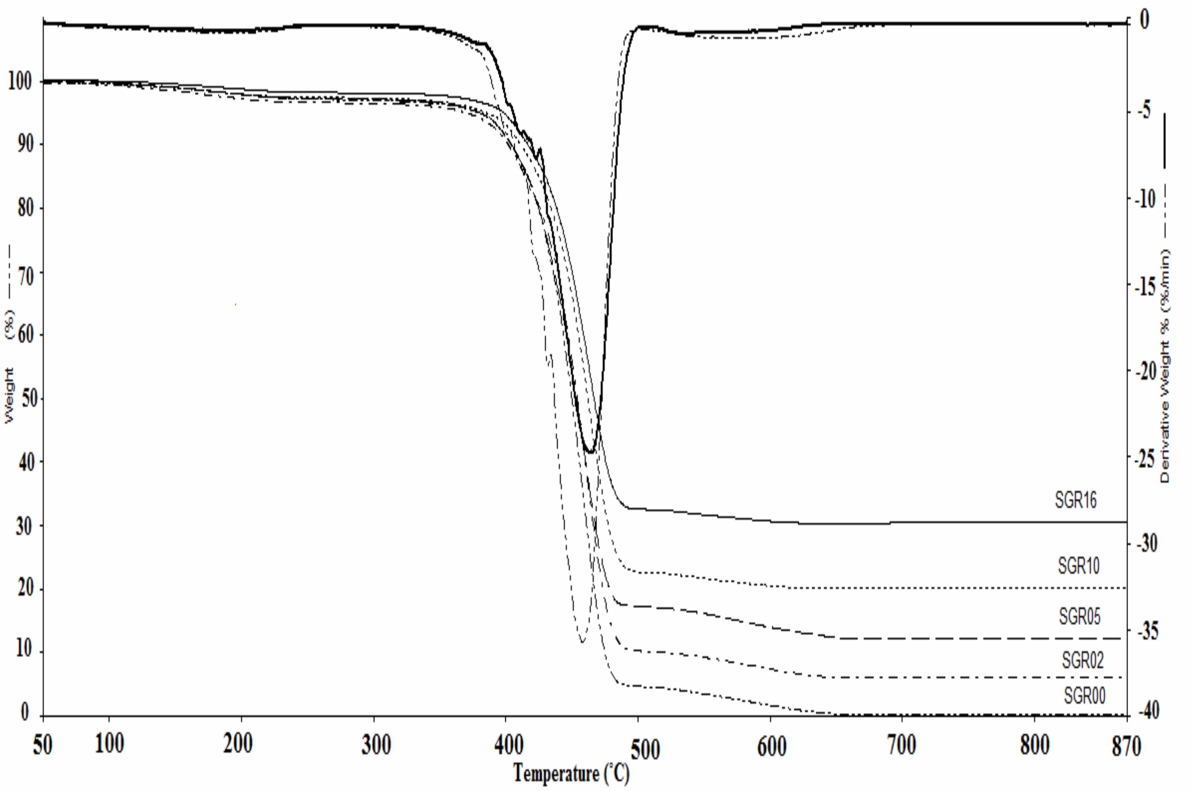

Figure 4.5: TGA curves of injection moulded SGF/PA6 composites subjected to 50% RH.

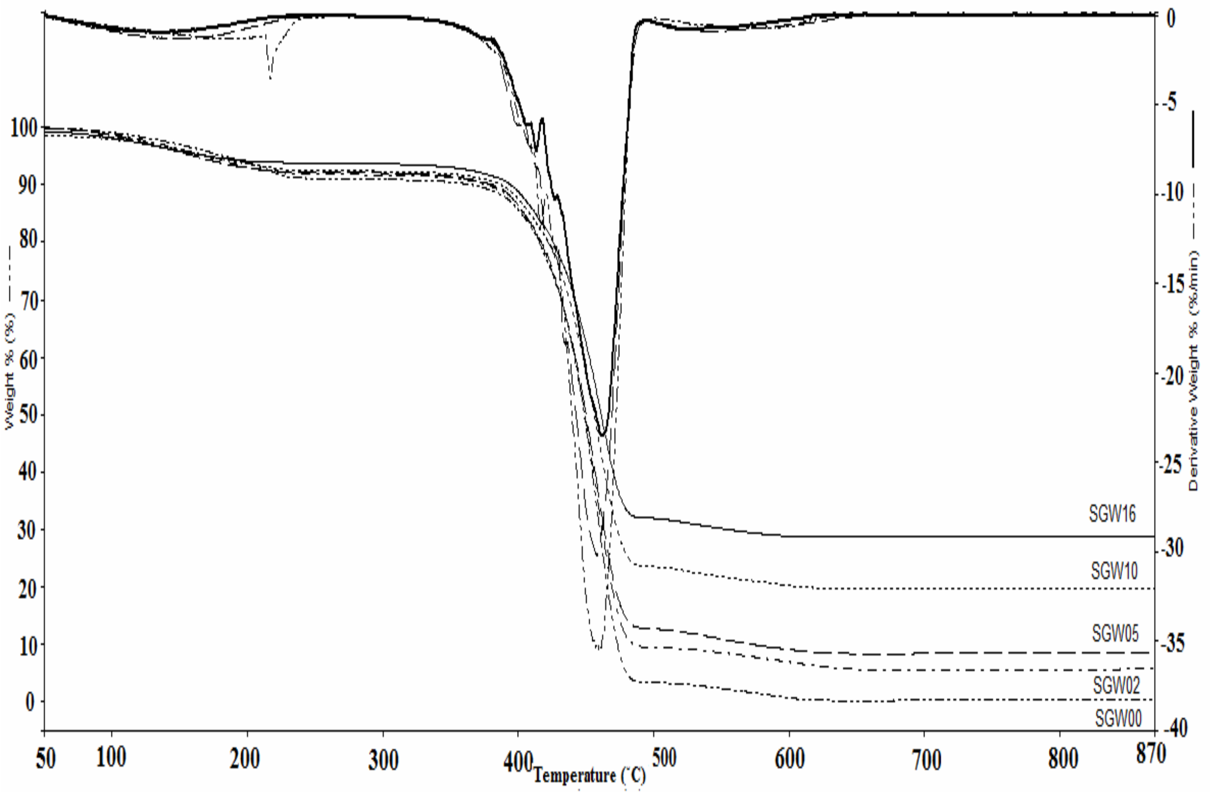

Figure 4.6: TGA curves of injection moulded SGF/PA6 composites subjected to wet condition.

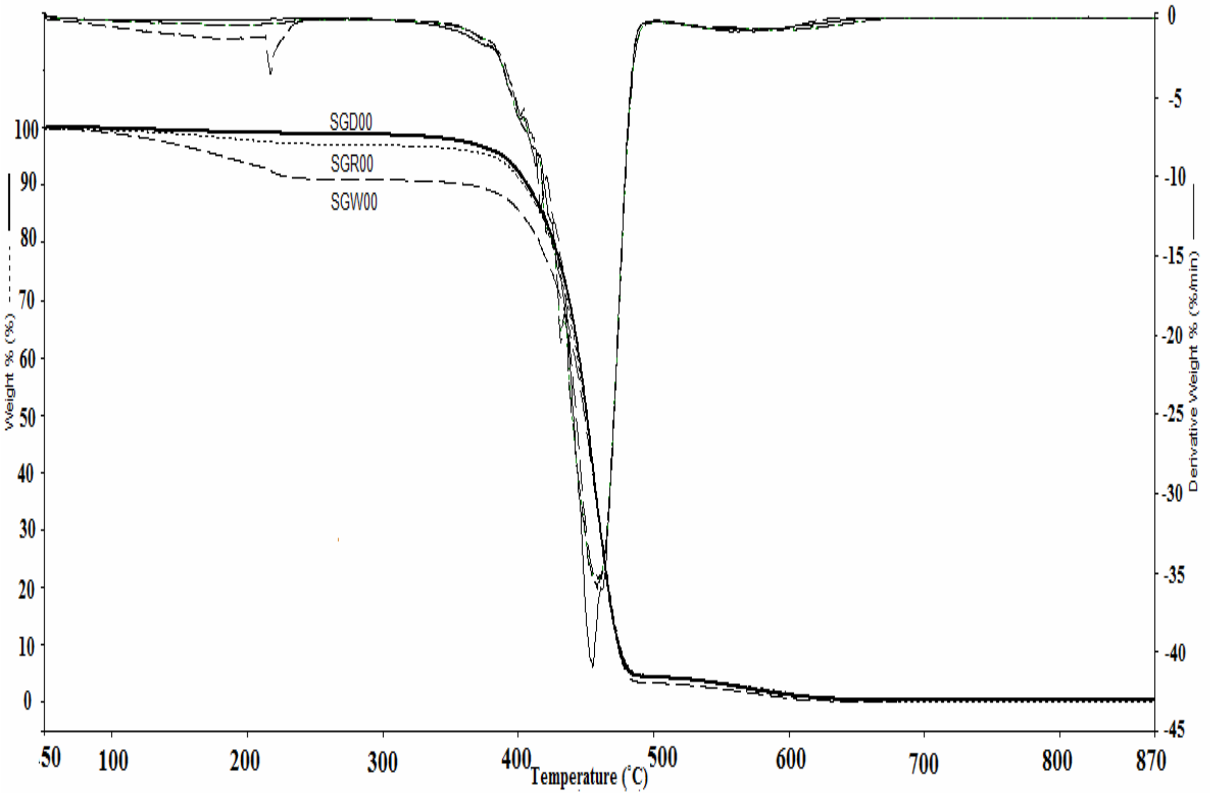

Figure 4.7: TGA curves of neat PA6 subjected to different environmental condition.

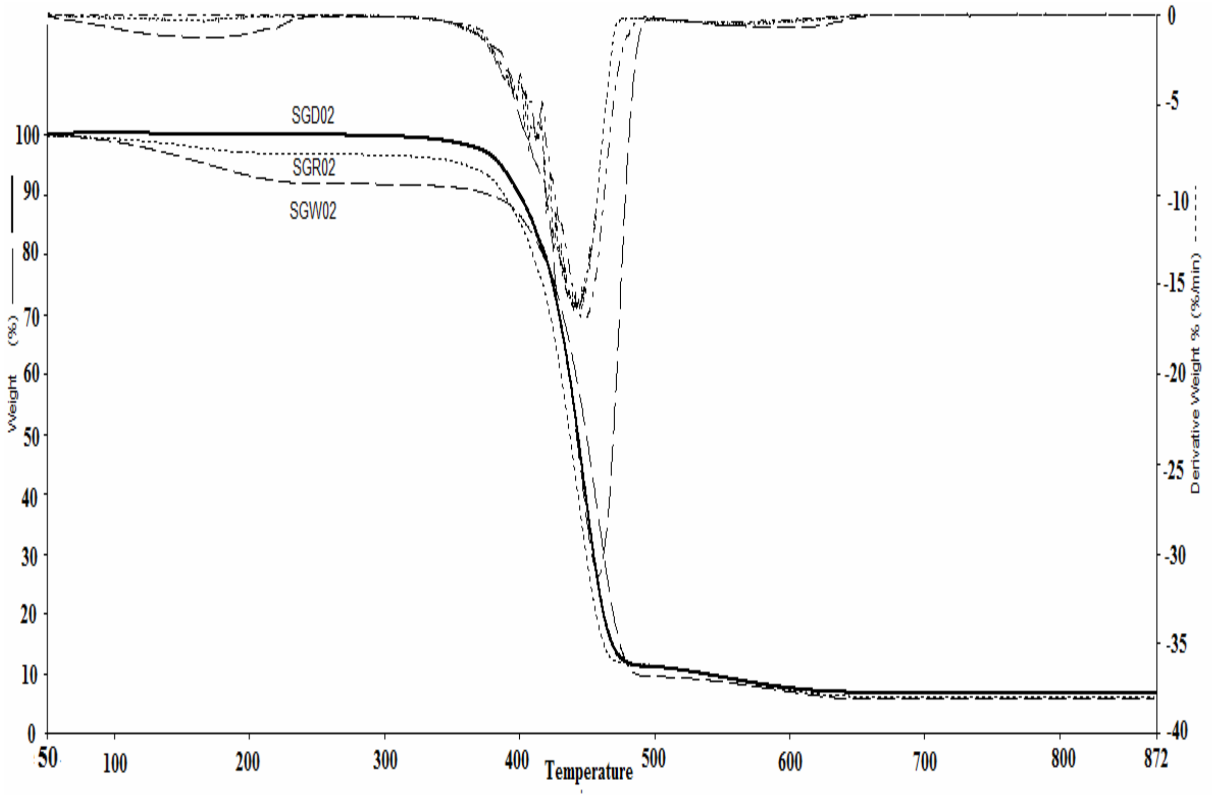

Figure 4.8: TGA curves of injection moulded 2% V_f SGF/PA6 composites subjected to different environmental condition.

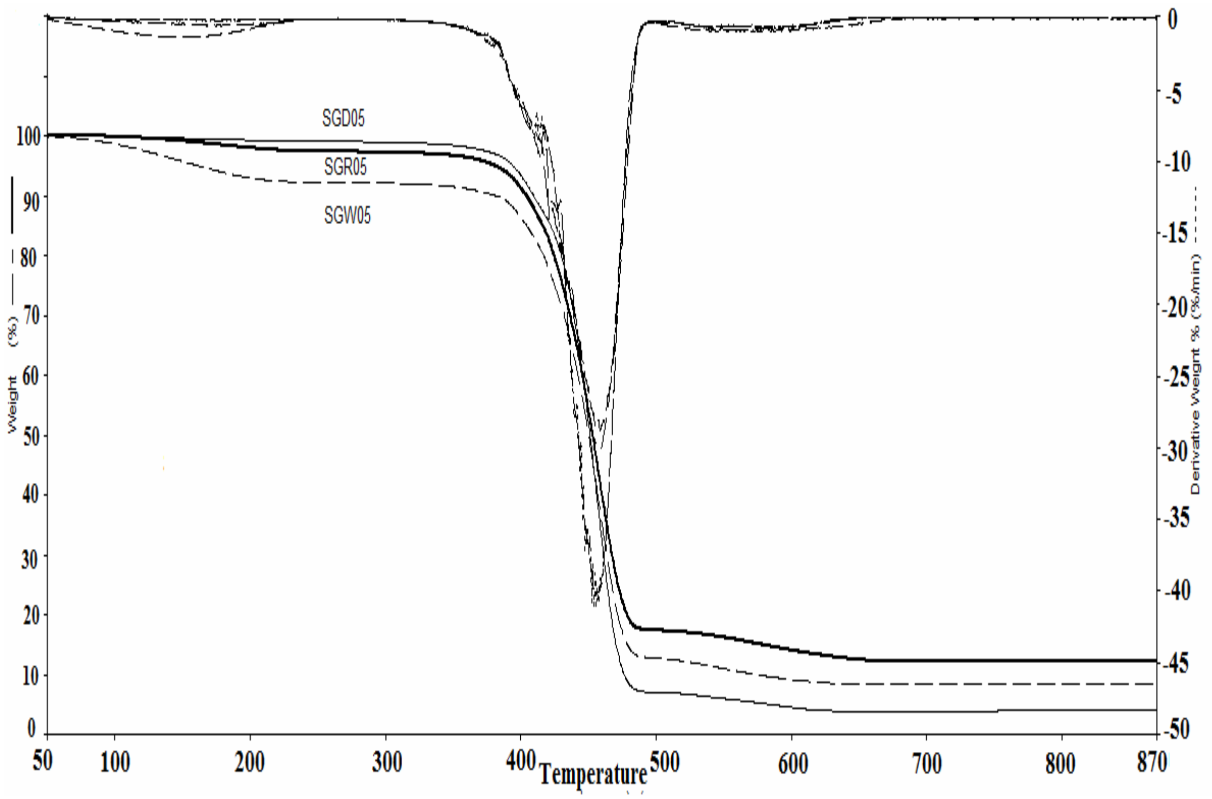

Figure 4.9: TGA curves of injection moulded 5% V_f SGF/PA6 composites subjected to different environmental condition.

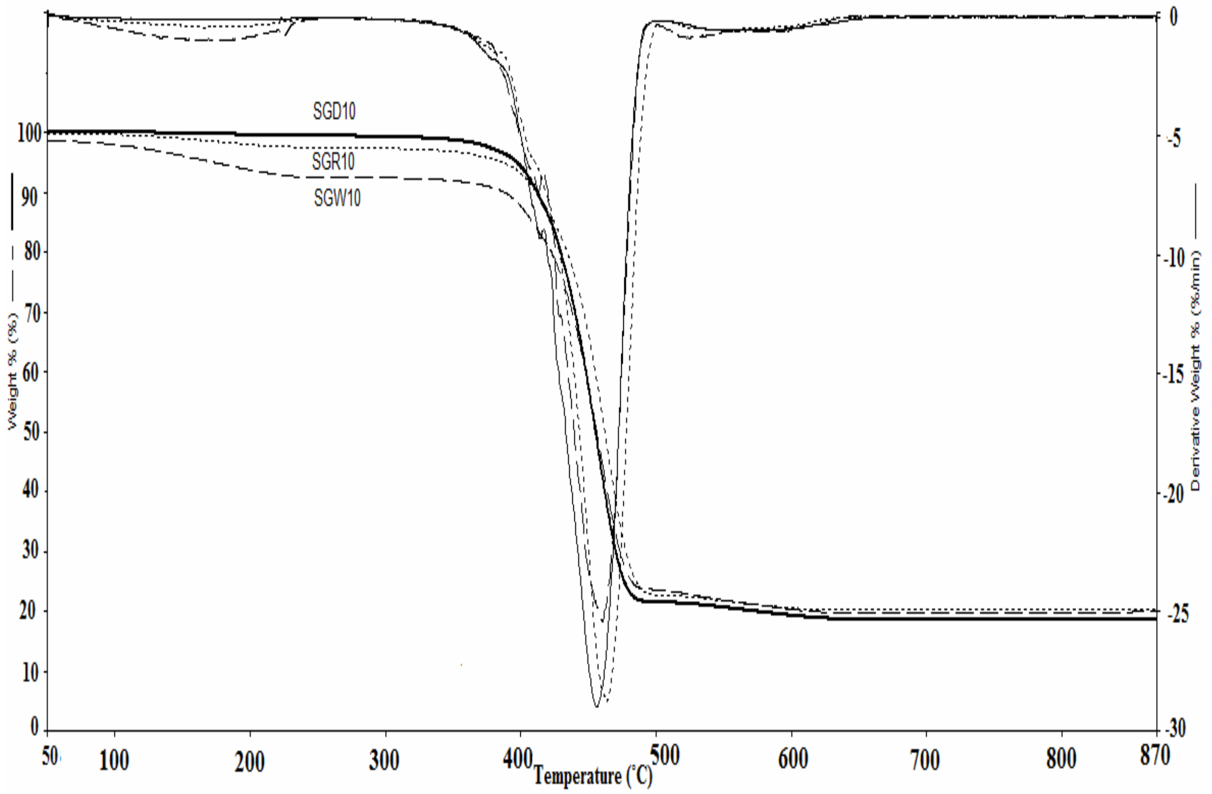

Figure 4.10: TGA curves of injection moulded 10% V_f SGF/PA6 composites subjected to different environmental condition.

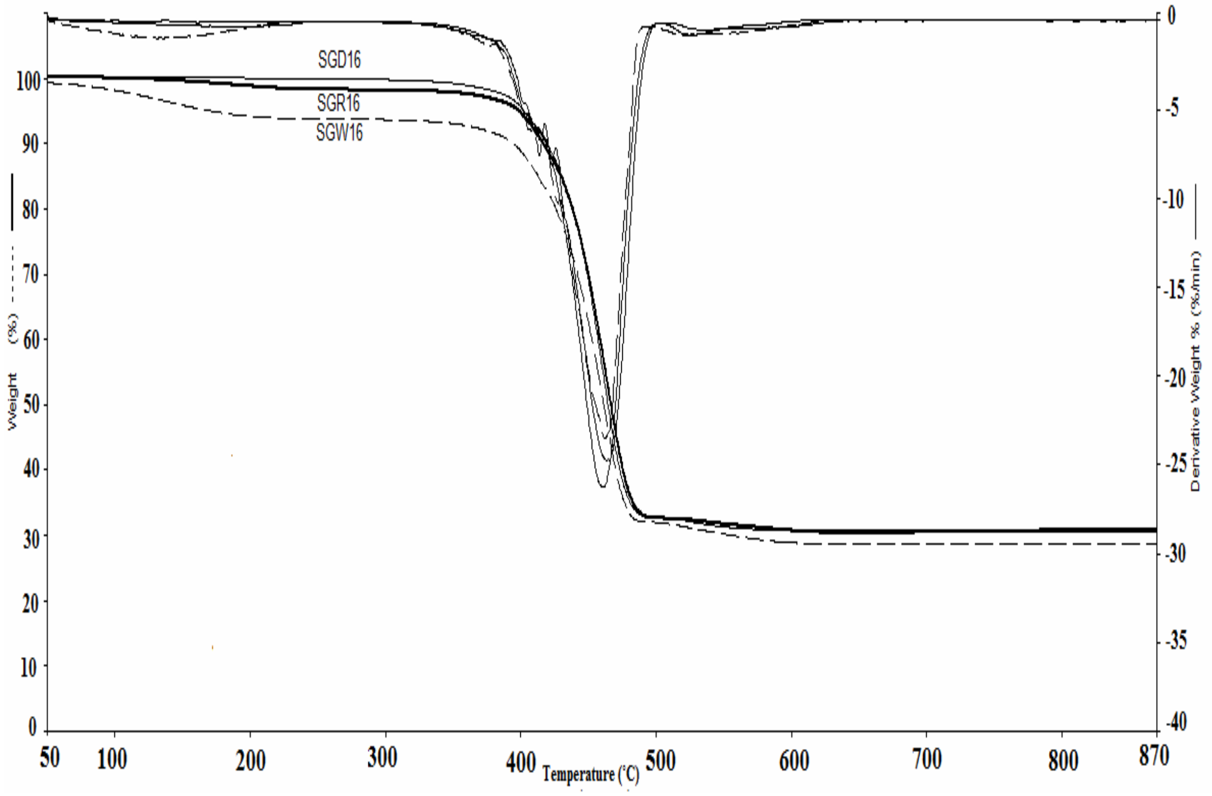

Figure 4.11: TGA curves of injection moulded 16% V_f SGF/PA6 composites subjected to different environmental condition.

4.3.2 Differential Scanning Calorimetry (DSC)

4.3.2.1 The Effect of Fibre Volume Fraction, V_f

The crystallisation and melting behaviour of SGF/PA6 composites was analyzed with DSC. It has been well established that DSC methods was successfully applied for an analysis of the structural changes in polyamide [79]. The mechanical properties of the composites are strongly influenced by the matrix molecular structure (crystalline structure, the orientation of the amorphous regions), especially on the degree of crystallinity. Heating scans were analysed for the melting temperature, T_m, heat of fusion, ΔH_m, and the degree of crystallinity, χ_c, while cooling scans were used to obtain the crystalline temperature, T_c and crystalline enthalpy ($-\Delta H_c$) For clarity, all the DSC curves shown here are shifted vertically.

In some polymers, the level of crystallinity can have a major effect on key properties such as stiffness, optical clarity, barrier resistance and brittleness. In some cases the larger heat of melting, will lead to a higher level of crystallinity, resulting to the polymer brittleness. To determine the degree of crystallinity, χ_c, the following expression was used:

$$\chi_c = \frac{\Delta H_m}{\Delta H_{mo}} \times 100\% \qquad (4.5)$$

Where:

ΔH_m – heat of fusion due to PA6 melting, measured through the melting peak

ΔH_{mo} – heat of fusion for PA6, 100% pure crystalline.

Generally, 230 (±20) J/g is a commonly accepted average value for PA6 [80-82].

Table 4.4 shows the melting and crystallization parameters of the neat PA6 and SGF/PA6 composites obtained by DSC. All V_f shows melting temperature at around 220˚C except for specimen 16% V_f at dry as moulded (DAM) where the melting temperature is around 216˚C. On the other hand, crystalline temperature was observed at 195˚C. It can be seen that there is no significant change in the melting and crystallisation temperatures of the composites as glass fibre is added. It was found from Figures 4.12-4.19 that all the heating and cooling scans show only one endothermic and exothermic peak respectively. This is contrary with PA6,6 where the heating scans show that PA6,6 has two melting peaks, at about 261˚C (α-form) and at 252˚C (β-form) as reported by Mehrabzadeh and Kamal [83]. The same trend is reported by Lee *et al.* [84] which indicate that there is no change in T_m for PP/clay/wood flour/compatibilizer hybrids subjected to 3 and 5 phr clay loading level. Akkaoui and Bayram [25] also agree that the T_m of PA6 in the composite does not change significantly with respect to glass mat content.

Table 4.4: DSC melting and crystallisation parameters of injection moulded SGF/PA6 composites at various environmental conditions.

V_f (%)	Condition	Heating		Cooling		χ_c (%)
		T_m (˚C)	ΔH_m (J/g)	T_c (˚C)	$-\Delta H_c$ (J/g)	
0	DAM	221	56	196	58	24
2		220	58	196	48	25
5		220	53	196	39	23
10		220	47	196	40	20
16		216	35	193	41	15
0	50% RH	220	54	196	50	23
2		220	46	196	43	20
5		221	46	196	47	20
10		220	43	196	42	19
16		220	38	196	41	17
0	Wet	220	49	196	48	21
2		220	47	196	45	20
5		220	46	196	44	20
10		221	40	196	36	18
16		220	34	196	33	15

A melting peak (T_m about 220°C), is a characteristic of the α form of PA6, appears in all fibre volume fraction studied. The melting peak could be attributed to the melting of the α crystalline form of PA6. This indicates that in the neat PA6 specimen, the α crystals were the dominant crystalline phase [85]. Mekawy and El-Megeed [86] in their study reported that polyamides can occur in more than one crystalline form (α and γ), depending on the conformation and packing of the polymer chains during polymer crystallization. Transforming between the phases occurs upon processing, annealing, and mechanical stresses. For moulded PA6, three different crystal structures were observed based on a different dependence of their properties on density. The α form crystals were obtained from crystallization at higher temperatures or annealing; γ crystals were obtained at lower temperatures.

From Table 4.4 it was found that the degree of crystallinity of SGF/PA6 composite at DAM is reduced for all fibre content. The same trend was also observed as specimens were subjected to 50% RH and wet condition. The presence of glass fibres leads to a decrease in the crystallinity of PA6 as a result of their hybrid structure. In addition, the different degree of crystallinity of SGF/PA6 composites is also contribute from the different arrangement of the glass fibres in the matrix and the architecture of the glass fibre distribution in the polyamide matrix as studied by Krucińska *et al.* [87]. Mekawy and El-Megeed [86] reported that the degree of crystallinity of PA6 decreases towards the surface of the glass fibre. This hypothesis is due to the fact that glass fibre has a lower coefficient of thermal conductivity and probably during crystallisation in the cooling process of SGF/PA6 composites. Caban & Nitkiewicz [88] in explaining the lower degree of crystallinity state that the glass fibre has a higher temperature than the surrounding polyamide matrix; therefore the heat can be transferred to the polyamide efficiently. This mean that the degree of crystallinity of the matrix could be lower when fibres in the composite are spaced closely together and higher when the fibres are placed far from each other.

The same behaviour was also observed in heat of fusion, ΔH_m. As glass fibres were added in 2%, 5%, 10% and 16% V_f, the heat of fusion, ΔH_m decreased from 56 to

35 J/g, 54 to 38 J/g and 49 to 34 J/g for specimens under DAM, 50% RH and wet condition respectively. Meanwhile, the addition of glass fibre from 2% to 16% V_f decreased the crystalline entalpy $-\Delta H_c$ from 58 to 41 J/g, 50 to 41 J/g and 48 to 33 J/g for specimen under DAM, 50% RH and wet condition respectively. Since the addition of glass fibre interfere the crystallization process, it is assumed that the decrease of $-\Delta H_c$ was closely related to the decrease of crystal size itself [75]. Wong and Truss [89] also observed the same behaviour where the overall crystallinity of the flyash-filled polypropylene composites was reduced. This indicates that, the presence of the filler is changing the crystallisation of the polymer, presumably near the surface of the filler.

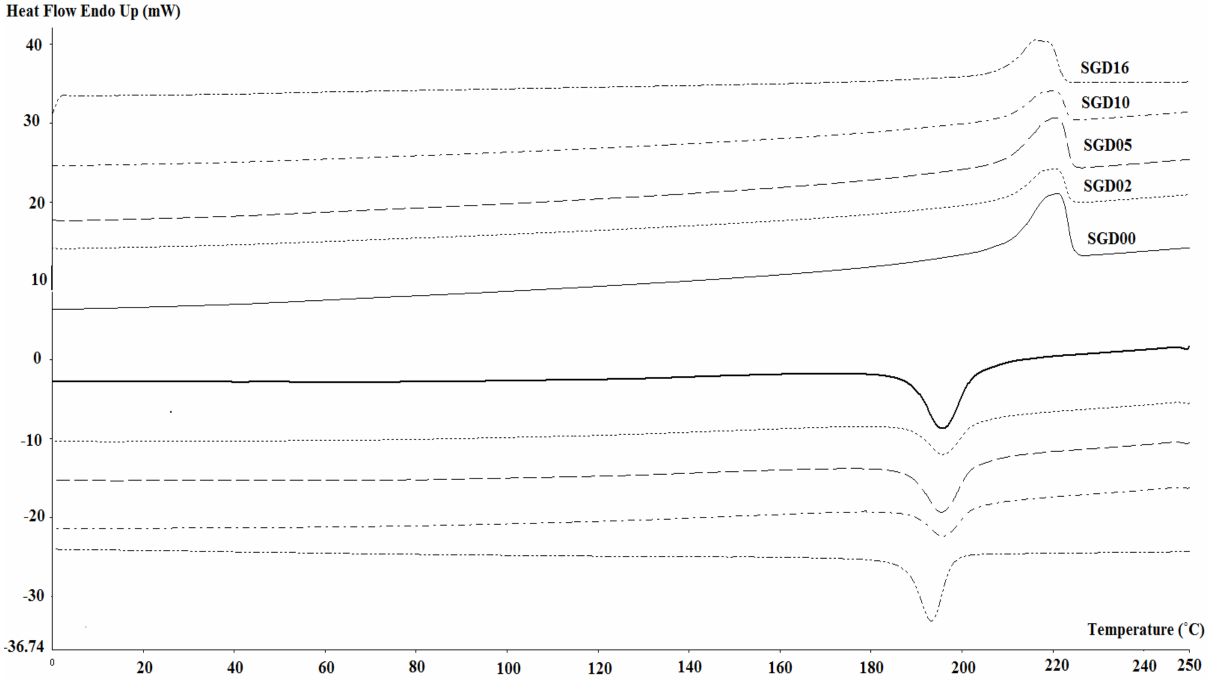

Figure 4.12: DSC results of injection moulded SGF/PA6 composites at various V_f at DAM.

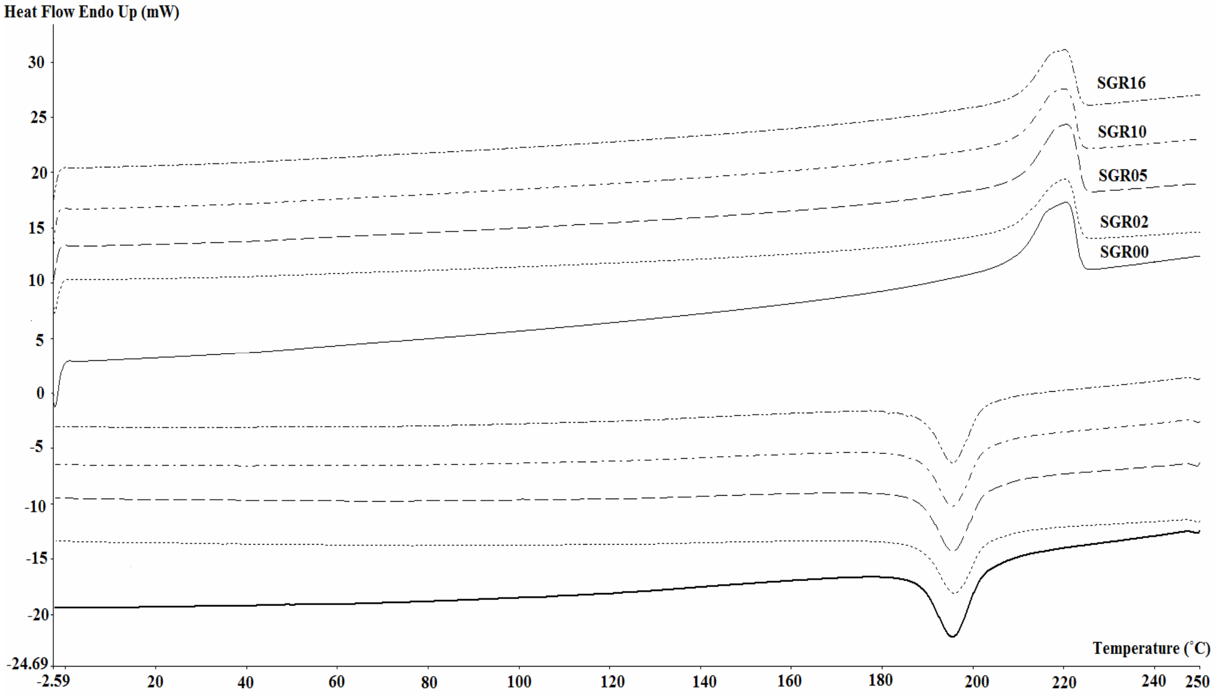

Figure 4.13: DSC results of injection moulded SGF/PA6 composites at various V_f subjected to 50% RH.

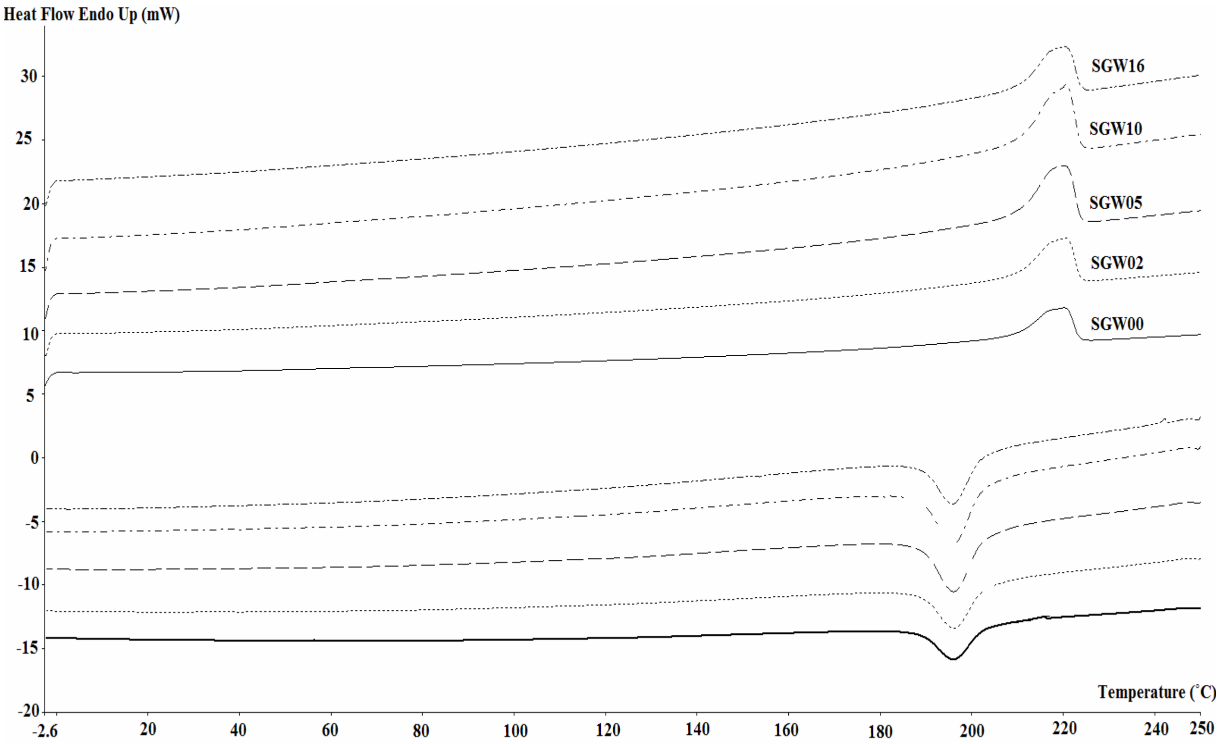

Figure 4.14: DSC results of injection moulded SGF/PA6 composites at various V_f subjected to wet condition.

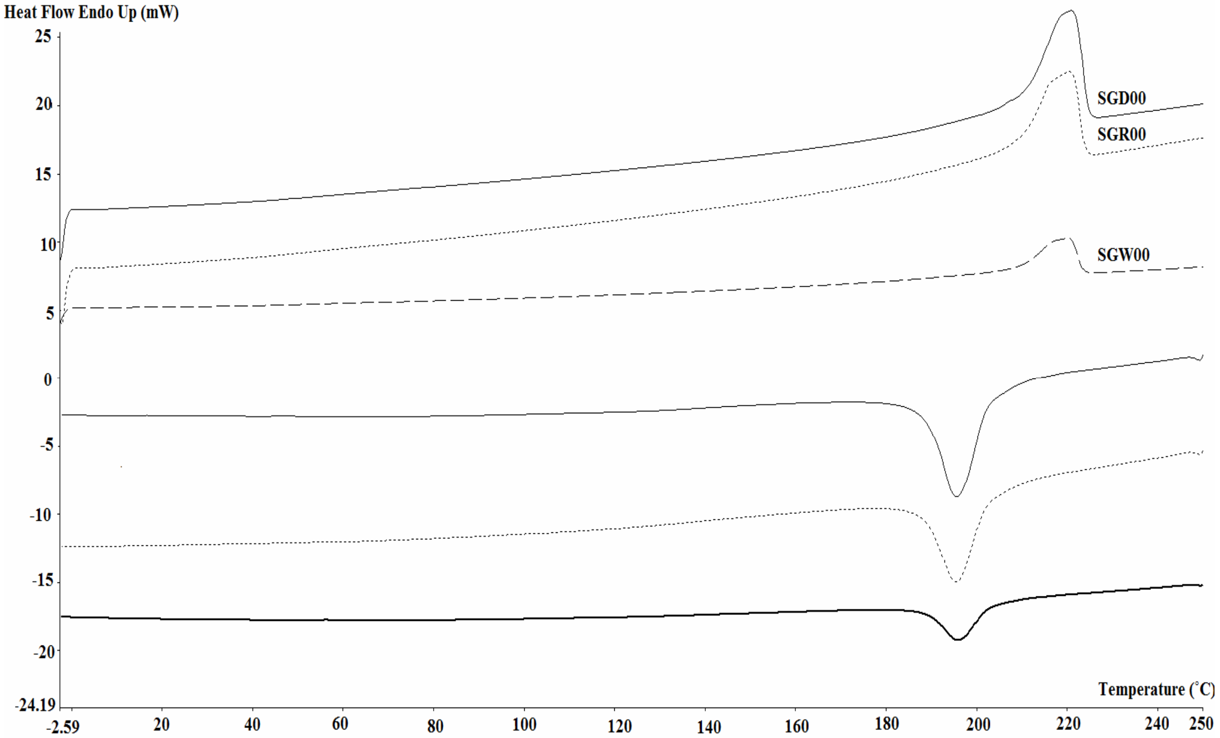

Figure 4.15: DSC results of neat PA6 subjected to different environmental condition.

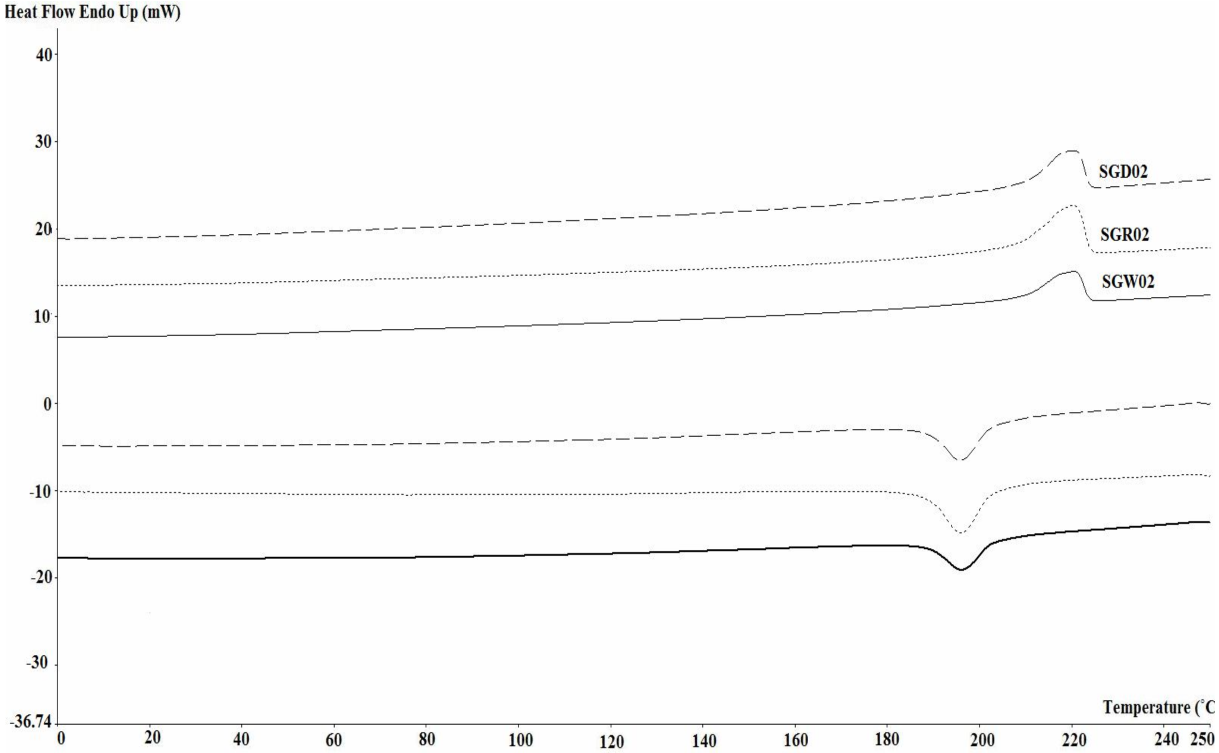

Figure 4.16: DSC results of injection moulded 2% V_f SGF/PA6 composites subjected to different environmental condition.

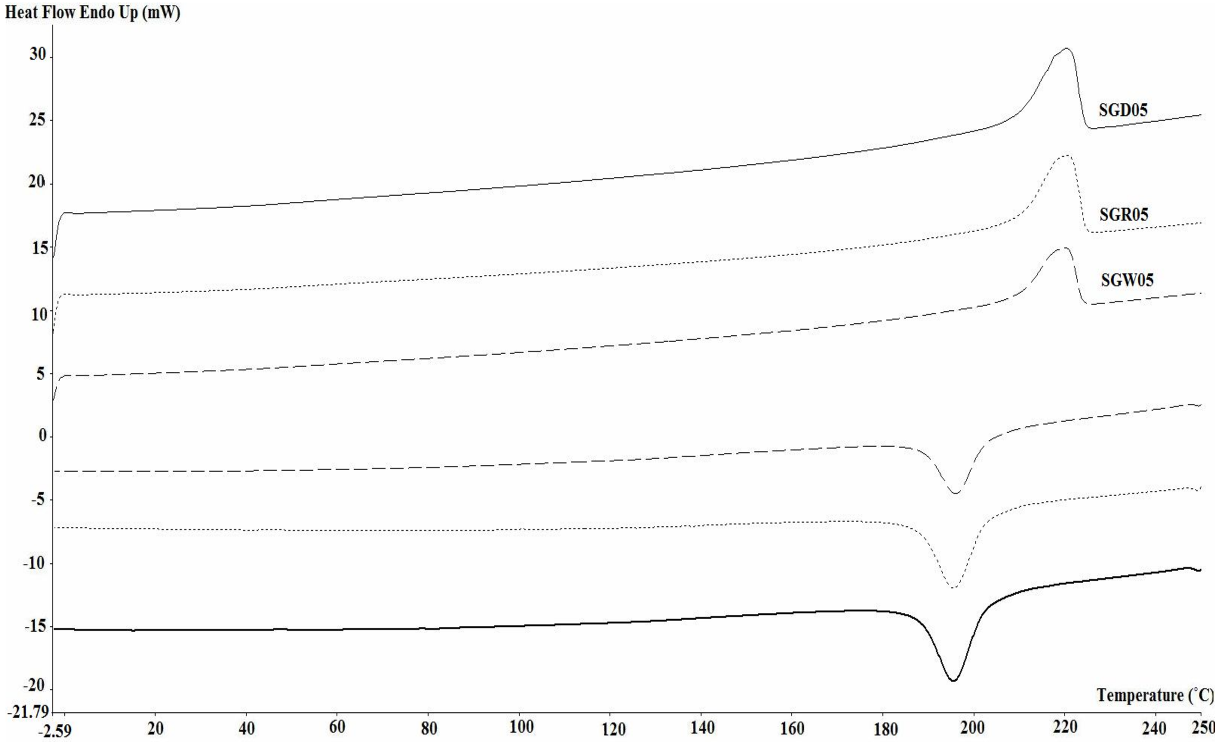

Figure 4.17: DSC results of injection moulded 5% V_f SGF/PA6 composites subjected to different environmental condition.

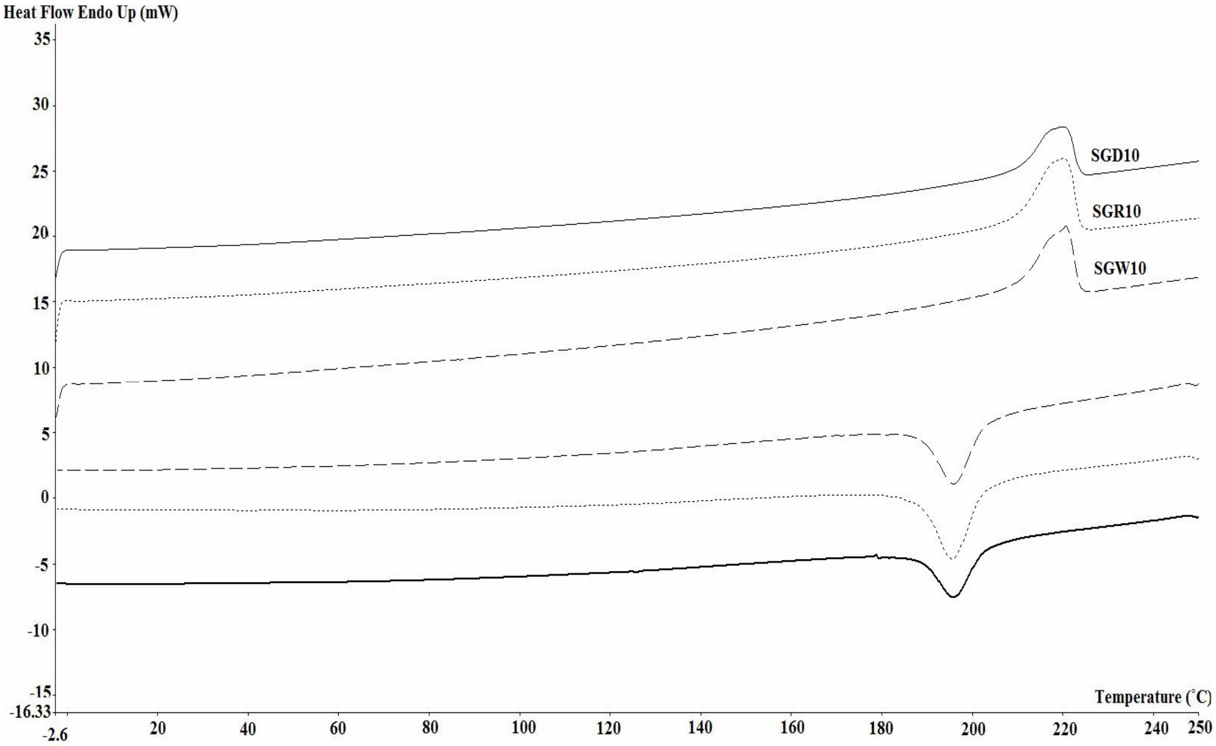

Figure 4.18: DSC results of injection moulded 10% V_f SGF/PA6 composites subjected to different environmental condition.

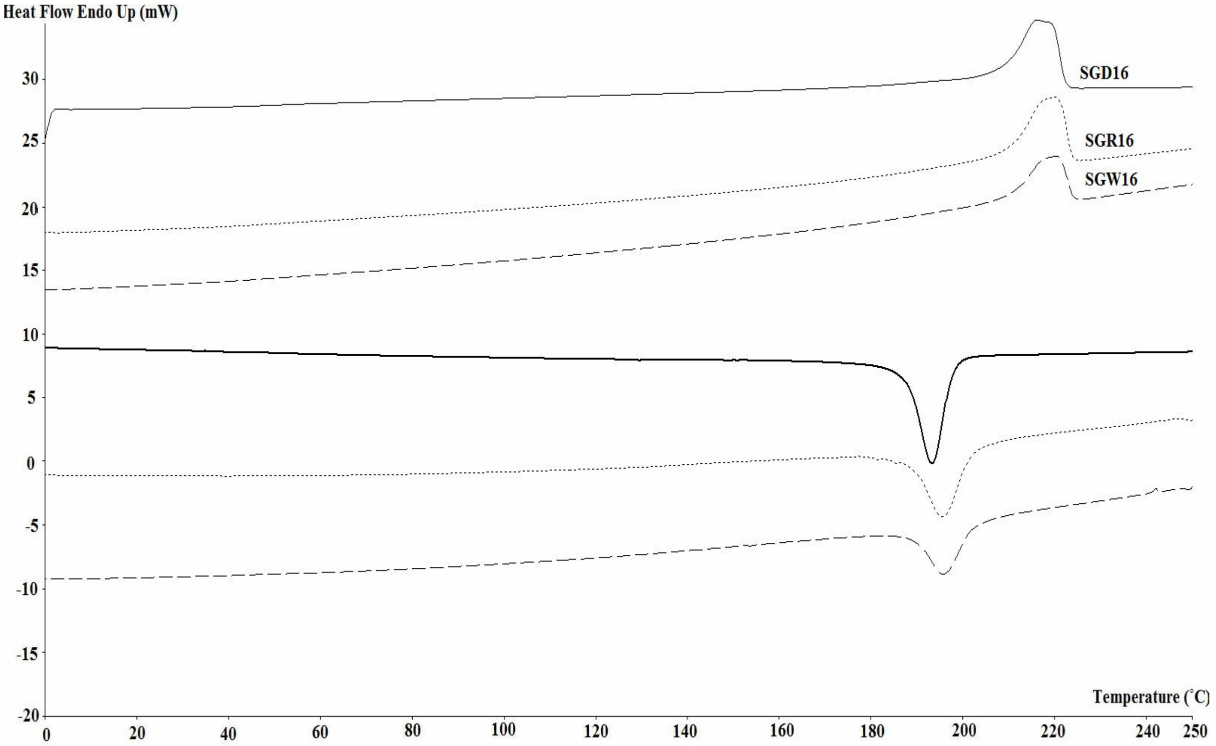

Figure 4.19: DSC results of injection moulded 16% V_f SGF/PA6 composites subjected to different environmental condition.

4.3.2.2 The Effect of Moisture

Conditioning may also bring changes in the nature of the crystalline state, which in turn is governed by the nature of the crystal structure, degree of crystallinity, size and number of spherulites and orientation. Table 4.4 indicates the degree of crystallinity, χ_c at different environmental condition. It shows that the χ_c reduce as moisture is introduce. Degree of crystallinity of pure PA6 reduces dramatically at 24 %, 23% and 21% for specimen under DAM, 50% RH and wet condition respectively. The same trend was also observed as glass fibre is introduced to the composites. This suggests that moisture will lower the degree of crystallinity matrix where it breaks up intermolecular hydrogen bonding resulting in a significant change in the polyamide matrix structure [90].

The ΔH_m of unreinforced PA6 is reduced at 56, 54, 49 J/g, for specimen under DAM, 50% RH and wet condition respectively. This is expected due to reduction in ΔH_m magnitude is directly proportional to the overall level of χ_c possessed by the polymer [91]. On the other hand, - ΔH_c also behave the same behaviour where it shows decrement at 58, 50 and 48 J/g for specimen under DAM, 50% RH and wet condition.

Pai *et al.* [92] who investigate the effect of moisture on thermal properties of PA6,6 reported a broad melting endotherm was observed as a result of water plasticizing effect on PA6,6. This study also suggests that moulding conditions of a PA6,6 material may ultimately effect the levels of crystallinity in the final part and establish a relationship between the amount of absorbed water for a given polyamide product and its processing variables.

4.4 Dynamic Mechanical Analysis (DMA)

In this study, results presented here are the tan δ and storage modulus against temperature and the effect of V_f and moisture on neat PA6 and SGF/PA6 composites were investigated.

4.4.1 The Effect of Fibre Volume Fraction, V_f

The curves in Figures 4.20, 4.21 and 4.22 obtained by the dynamic mechanical analyzer (DMA), show the variation of tan δ of SGF/PA6 composites as a function of temperature. Over a temperature range of -100ºC to 150ºC, two transition regions as indicated by two damping maxima, were recorded. There are ß-transition ($T_ß$) at a lower temperature and α-transition (T_α) at a higher temperature and usually T_α refers to glass transition temperature (T_g).

Tan δ expressed as the ratio of loss modulus to the storage modulus is desirable to avoid catastrophic failure. For DAM specimen, the α- and β-relaxation peaks are about 60˚C and -67˚C, respectively and the values of 17˚C and -77˚C for 50% RH and -24˚C for α- relaxation peak under wet condition are obtained. In general, the α-transition of PA6 is related with the breakage of the hydrogen bond network, while β-transition is mainly due to the movement of the carbonyl group in amorphous phase. A secondary glass transition (β-transition) is important for the impact strength of a polymer as it creates the possibility to dissipate energy in situations of shock loading, so that the polymer is less brittle [7, 101].

Clearly from the Figures 4.20, 4.21, and 4.22 show variations of glass fibre content do not affect the T_g of composites significantly. On the other hand, increases in glass fibre content causes gradual decrease of tan δ magnitude. Previous study [103-105] reported that the degree of crystallinity of polymer have an essential effect on maximum values of tan δ curve and the higher the degree of crystallinity the higher maximum of tan δ.

The curves in Figures 4.23, 4.24 and 4.25, show the variation of storage modulus of SGF/PA6 composites as a function of temperature. Storage modulus or well known as elastic modulus (E') represent the ability of the material to return or store energy due to elasticity [95]. Figure 4.23 shows that there is no significant change in T_g with increase in fibre loading for DAM specimens. On the other hand, a slight increment in 50% RH was observed as temperature showed an increasing from -7 to -5˚C with fibre loading. Specimens subjected to wet condition showed the same observation as T_g increasing from -51 to -49˚C. This suggests that the addition of glass fibre has a slight effect on the viscoelastic behaviour for the reinforced materials in comparison with the neat materials.

In terms of storage modulus intensity, it was apparent that the storage modulus of SGF/PA6 composites were higher than those of the neat PA6 throughout the whole temperature range (–100 - 150°C). This indicates that there is a high degree of stress transfer at the interface. Furthermore the presence of even small amount of glass fibre is sufficient to inhibit ductile energy dissipation away from the fracture surface [96, 97]. Therefore, the thermoviscoelastic behaviour of all V_f of SGF/PA6 composites is characterized by an increase of storage modulus in the glassy region with respect to the neat PA6 and by a decrease of T_g [98]. This is in line with the study reported by Koszkul & Kwiatkowski where SGF/PA6 composites were found to show the viscoelastic characteristic on the dynamical mechanical properties of SGF/PA6 composites [99].

It is well known that composite becomes stiffer with further addition of glass fibre. Theoretical considerations show that the thermal expansion coefficient and stiffness of a composite are closely related. The stiffer the composite, the lower the thermal expansion will be, while the composite will expand most in the direction of lowest stiffness. It is found that the theory accurately predicts the relationship between the thermal expansion and stiffness of SGF/PA6 composites as reported by Laura *et al.* [100]. Furthermore, hardening occurs with reinforcement with glass fibres as reported by SchoBig *et. al.* [94] in glass fibre reinforced polyprolylene and polybutene.

In this study, tan δ_{25} was chosen because most of the properties were measured at room temperature (Table 4.5). Specimens at DAM showed reduction in tan δ_{25} value with increase in fibre loading. The same behaviour was also observed in specimens subjected to 50% RH and wet condition. On the other hand, the transition width of α-transition region ($W_{\sqrt{2}}$) also becomes lower than that of the pure matrix as fibre content increase in DAM specimens. By contrast, as specimens were subjected to 50% RH and wet condition, ($W_{\sqrt{2}}$) show a reduction value in α-transition. However, in β-transition region ($W_{\sqrt{2}}$) shows inconsistent value with increment in fibre content. This suggests that there are molecular relaxations occurring at the interfacial region of the composite [106].

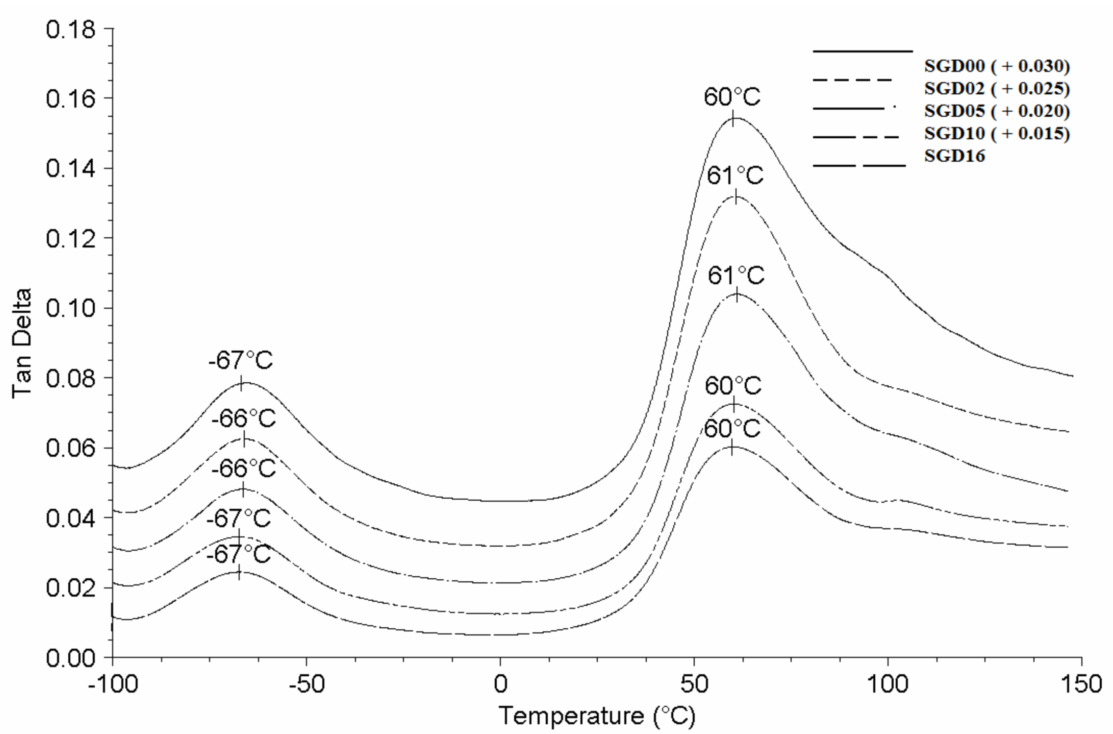

Figure 4.20: The tan delta-temperature behaviour of injection moulded SGF/PA6 composites at DAM.

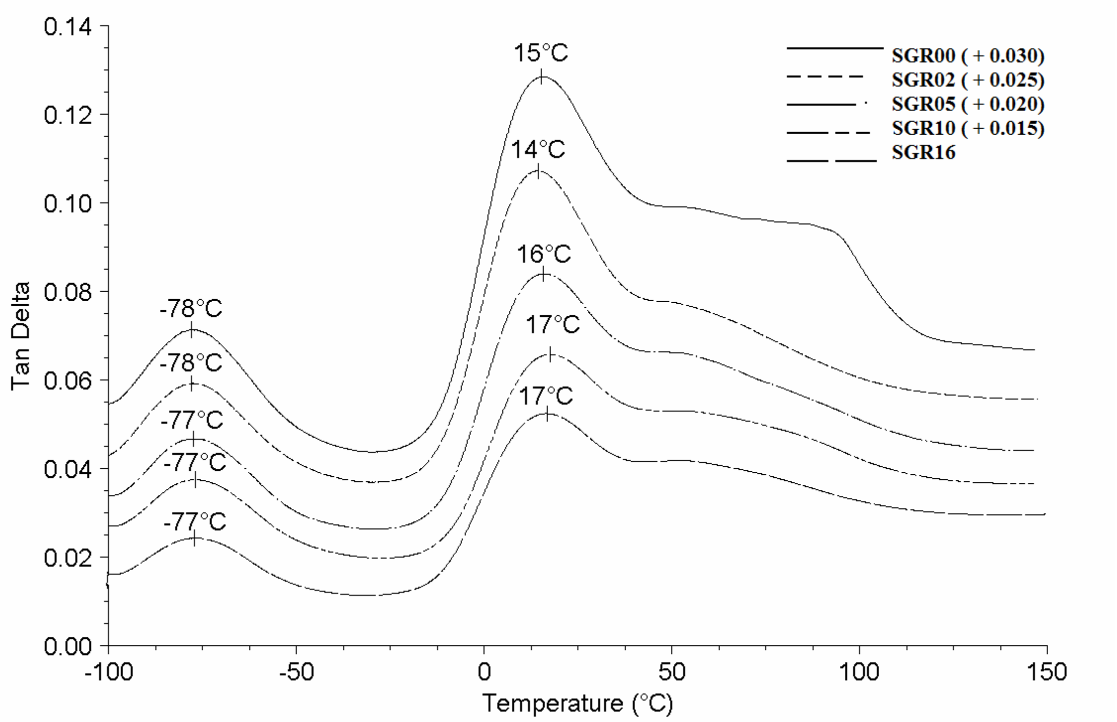

Figure 4.21: The tan delta-temperature behaviour of injection moulded SGF/PA6 composites subjected to 50% RH.

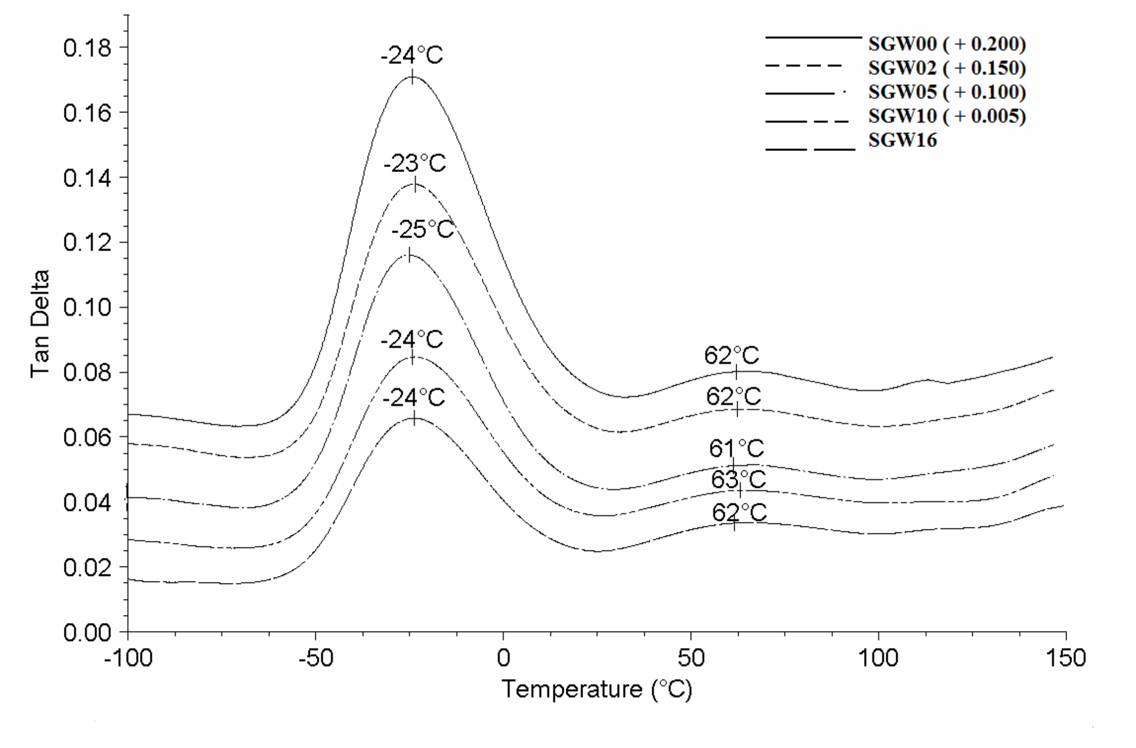

Figure 4.22: The tan delta-temperature behaviour of injection moulded SGF/PA6 composites subjected to wet condition.

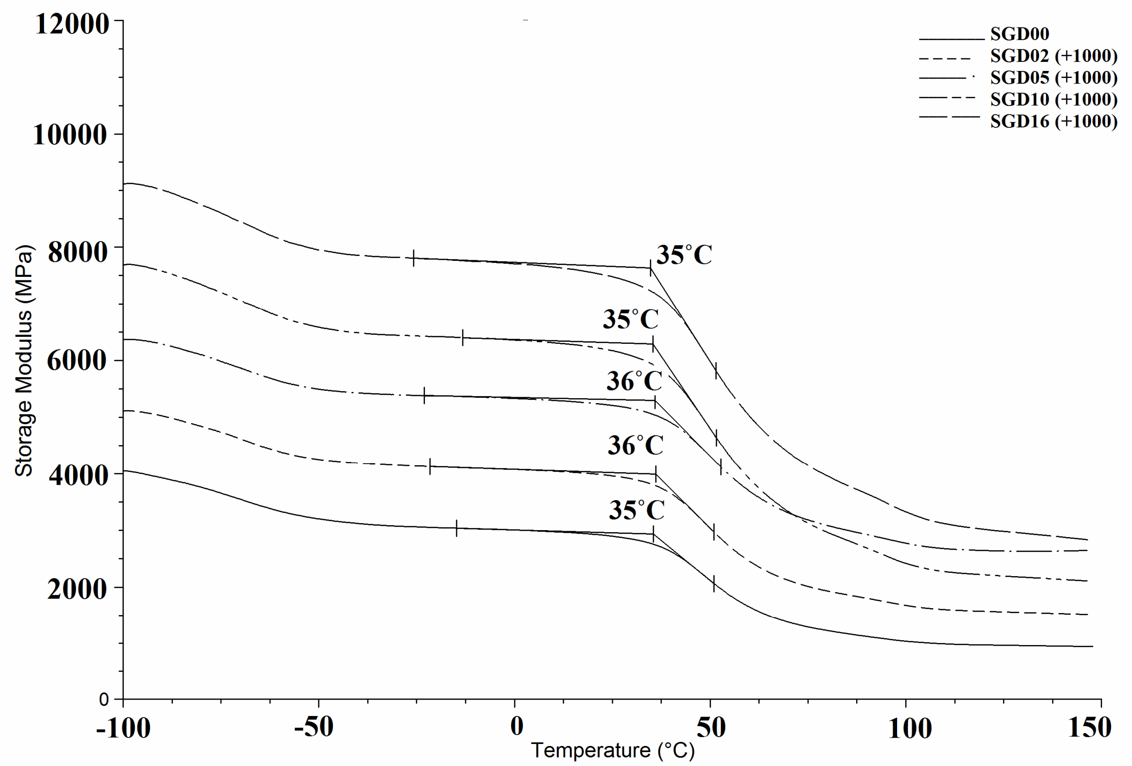

Figure 4.23: The storage modulus-temperature behaviour of injection moulded SGF/PA6 composites at DAM.

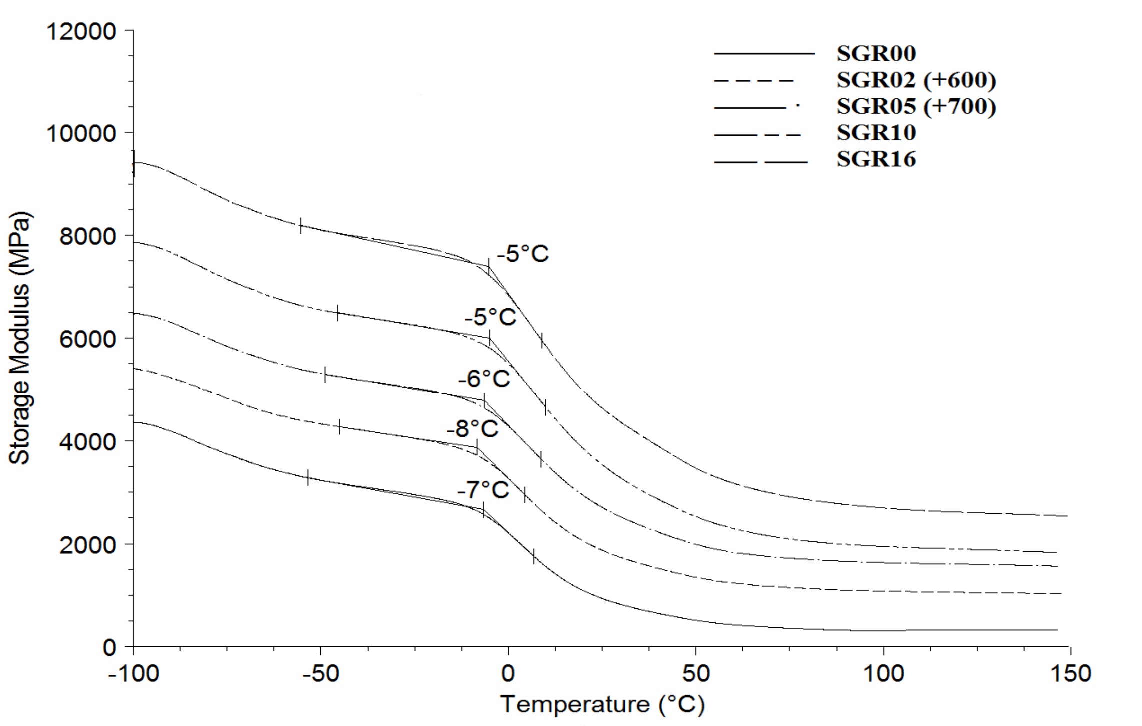

Figure 4.24: The storage modulus-temperature behaviour of injection moulded SGF/PA6 composites subjected to 50% RH.

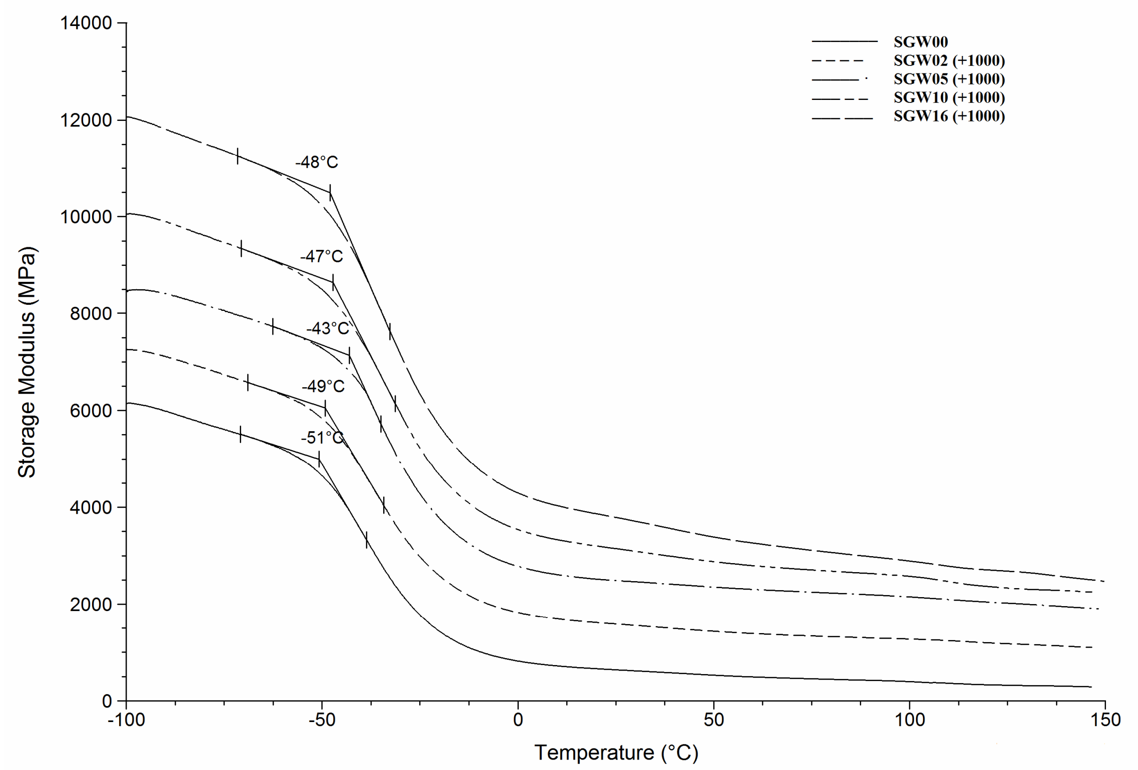

Figure 4.25: The storage modulus-temperature behaviour of injection moulded SGF/PA6 composites subjected to wet condition.

Table 4.5: DMA thermomechanical data of injection moulded glass fibre composites at various environmental conditions.

Sample	V_f (%)	Condition	tan δ_{25} [a] (x 10^{-2})	α-transition					β-transition				
				tan δ_{max} [b] (x 10^{-2})	T_α [c] (°C)	T_i [d] (°C)	T_e [e] (°C)	$W_{\sqrt{2}}$ [f] (°C)	tan δ_{max} [g] (x 10^{-2})	T_β [h] (°C)	T_i [i] (°C)	T_e [j] (°C)	$W_{\sqrt{2}}$ [k] (°C)
SGD00	0	DAM	1.80	12.60	60	48	88	40	5.08	-67	-66	-49	17
SGD02	2		1.19	10.60	61	48	79	31	3.69	-66	-66	-52	14
SGD05	5		1.28	9.20	61	48	83	35	3.70	-66	-82	-50	32
SGD10	10		1.16	6.70	60	47	82	35	2.93	-67	-84	-53	31
SGD16	16		0.94	6.00	60	46	83	37	2.44	-67	-83	-53	30
SGR00	0	50% RH	8.37	10.50	15	1	63	62	4.83	-78	-95	-60	35
SGR02	2		6.58	8.60	14	1	36	35	3.80	-78	-93	-60	33
SGR05	5		5.93	7.20	16	1	66	65	3.60	-77	-94	-59	35
SGR10	10		4.83	5.80	17	3	80	77	3.07	-77	-94	-59	35
SGR16	16		4.34	5.10	17	1	81	80	2.43	-77	-95	-59	36
SGW00	0	Wet	7.00	12.70	-24	-39	-6	33	–	–	–	–	–
SGW02	2		8.72	10.10	-23	-39	-5	34	–	–	–	–	–
SGW05	5		9.32	9.40	-25	-35	-3	32	–	–	–	–	–
SGW10	10		6.44	7.20	-24	-39	-5	34	–	–	–	–	–
SGW16	16		4.74	6.50	-24	-39	-5	34	–	–	–	–	–

Keynotes:

a: loss tangent value at the temperature of 25˚C.
b: maximum value of tan δ in α-transition region.
c: temperature at the maximum value of tan δ in α-transition region.
d: initial temperature of transition width in α-transition region.
e: end temperature of transition width in α-transition region.
f: transition width in α-transition region.
g: maximum value of tan δ in β-transition transition region.
h: temperature at maximum value of tan δ in β-transition transition region.
i: initial temperature of transition width in β-transition transition region.
j: end temperature of transition width in β-transition transition region.
k: transition width in β -transition transition region.

4.4.2 The Effect of Moisture

As the SGF/PA6 composites subjected to different condition, a clear trend of reduction in T_g was observed in DAM, 50% RH and wet condition in both storage modulus and tan δ. The T_g reduces gradually from 60˚C to 15˚C and -24˚C for neat PA6 (Figure 4.26). The same behaviour was also observed for 2, 5, 10 and 16% V_f (Figures 4.27, 4.28, 4.29 and 4.30). The presence of moisture makes the polymer chain more flexible and moveable. As a result, reduce the T_g in which the modulus and strength drop significantly; however some polyamides containing aromatic monomers with a high T_g, have little change in properties with changing moisture as the T_g remains above room temperature [34].

In terms of storage modulus magnitude (Figures 4.31, 4.32, 4.33, 4.34 and 4.35), composites in wet condition showed the highest value followed by 50% RH and DAM. This is expected as composite in wet condition has the ability to store more energy compared to 50% RH and DAM specimens. An explanation for this is, as structural materials subjected to dynamic loading; it should produce high stiffness along with high damping. Thus, high storage modulus will eventually enhanced the ability to absorb energy before failure as well as high loss modulus to dissipate the energy. High damping is also desirable to avoid catastrophic failure.

Theoretically when water diffuses into a fibre, water molecules may interrupt the original hydrogen bonds between the polymeric molecules of the fibre. This interruption could result in temporary reduction of the rigidity of the material and therefore the observed increased in deformation under the action of load [48]. Water can be considered as a plasticizer for polar polymers. The T_g of polyamide is greatly reduced by existing of water. Strong hydrogen bonds in polyamides act similar to crosslink in raising T_g. Small amount of water (about 5% or less) may break these bonds and cause a large reduction in T_g. Water also affect the secondary glass transitions in many cases, and it also often in the region -50˚C to -100˚C.

The reduced T_g in the presence of water results in a strong reduction of the amorphous modulus in the temperature range around T_g, which leads to a decrease of the modulus of the semi-crystalline polymer. Due to the reduction of the matrix modulus, also polyamide nanocomposites suffer from a modulus reduction after moisture conditioning as reported by Vlasveld *et. al*. [107].

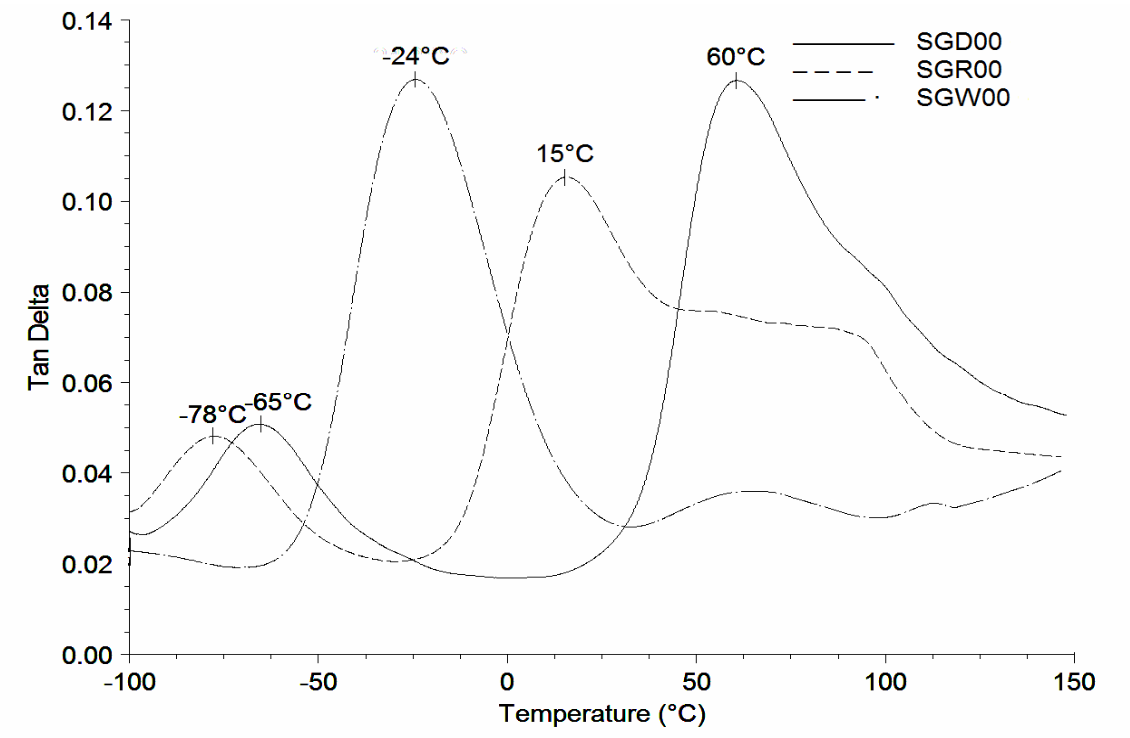

Figure 4.26: The tan delta-temperature behaviour of injection moulded neat PA6 subjected to different conditions.

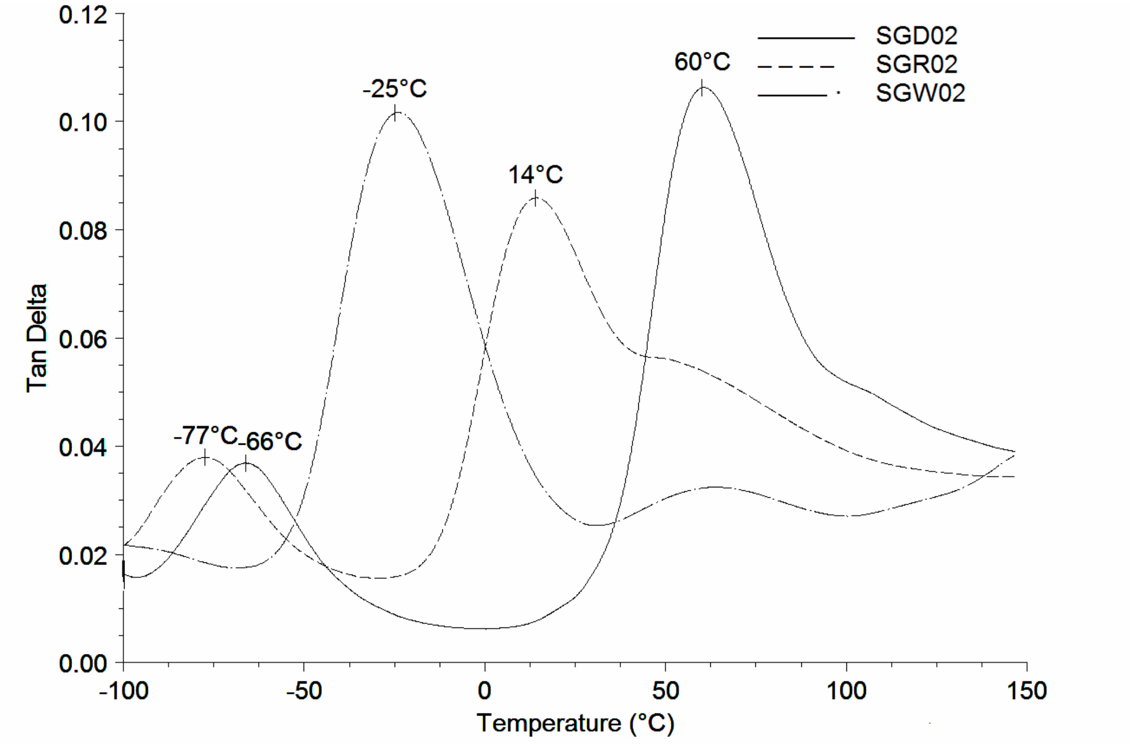

Figure 4.27: The tan delta-temperature behaviour of injection moulded 2% V_f SGF/PA6 composites subjected to different conditions.

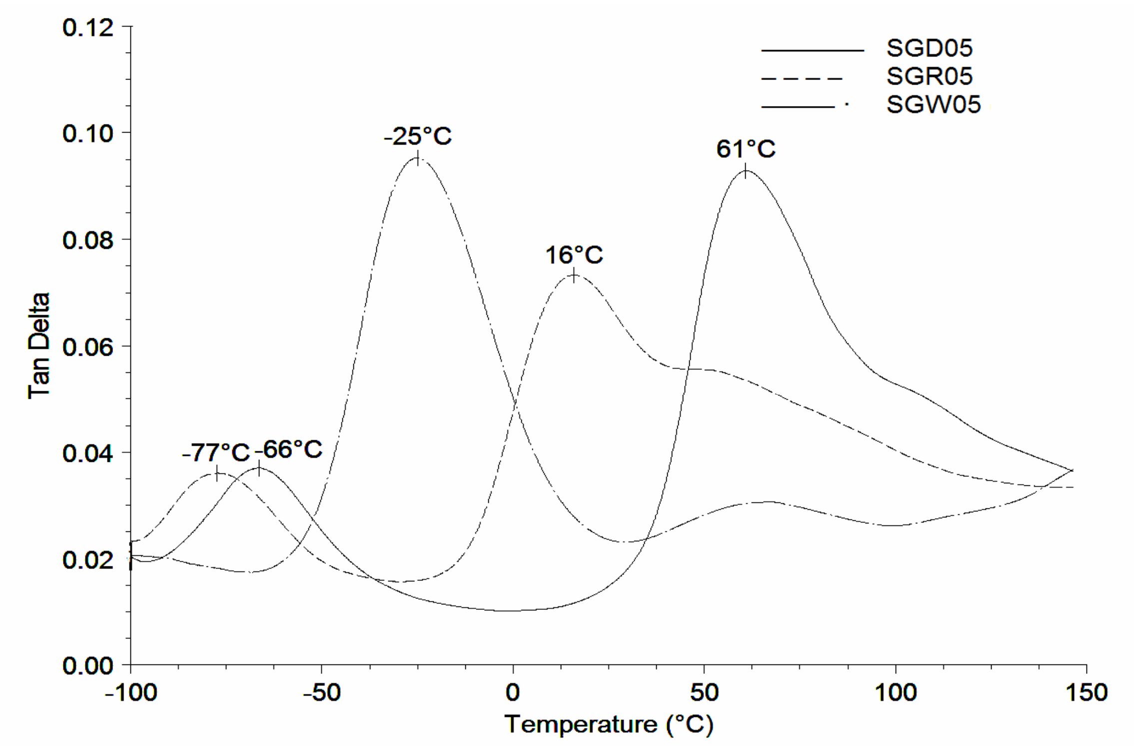

Figure 4.28: The tan delta-temperature behaviour of injection moulded 5% V_f SGF/PA6 composites subjected to different conditions.

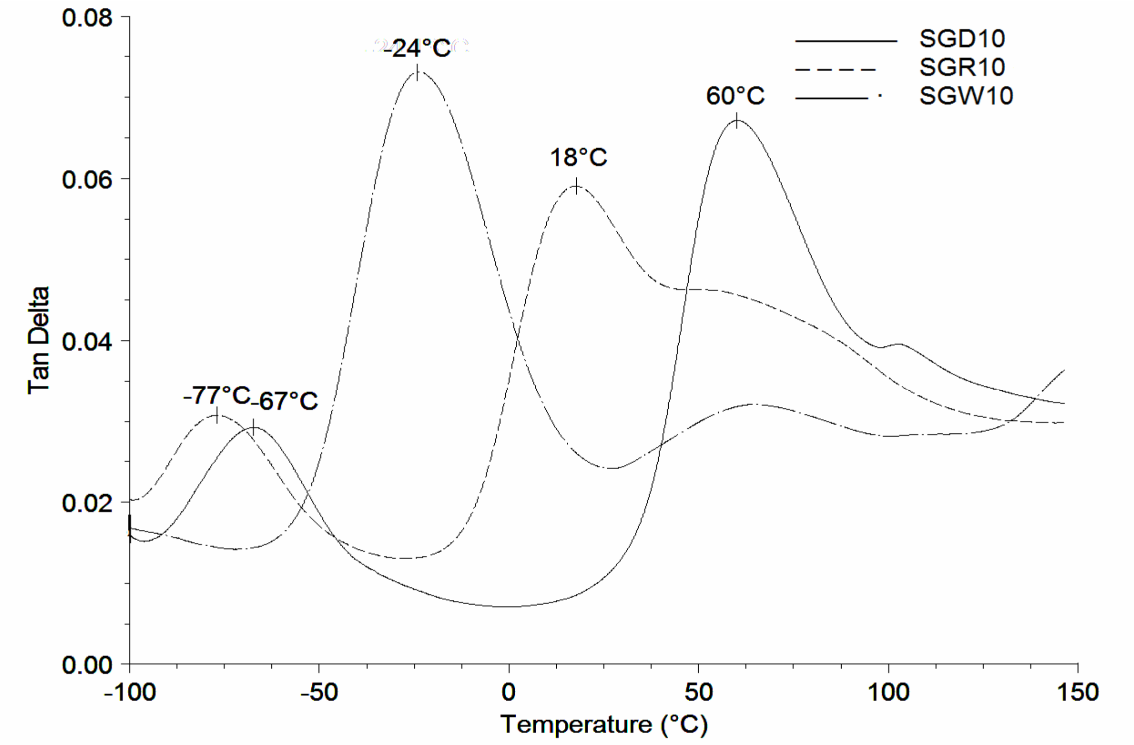

Figure 4.29: The tan delta-temperature behaviour of injection moulded 10% V_f SGF/PA6 composites subjected to different conditions.

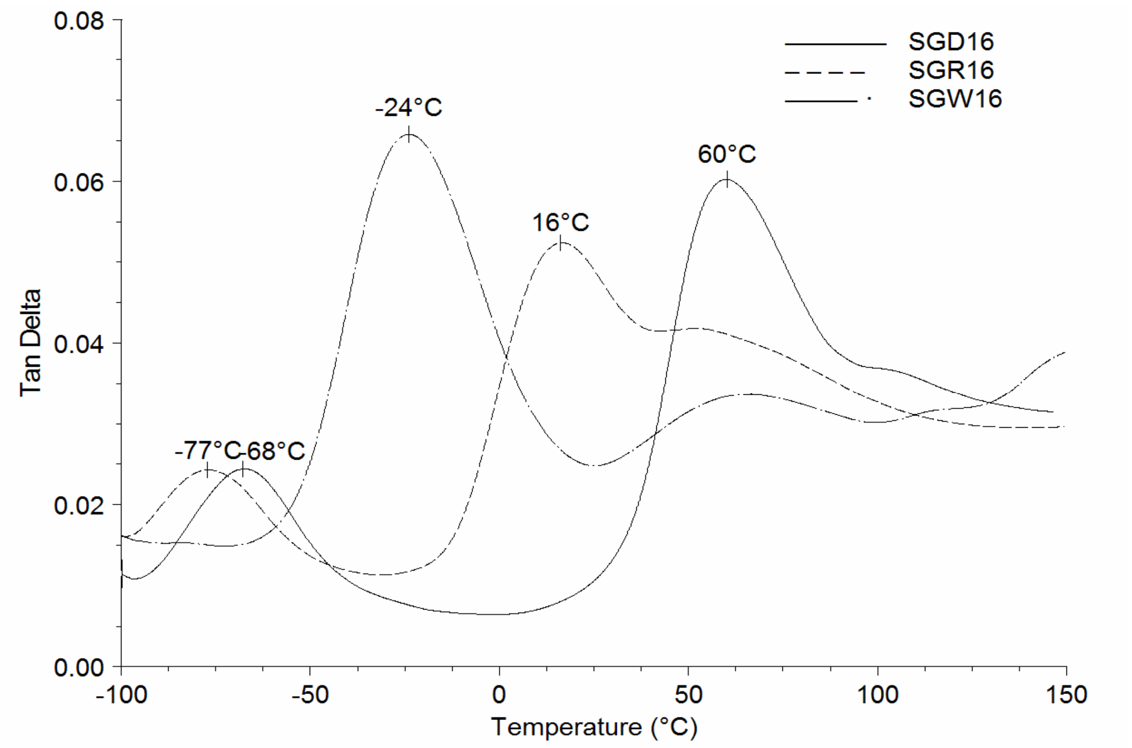

Figure 4.30: The tan delta-temperature behaviour of injection moulded 16% V_f SGF/PA6 composites subjected to different conditions.

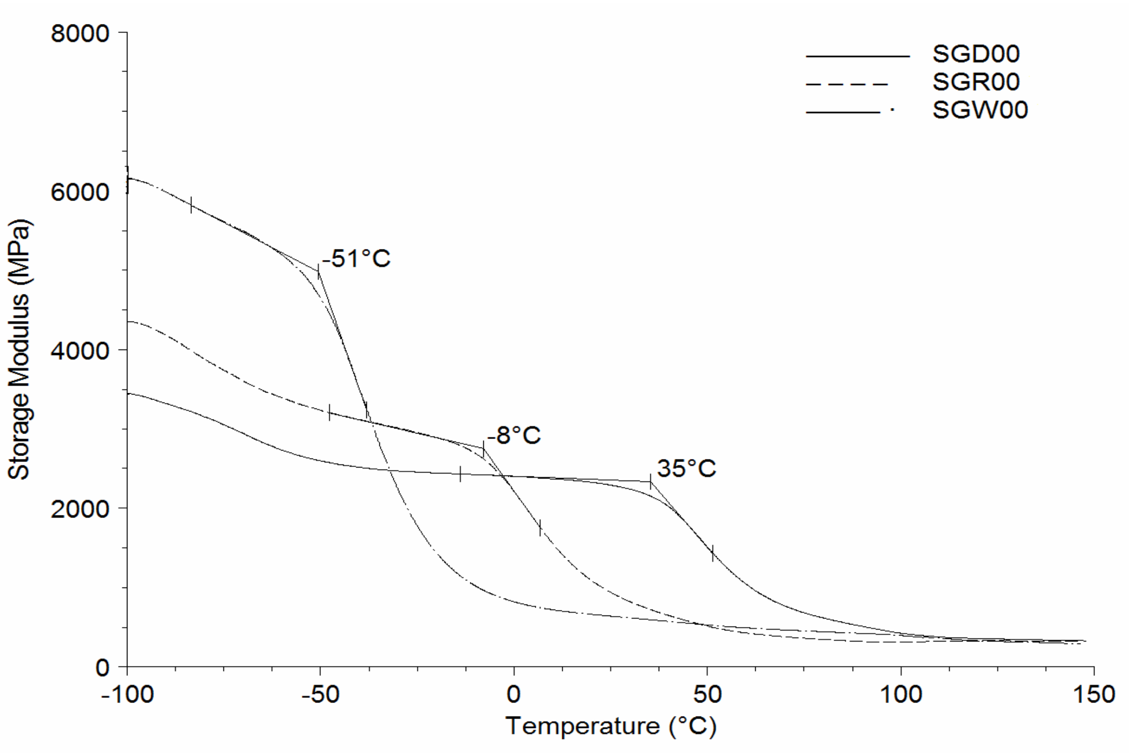

Figure 4.31: The storage modulus-temperature behaviour of injection moulded neat PA6 subjected to different condition.

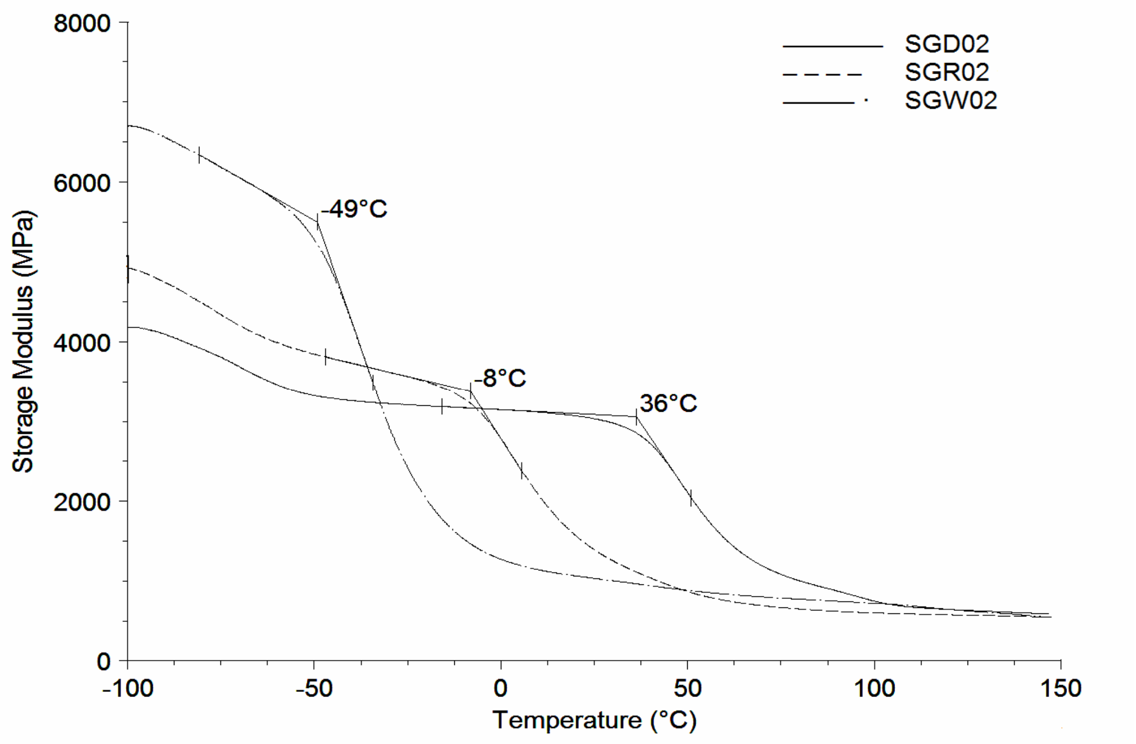

Figure 4.32: The storage modulus-temperature behaviour of injection moulded 2% V_f SGF/PA6 composites subjected to different condition.

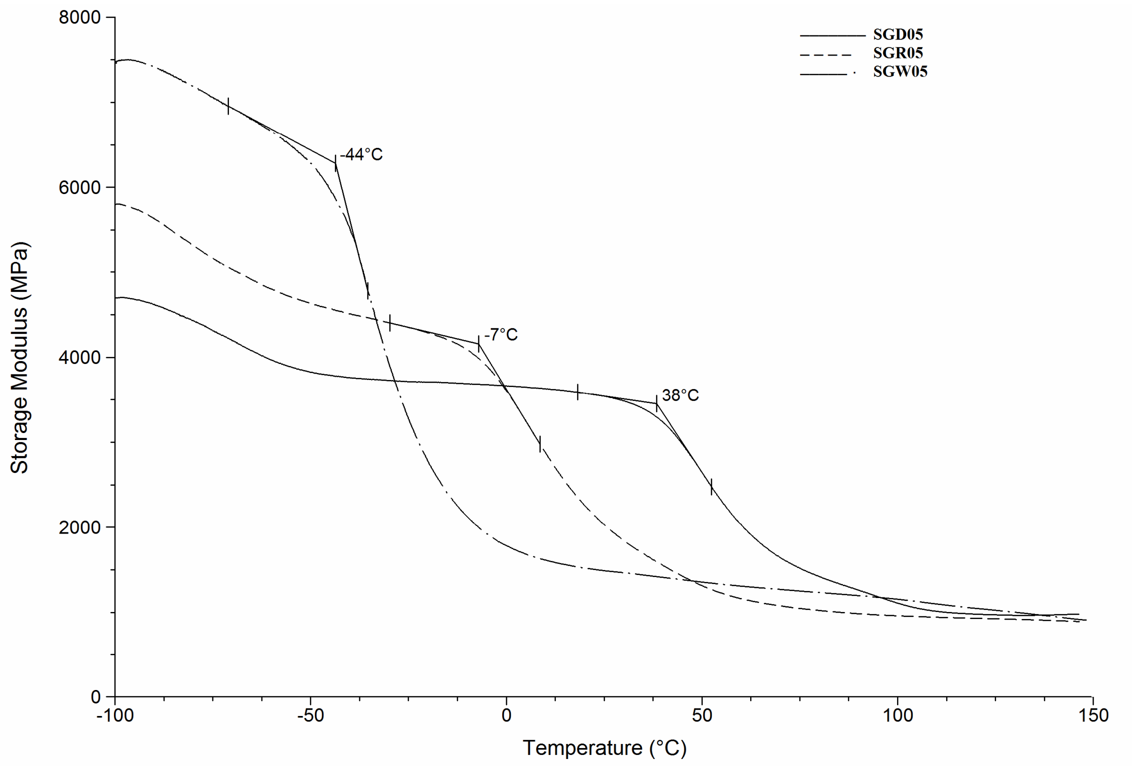

Figure 4.33: The storage modulus-temperature behaviour of injection moulded 5% V_f SGF/PA6 composites subjected to different condition.

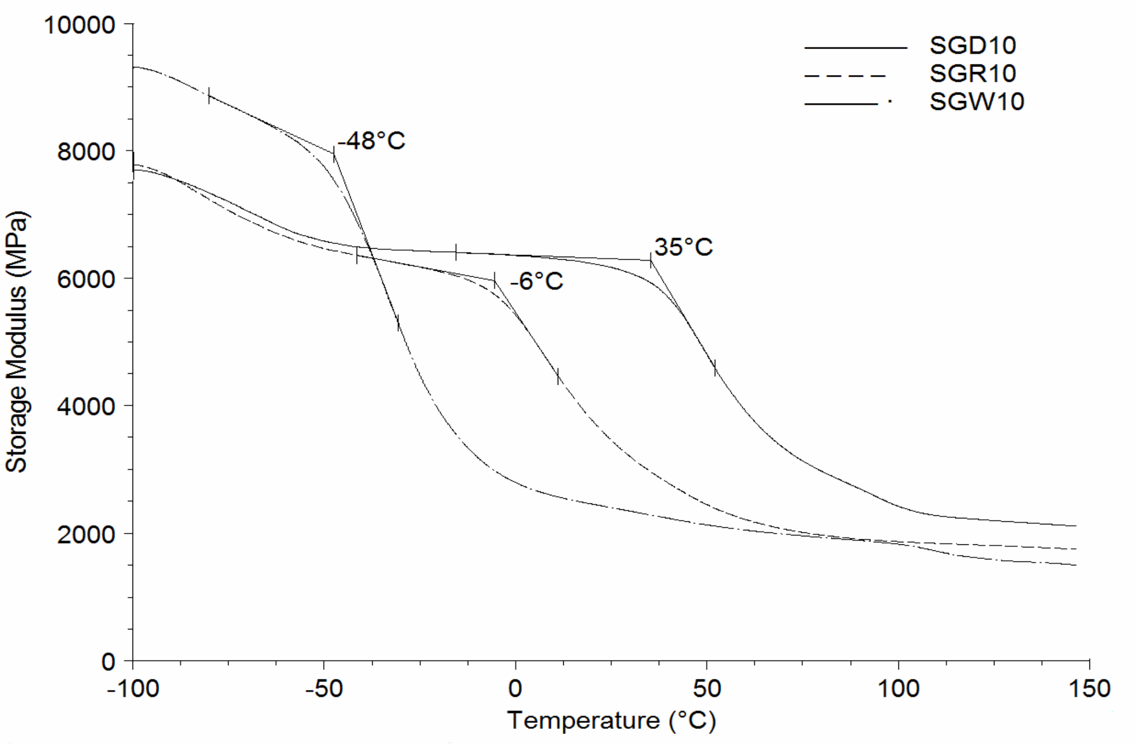

Figure 4.34: The storage modulus-temperature behaviour of injection moulded 10% V_f SGF/PA6 composites subjected to different condition.

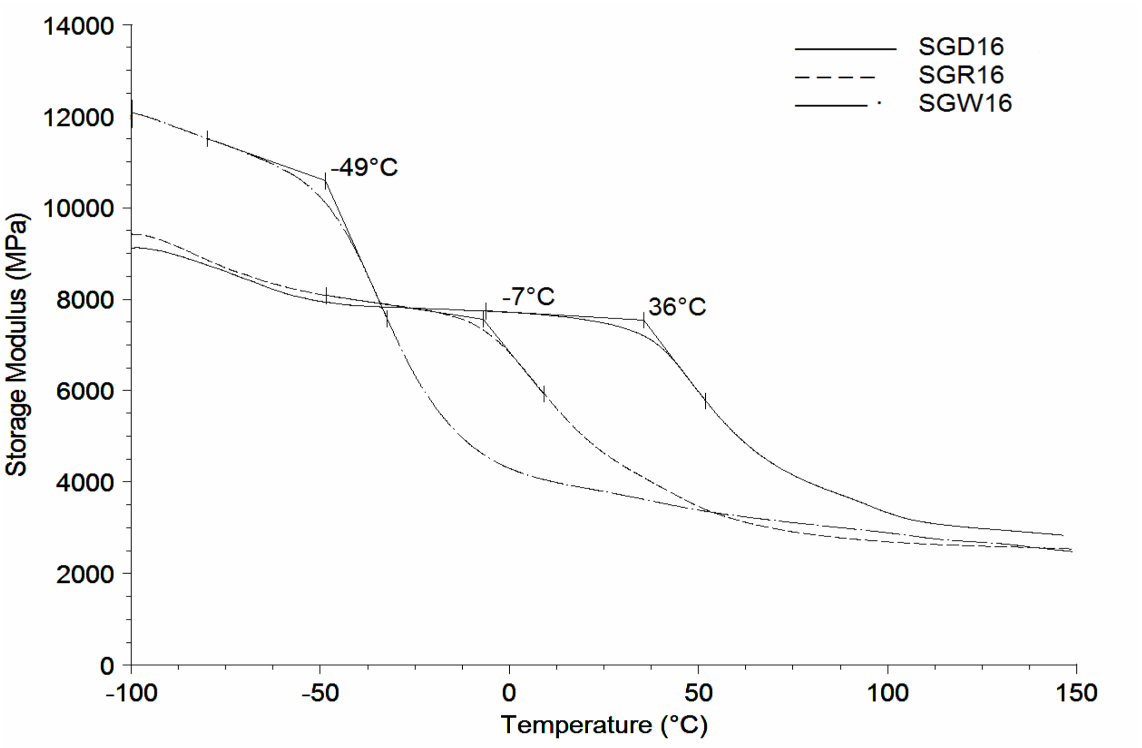

Figure 4.35: The storage modulus-temperature behaviour of injection moulded 16% V_f SGF/PA6 composites subjected to different condition.

4.5 Tensile Properties

The mechanical properties of composites are heavily influenced both on the reinforcement fibres and on the properties of the matrix. Depending on their application areas, reinforcement such as fibre materials is added to plastics to improve their mechanical properties and to reduce cost compared to the traditional materials [12]. In this study, the tensile properties were investigated through four different effects which are the effects of fibre volume fraction, moisture, strain rate and extensometer.

4.5.1 Neat Polyamide 6

Neat PA6 are hard and have a tough structure. Due to different failure mechanism, the PA6 discussion is done separately. As can be seen from Figure 4.36 the tensile strength for PA6 was found to be 75.88 MPa, while it reduced to 73.37, 76.16, and 72.50 MPa with strain rate of 1.67×10^{-3} s^{-1}, 3.30×10^{-3} s^{-1} and 6.67×10^{-3} s^{-1} respectively under DAM. However, when PA6 is subjected to 50% RH and wet condition the increment of 22%, 28% and 29% for 50% RH and 3.84%, 4.68% and 5.62% for wet condition respectively was observed. Tensile modulus (Figure 4.37) also behaves the similar trend where it shows decrement for specimen under DAM and wet condition and significant increment in tensile modulus as PA6 is subjected to 50% RH. The inconsistent value in tensile strength and tensile modulus of neat PA6 is due to the changes of failure mechanism under high strain rate. By contrast, for all three conditions studied, show decrement in fracture strain (Figure 4.38). It was found that decrement about 27.85%, 75.84%, 75.90% for specimens at DAM, 23.50%, 27.70%, 31.31% for specimens subjected to 50% RH and 6.95%, 8.00%, 12.48% for wet condition was observed respectively. This indicates that PA6 failed in brittle manner as strain rate increased.

In addition, at low strain rate of 0.33 x 10^{-3} s^{-1} neat PA6 exhibited the highest fracture strain of 18.13%, 28.30% and 29.64% respectively for specimens under DAM, 50% RH and wet condition due to matrix ductility which dominates the tensile strength especially at lowest strain rate [54]. The largest fracture strain at lowers strain rate suggests that there is high absorb energy in neat PA6.

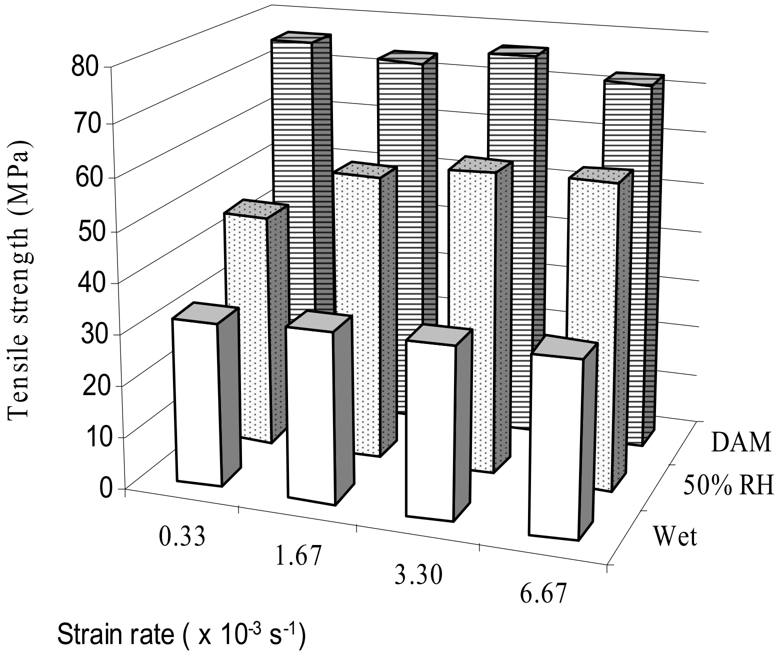

Figure 4.36: Tensile strength of neat PA6 at different environmental condition.

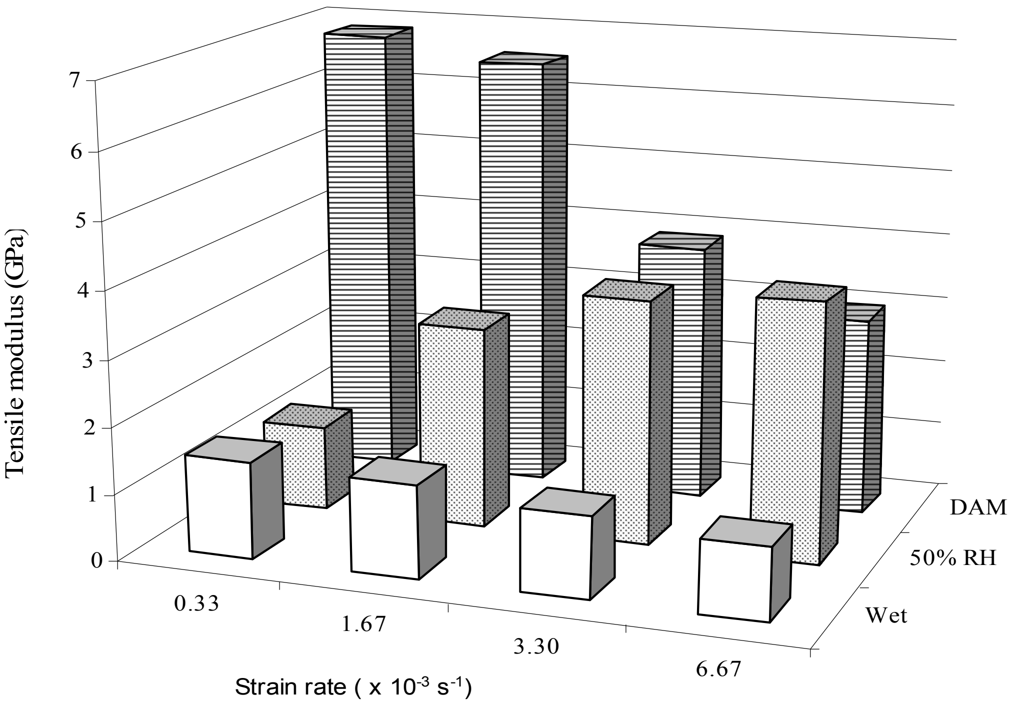

Figure 4.37: Tensile modulus of neat PA6 at different environmental condition.

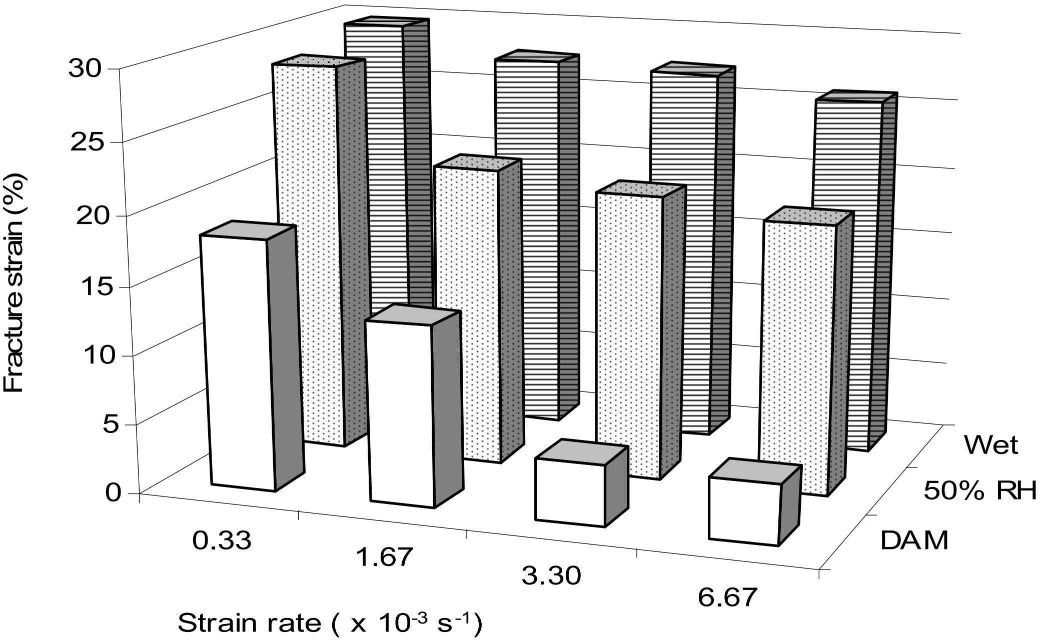

Figure 4.38: Fracture strain of neat PA6 at different environmental condition.

4.5.2 The Effect of Fibre Volume Fraction (V_f)

Mechanical results show that SGF/PA6 composites provide a significant enhancement to the tensile modulus and strength. Result proved that SGF/PA6 composite is hard and brittle. The ultimate strength of composites is a direct indicator of the strength of the interfacial bonds since the applied stress is more efficiently transferred through the interface [69].

Figure 4.39 show the effect of glass fibre concentration on the mechanical properties of SGF/PA6 composites at DAM. Results shown that tensile strength of 2% V_f is 73.36 MPa and increased to 93.60, 133.53, 157.93 MPa with the addition of 5%, 10% and 16% V_f respectively subjected to strain rate of 0.33 x 10^{-3} s^{-1}. SGF/PA6 composites at wet condition and 50% RH (Figures 4.40 and 4.41) also show the same increment as fibre content increased. For specimens exposed 50% RH, the increment is 41.89 for 2% V_f and increased to 54.50, 86.70 and 110.46 MPa for 5%, 10% and 16% V_f respectively. On the other hand, as composites was exposed to wet condition, the increment were 42.40, 62.69 and 76.07 MPa for 5%, 10% and 16% V_f respectively. Therefore, with the increase in the fibre loading from 2% to 16%, there is a progressive increase in the tensile strength and modulus of the composites.

As expected, the tensile strength of SGF/PA6 composites increased by increasing glass fibre loading. This indicates that fibre loading play a major role in the strength of glass fibre composites as glass fibres have a much higher strength and stiffness than PA6 matrix. An increase in tensile strength also means that the stress has been transferred from the PA6 matrix to the glass fibre particle efficiently. Strong interfacial bonding between the fillers and the matrix caused efficient stress transfer when strain is applied on a tensile specimen [111]. In general, the improvement of the interfacial adhesion of the SGF/PA6 composites will subsequently increase the yield stress of the SGF/PA6 composites. In addition, the interfacial influence may vary from one composite system to another due to variation in the properties of fibres and matrix. Good adhesion between filler and plastic is desirable because it improves strength, but unfortunately it increases the tendency to brittle failure and makes the material more notches sensitive. If there is good adhesion between the filler and the matrix, a decrease of the elongation at break, even with small amounts of filler, can be expected. On the other hand, the elongation at break may decrease more gradually if the adhesion is poor [112]. The increment in tensile strength suggests improvement in interfacial adhesion that eventually lead to an increasing the yield stress of the SGF/PA6 composites. Unreinforced PA6 are hard and have a tough structure. Therefore, high fibre content in the plastic provides dimensional stability by eliminating the deflection [113].

Nicholson [77] reported that, once the glass fibre reinforced composite is fully formed, the fibre is capable of carrying twenty times the stress of the matrix. The increase in tensile strength at high fibre volume fraction due to the improvement of fibre-matrix adhesion is clearly higher than that at the low fibre volume fraction. At high fibre volume fraction, total interfacial area between fibres and matrix is also increased and there are more places to form interfacial cracks in the composite system with weak fibre-matrix adhesion. Therefore, the effect of fibre-matrix adhesion on the transverse tensile strength at a high fibre volume fraction becomes more pronounced and the composite become more sensitive to the difference in the fibre matrix adhesion. Hence, more percentage of fibres in the composites has resulted more interfacial areas and thus more matrix damages were inducted by misfit strain for glass/epoxy composites as reported by Ray [111].

On the other hand, tensile modulus also increases steadily with the addition of glass fibres. It can be see clearly from Figure 4.42, tensile modulus for 2% V_f is 3.70 GPa, increased to 5.00, 6.98, 9.30 GPa for 5%, 10% and 16% V_f respectively at $0.33 \times 10^{-3}\ s^{-1}$ subjected to short travel extensometer. For specimens subjected to 50% RH

(Figure 4.43), the tensile modulus is improved from 2.27 for 2% V_f to 3.27, 4.57 and 7.08 GPa for 5%, 10% and 16% V_f respectively. Meanwhile, wet condition (Figure 4.44) also show the same trend where is increased linearly from 1.57 GPa at 5% V_f, to 2.91 and 4.18 GPa for 10% and 16% V_f respectively. The increment in tensile modulus is attributed to the increased stiffness and brittleness of composites by addition of glass fibre. Moreover, these interactions might stiffen the polymer chains close to the fibres to resist against the applied tension leading to an improved tensile modulus with increasing glass fibre content [69].

The effect of glass fibre loading on the fracture strain of SGF/PA6 composites is shown in Figures 4.45-4.47. The elongation at break for composite is greatly affected by the presence of glass fibre. The elongation at break improved slightly with the incorporation of 2%, 5%, 10% and 16% V_f for DAM and 50% RH at 0.33×10^{-3} s^{-1} subjected to short travel extensometer. The elongation at break increased from 2.40% for 2% V_f, to 2.56%, 3.22% and 3.24%, for 5%, 10% and 16% V_f for specimens under DAM. The same increment was also observed for specimen under 50% RH from 6.66% for 2% V_f, to 3.54%, 3.77% and 3.84% for 5%, 10% and 16% V_f respectively. This observation seems to contradict with the trend frequently observed in composites material as a reduction in fracture strain is expected with increasing fibre content. Nevertheless, for wet condition, the tensile strain drops dramatically from 14.50% for 5% V_f to 7.72% and 5.45% for 10% and 16% V_f. This observation suggests that the addition of even very low levels of reinforcement leads to a very large reduction in the ductility of the material. Theoretically with an increase in fibre content, the elongation at break declines slightly. However in this study, only wet condition obeys this rule. This suggests that SGF/PA6 composites in wet condition showed poor adhesion between the fibres and the matrix.

The loss of ductility is confirmed by the addition of fibre as reported by Oksman and Clemons who claim that the polypropylene wood fibre composite elongation at break is dramatically decreased compared to unfilled polypropylene. The addition of MAPP decreases the elongation at break further while impact modifiers increased it [109]. Increasing stress and decreasing strain at break with increasing fibre content is also reported by Thomason [68] in glass reinforced polyamide and SchoBig [94] in glass fibre reinforced polypropylene and polybutene.

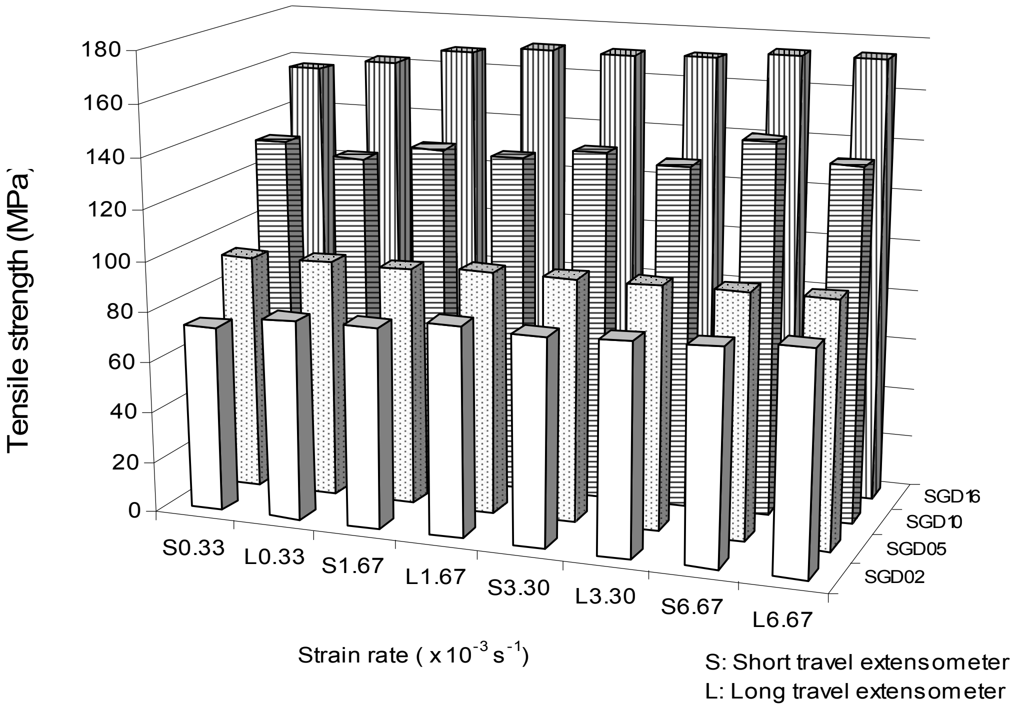

Figure 4.39: Tensile strength of injection moulded SGF/PA6 composites at DAM.

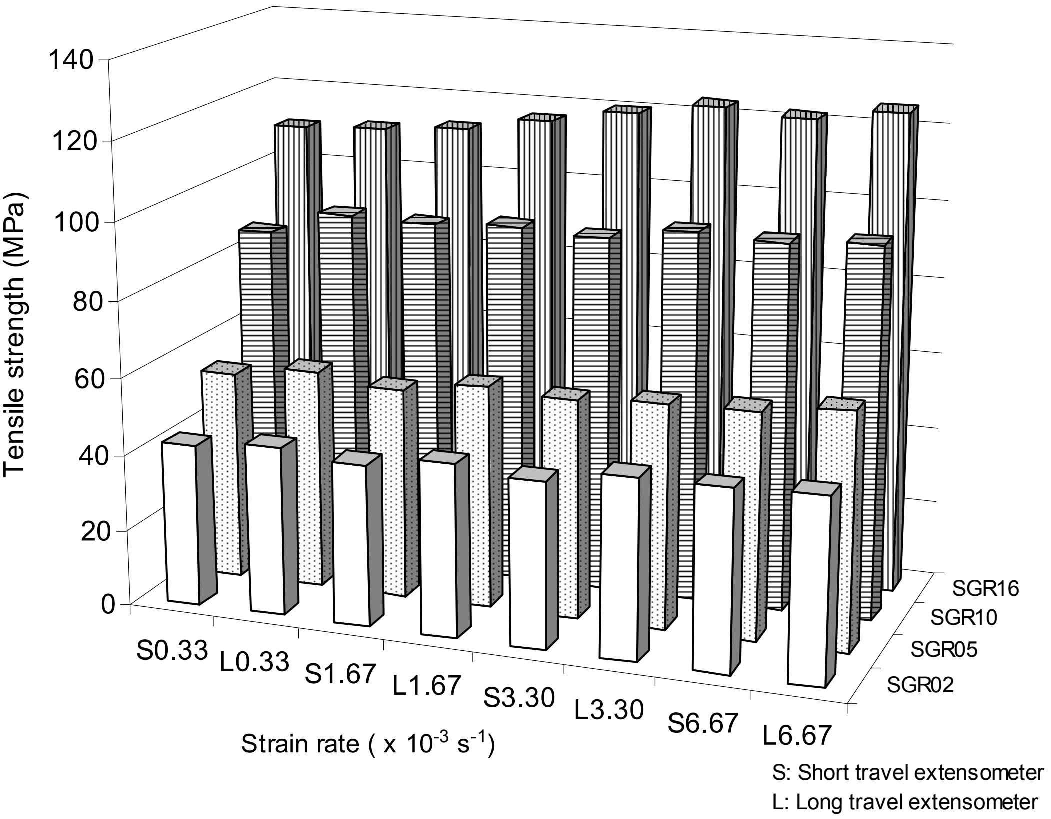

Figure 4.40: Tensile strength of injection moulded SGF/PA6 composites subjected to 50% RH.

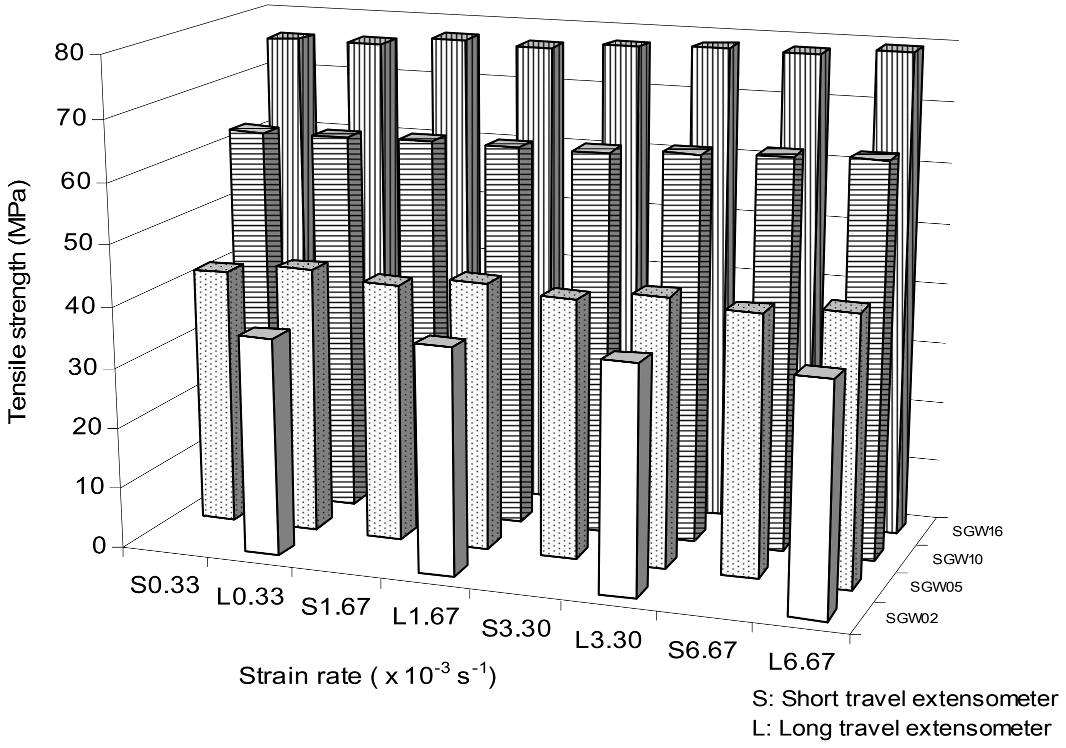

Figure 4.41: Tensile strength of injection moulded SGF/PA6 composites subjected to wet condition.

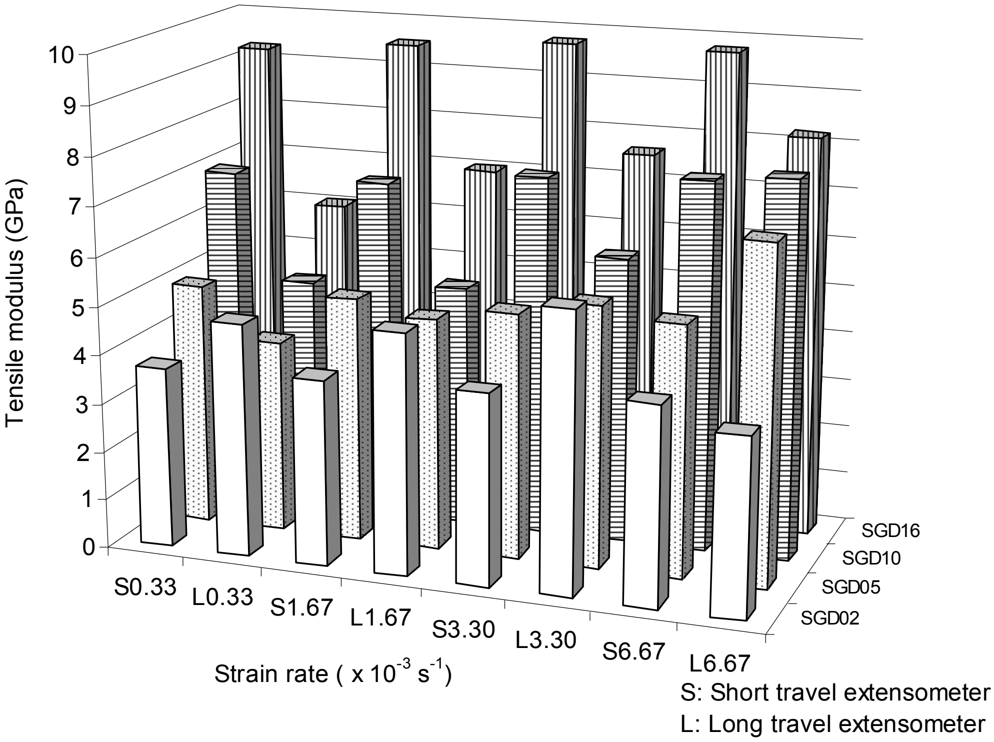

Figure 4.42: Tensile modulus of injection moulded SGF/PA6 composites at DAM.

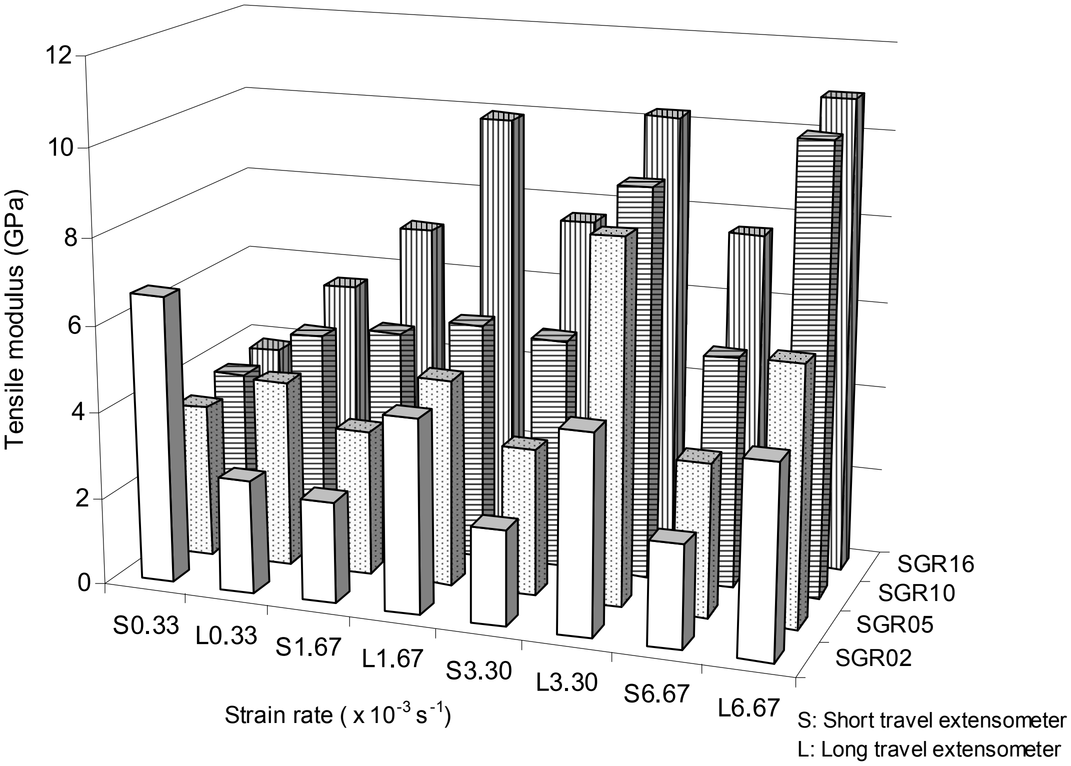

Figure 4.43: Tensile modulus of injection moulded SGF/PA6 composites subjected to 50% RH.

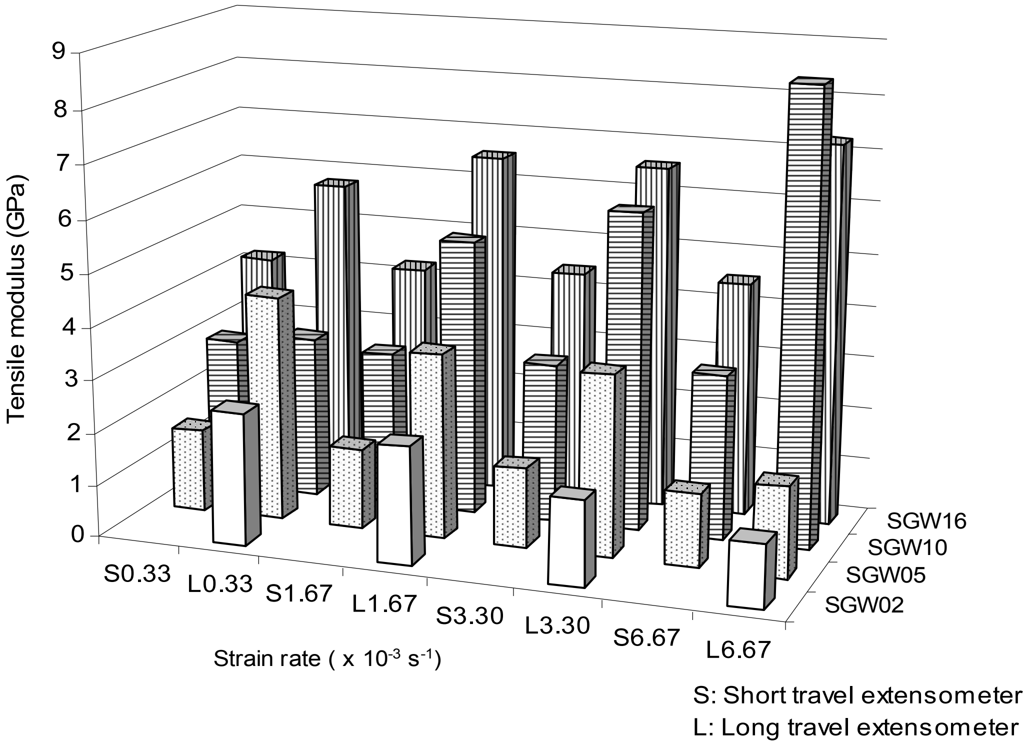

Figure 4.44: Tensile modulus of injection moulded SGF/PA6 composites subjected to wet condition.

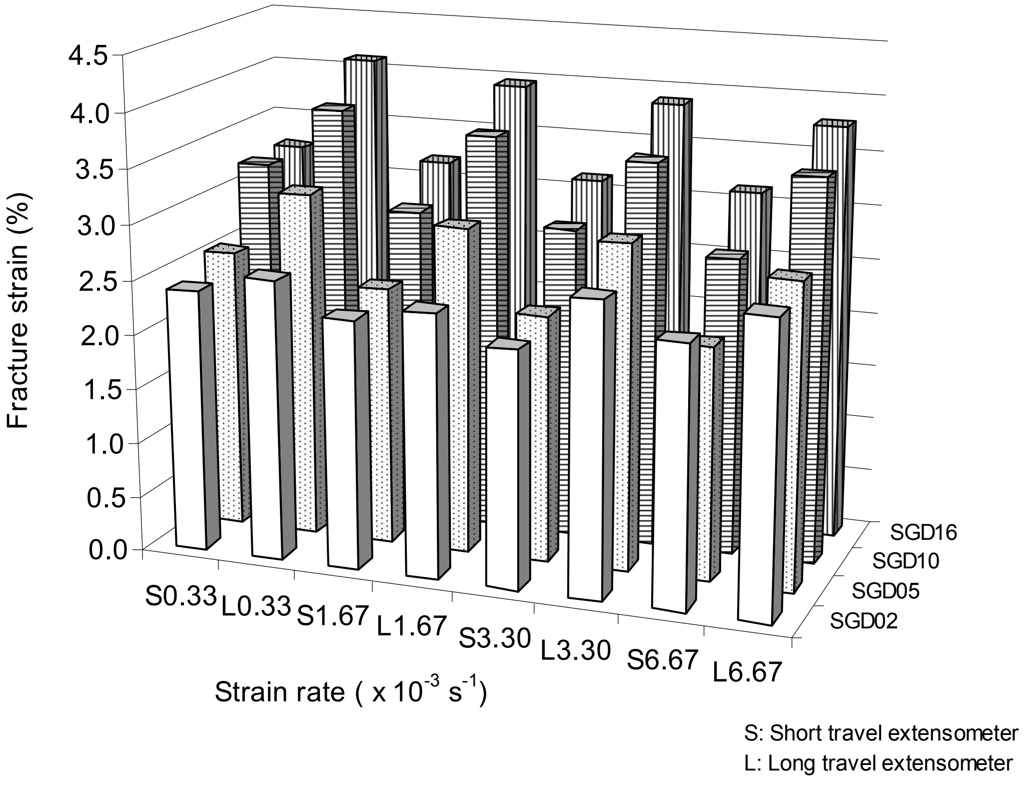

Figure 4.45: Fracture strain of injection moulded SGF/PA6 composites at DAM.

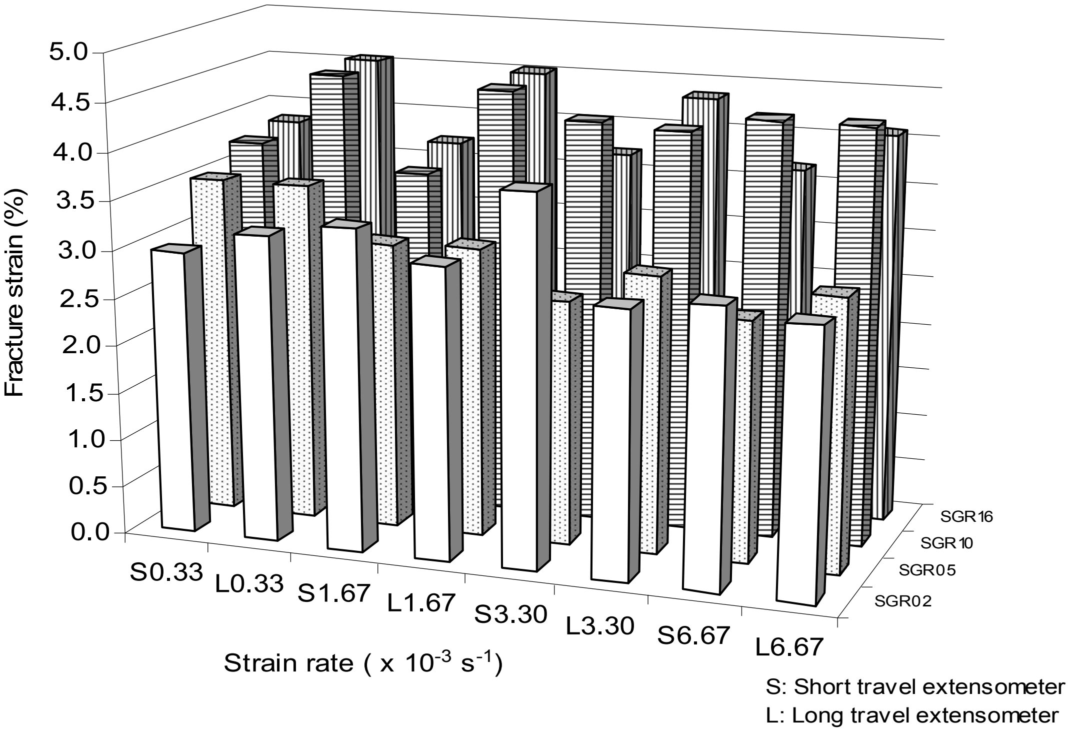

Figure 4.46: Fracture strain of injection moulded SGF/PA6 composites subjected to 50% RH.

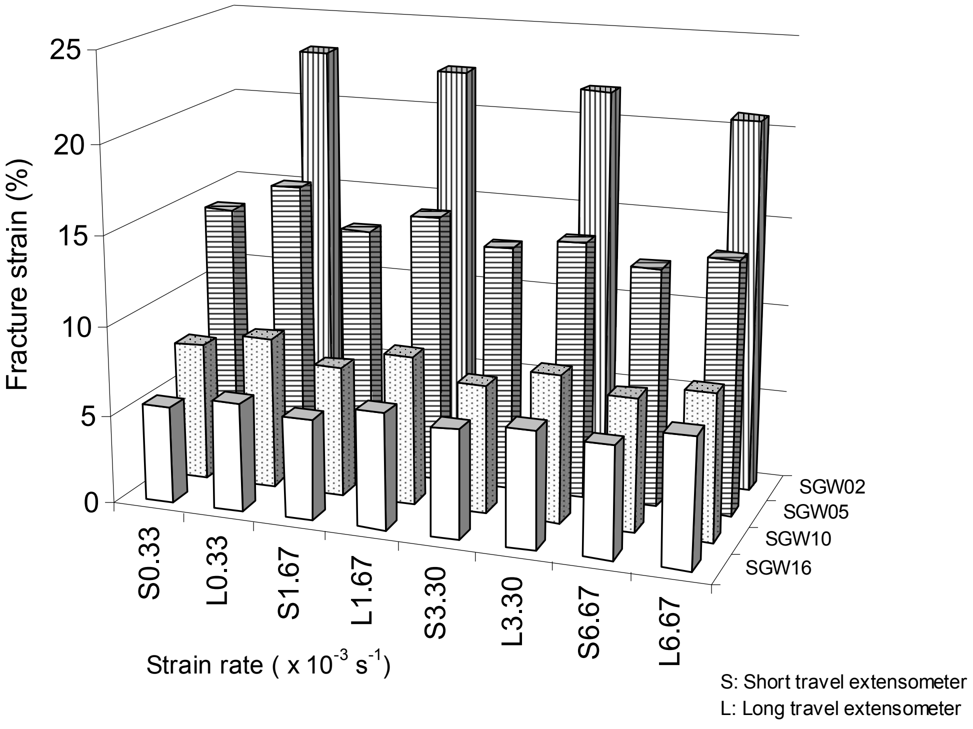

Figure 4.47: Fracture strain of injection moulded SGF/PA6 composites subjected to wet condition.

4.5.3 The Effect of Moisture

Changes in moisture content from specimen under DAM, 50% RH to wet condition affect significantly the tensile strength and modulus and eventually increase the fracture strain. Figures 4.39-4.47 show the influence of moisture on the tensile strength and modulus as well as fracture strain. All the conditioned samples show significantly lower performance compared to the DAM samples. The 16% V_f SGF/PA6 composites showed tensile strength reduced significantly from 157.93 to 110.46 and 76.07 MPa for specimen under DAM, 50% RH and wet condition respectively at strain rate of 0.33 x 10^{-3} s^{-1} subjected to short travel extensometer. The same trend was also observed in tensile modulus where a slight decrement is also observed from 9.30 GPa, 7.08 GPa and 4.18 GPa as moisture is introduce. These results suggest that the tensile strength and tensile modulus is heavily influence by introduction of moisture where it lowers the strength of SGF/PA6 composites dramatically. The lowest value of tensile strength and tensile modulus was achieved by the SGF/PA6 subjected to wet condition. This is because, as the moisture increase, the moisture attack on the interface becomes more significant, resulting in reduction in stress transfer and overall reduction in tensile properties. In spite of reducing the tensile strength and tensile modulus, the absorbed moisture has also significantly changed the mode of fracture of the composite from being brittle, to a ductile fracture with relatively higher fracture strain [52]. Whereas, the fracture strain increase significantly from 3.24%, 3.84% and 5.45% for specimen under DAM, 50% RH and wet condition respectively.

Generally, conditioning these composites in boiling water for 24 hours leads to a dramatic drop in both tensile modulus and tensile strength. At the same time, the increase in fracture strain upon exposure to a wet environment most likely due to the high level of matrix plasticization cause by moisture absorption [35]. As the plasticizer concentration increases, the yield stress decreases and the type of failure changes from brittle fracture to necking rupture. The tensile strain for all water-immersed specimens was found to increase compared to DAM and 50% RH specimens. Moisture makes the interfacial stress transfer less efficient when moisture is adsorbed at the interface. With less efficient interfacial stress transfer, a larger part of the load is carried by the matrix. After moisture absorption, the energy has been increased further owing to plasticization and the level of radial interfacial stress in the SGF/PA6 composites would be significantly reduced by the swelling due to moisture absorption [23,113].

The decrease in tensile properties after water immersion can be related to the weak fibre matrix interface due to water absorption as observed by Stamboulis *et al.* [114] in their study on flax fibres. Flexural strain for water immersed samples has increases dramatically compared to dry samples. It has been reported that the water molecule act as a plasticizer agent in the composites materials, which normally leads to an increase of the maximum strain for the composites after water absorption. This is in line with the study done by Bader and Collins [17], who claim that, the glass fibre reinforced PA6 which expose to moisture suffer a much more drastic reduction in stiffness and strength compared to composites at DAM. Thus, coupling agent is required in order to minimize further reduction in mechanical properties.

Scanning electron micrograph (Figures 4.48 and 4.49) shows the fractured surface of injection moulded SGF/PA6 composites at DAM and wet condition. It reveals total loss of adhesion at the fibre/polymer interface and massive matrix failure. Water acts as plasticizer decreasing the T_g value and increasing the flexibility of the matrix. In this study, specimens that have been conditioned to boiling water showed matrix material with a much more ductile behaviour, compared with specimens investigated in their DAM state.

It is well known that, glass fibre act as inert in the water absorption process of PA6 matrix. However, fibre matrix interface has a capability to absorb water resulting in permanent loss of properties of the interface. Figure 4.49 shows the ductile area, where the conical crack in the matrix, initiating from the fibre crack has developed. This figure proved that matrix cause dominated failure with the reduction in glass transition temperature coupled with the lowering of the stress transfer capability of the interface [156]. Obviously from this figure, the absorbed water has a great influence on both matrix ductility and bonding. The quality of the bonding also influences the ductility of the matrix, as a strong bond puts a high constraint on the matrix.

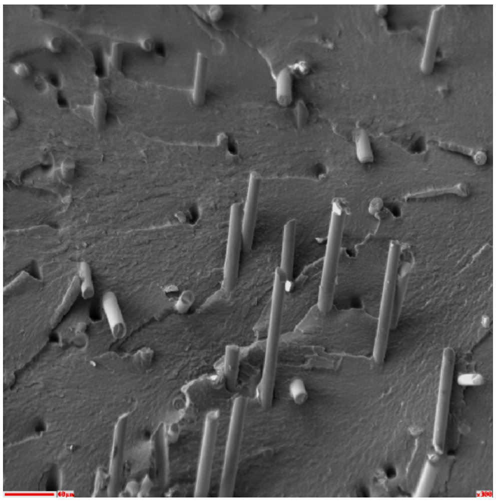

Figure 4.48: Tensile specimen fracture surface of injection moulded 2% V_f SGF/PA6 composites at strain rate of 6.67×10^{-3} s^{-1} (20 mm/min) subjected to DAM.

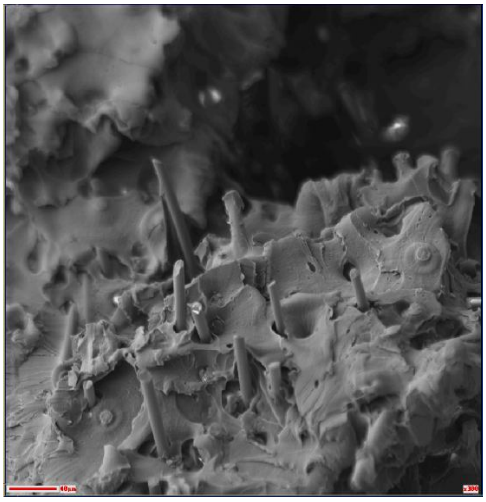

Figure 4.49: Tensile specimen fracture surface of injection moulded 2% V_f SGF/PA6 composites at strain rate of 6.67×10^{-3} s^{-1} (20 mm/min) subjected to wet condition.

4.5.4 The Effect of Strain Rate

The aim of this study is, to study the effect of strain rate on the tensile behaviour of neat PA6 and SGF/PA6 composites. Dependence of the tensile strength and tensile modulus on strain rate is shown in Figures 4.39-4.44. Strain was measured by means of an extensometer that was designed for the purpose of dynamic testing. It is worthy to note that strain rates have been estimated exclusively on the basis of strain gauge responses. The nominal strain rate is the ratio of the crosshead speed to the initial gauge length of the sample [117]. According to the definition of nominal strain rate above, it can be calculated that the corresponding nominal strain rates were 0.33 x 10^{-3} s^{-1}, 1.67 x 10^{-3} s^{-1}, 3.3 x 10^{-3} s^{-1} and 6.67 x 10^{-3} s^{-1} corresponding to crosshead speed of 1, 5, 10 and 20 mm/min respectively.

It is shown that, the tensile strength and tensile modulus tend to slightly increase with the increment of the strain rate for all V_f as a result of the combination of high strength of glass fibre and PA6 matrix. It was found that tensile strength increases with strain rate from 157.93 MPa, 168.23 MPa, 170.64 MPa and 173.83 MPa for specimen 16% V_f at DAM subjected to short travel extensometer. The same behaviour was also observed in specimen subjected to 50% RH and wet condition where the increment in 110.46 MPa, 113.17 MPa, 120.40 MPa and 121.86 MPa was observed for specimen under 50% RH whereas specimen in wet condition showed an increment in 76.07 MPa, 77.48 MPa, 77.80 MPa, and 78.17 MPa. This proved that a SGF/PA6 composite is a strain rate dependent material. The stiffening behaviour becomes more significant as the strain rate increases. Indeed, in terms of tensile strength and modulus, the ultimate properties increase significantly at high strain rate. This experimental finding is consistent with those obtained in other works [32, 55, 118]. These authors have pointed out that the tensile strength increases greatly with strain rate. At higher strain rates, the strength increases while simultaneously a reduction of the fracture strain was observed

[94]. However, there is slightly difference in the case of neat PA6 subjected to DAM where it shows the instability in tensile strength as strain rate increase.

Results showed that the higher the strain rate the higher the tensile strength, hardness, yield strength and elastic modulus. It is believed that the strain rate play a role towards the mechanical properties of SGF/PA6 composites. Higher strain rates also lead to higher yield strength. The highest ultimate tensile strength was recorded when the strain rate at 6.67 x 10^{-3} s^{-1} which gave the strength at the value of 173.83 MPa while at the lowest strain rate 0.33 x 10^{-3} s^{-1} the tensile strength was recorded at 157.93 MPa for specimen 16% V_f at DAM subjected to short travel extensometer. The different tensile strength between the higher and lower strain rates is 15.90 MPa. The ultimate strength for the SGF/PA6 composites was proportionally increased with the increment of the strain rates. Abdullah *et al.* [119] reported the different strains rates influence the ultimate tensile strength, Young's modulus and deformation behaviours. With variety of strain rates, many different deformation behaviours will be observed which include sliding, multi-sliding, phase transformative, twisting, necking and brittle deformation before breaking.

Tensile modulus also showed a general increase with strain rate in both modes in tension as well as in compression as reported by Hansen *et al.* [120]. Nevertheless, Yamakawa *et al.* [121] observed a reduction in the polyamide's toughness with increasing strain rate, particularly when the specimens were tested at higher strain rate under dynamic loading conditions (tensile-impact testing, at 3.7 m/s). This effect was caused by the polymer's viscoelastic properties and was more obvious in the thicker sheet.

The tensile modulus values were increased when the strain rates increased from the lower to higher strain rates. The Young's Modulus of 9.80 GPa of 16% V_f with 6.67 x $10^{-3}s^{-1}$ strain rates was recorded higher than the other strain rate values. This finding revealed the SGF/PA6 composites showed superior tensile performance especially at higher strain rates. The same trend was also reported by Ju [123] who studied the strain rate effect on tensile behaviour of the helical multi-shell gold nanowires.

Dependence of the fracture strain on strain rate is shown in Figures 4.45-4.47. It was found that the elongation at break was also affected by the strain rates. The finding revealed that, the fracture strain showed a slight decreased with an increase of strain rate for all condition investigated. This phenomenon is more obvious when composites were subjected to wet condition. It was found that the fracture strain decreased consistently compared to 50% RH and DAM specimens. As the strain rate increases there appears to be a stiffening mechanism that takes place resulting in lower fracture strain. Nonetheless, this observation is in disagreement with the study reported by Zhou and Mallick [53] in SGF/PA6 composites who reported that the failure strain is not affected by the strain rate in the range considered. They claim that for high values of strain rate, molecular rearrangement does not have time to take place.

However, from the study reported by Abdullah *et al.* [119], their finding revealed that the elongation increased with the increment of strain rates. The percents of elongation at break for the 0.17 x 10^{-3} s^{-1} of strain rates were recorded higher, which is more than 30%. Higher plastic deformation occurred at 100 min^{-1} and before the necking pattern was developed which lead to the wire fracture. Wu *et al.* [124], in his study reported the ductility of superaustenitic stainless steel increases significantly with an increase in the strain rate, due to these materials tend to rupture naturally as the strain-hardening increases. Shohji *et al.* [125] in his study also observed an increment in the tensile strength with increasing strain rate for Sn–Ag based lead-free solder. However, the elongations decrease markedly with increasing strain rate over 10^{-3} s^{-1}.

SEM fractographs of injection moulded SGF/PA6 composites tensile specimens tested at low strain rates 0.33 x 10^{-3} s^{-1} and high strain rates 6.67 x 10^{-3} s^{-1} at room temperature are shown in Figures 4.50 and 4.51 respectively. As expected, a slightly more homogeneous pull out hole is observed in the sample failed at highest strain rate. At high strain rate, the testing time is short for the fibres to be pulled out of the matrix. Thus, when a crack initiates at the matrix or interface, it has to propagate across the matrix and the interfaces. This suggests that the material cannot elongate much resulting in high stress to fracture. In addition, the accumulation of micro-cracks leads to a prompt damage localisation requiring hence high energy dissipation [118, 157, 158]. On the other hand, at lower strain rate the testing time is longer, the cracks have enough time to penetrate into the weakest sites and propagate in the matrix or the interfaces. This suggests that the cracks do not propagate in a straight line and can select their propagation orientation and path. In other words, the material can elongate more and need minimum stress to fracture.

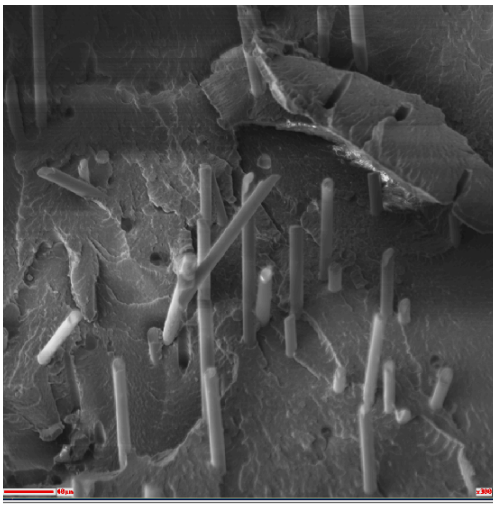

Figure 4.50: Tensile specimen fracture surface of injection moulded 2% V_f SGF/PA6 composites at strain rate of 0.33×10^{-3} s^{-1} (1 mm/min).

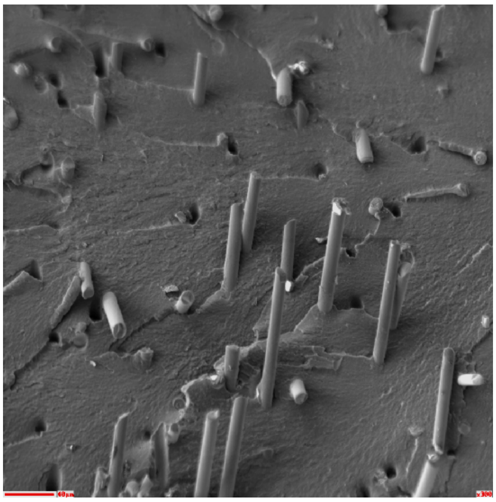

Figure 4.51: Tensile specimen fracture surface of injection moulded 2% V_f SGF/PA6 composites at strain rate of 6.67×10^{-3} s^{-1} (20 mm/min).

4.5.5 The Effect of Types of Extensometer

In this study, two types of extensometers with the requisite sensitivity were used to measure the longitudinal and the width strains on a dumb-bell shaped specimen. They are long travel extensometer and short travel extensometer. The long travel extensometer measures specimen elongation up to 500% strain from its original length of 50 mm and it is suitable to measure ductile sample. On the other hand, short travel extensometer is more suitable for brittle composites. It can only be extended up to 20% strain from its original length at 50 mm.

For all testing conditions investigated, i.e fibre volume fraction, moisture and strain rate, all samples shows that long travel extensometer give higher extension compared to short travel extensometer. This is a due to high inertia of moving parts when the sample is pull from their initial length. Therefore, surface of the specimen can be slippery.

It can be seen from Figures 4.45-4.47, the measured tensile strain value of short travel extensometer is much lower than the long travel extensometer. This suggests the accuracy and sensitivity of short travel extensometer in determining the tensile strain and modulus of SGF/PA6 composite which is well known for it brittleness. Meanwhile, this difference is due to the inertial effects of the gripping system. Higher inertia effect is produce by long travel extensometer and the extensometer may have slipped on the specimen during the test.

The load transfer from the matrix to reinforcement is both qualitatively and quantitatively different for short and long travel extensometers. In long travel extensomer, the load transfer is less effective due to slippage and high inertia resulting in higher fracture strain. The same improvement was also observed in tensile modulus. The same failure mechanism was also observed in particulate-reinforced metal-matrix composite, where when matrix creeps, load transfer is less effective than when the matrix deforms by slip; also, load transfer at elevated temperatures decreases with increasing applied stress [73, 126]. Therefore, it can be conclude that without extensometer, however, one must find alternatives with which the elongation, strain, and modulus can be calculated.

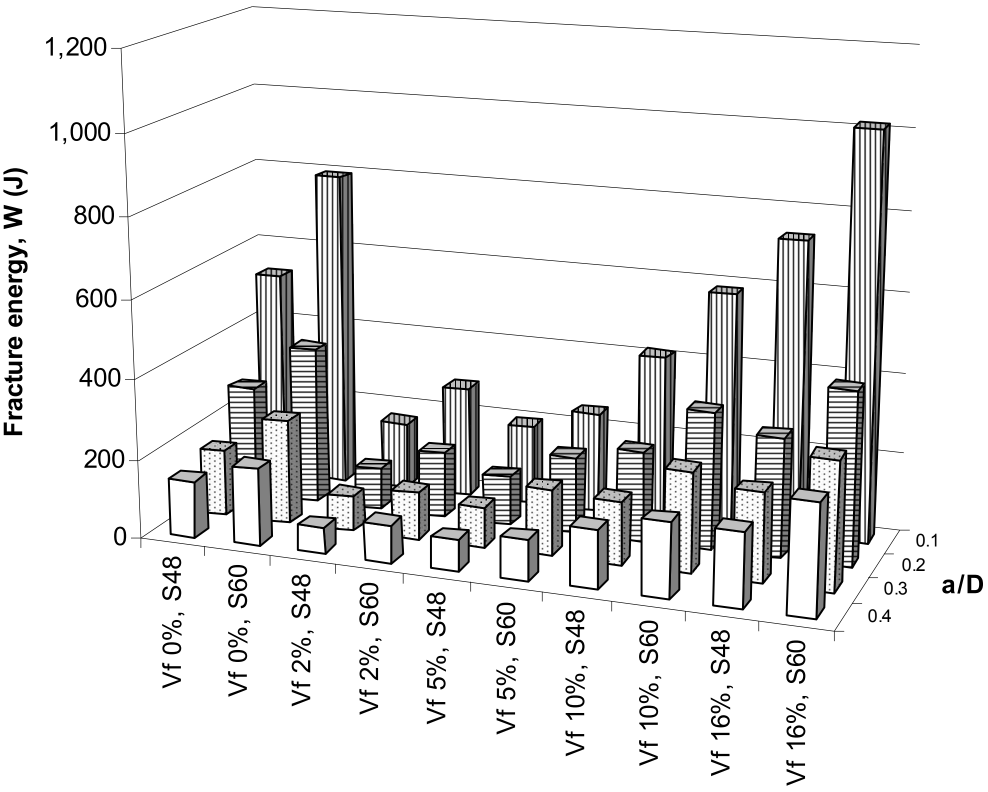

Figure 4.52: Fracture energy, W values of injection moulded SGF/PA6 composites subjected to different support span.

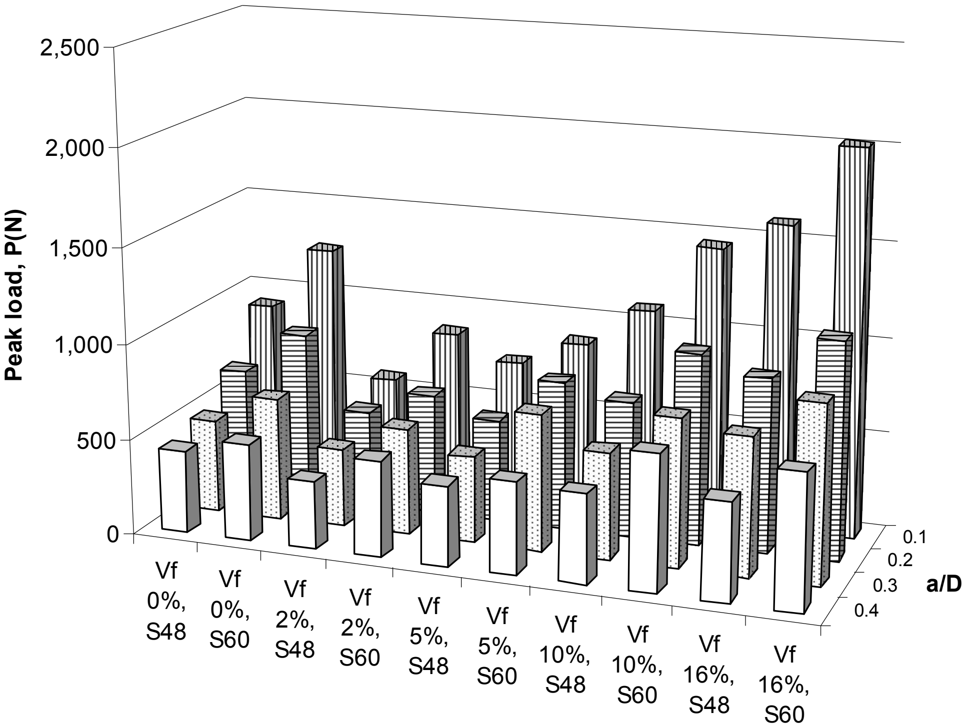

Figure 4.53: Peak load values of injection moulded SGF/PA6 composites subjected to different support span.

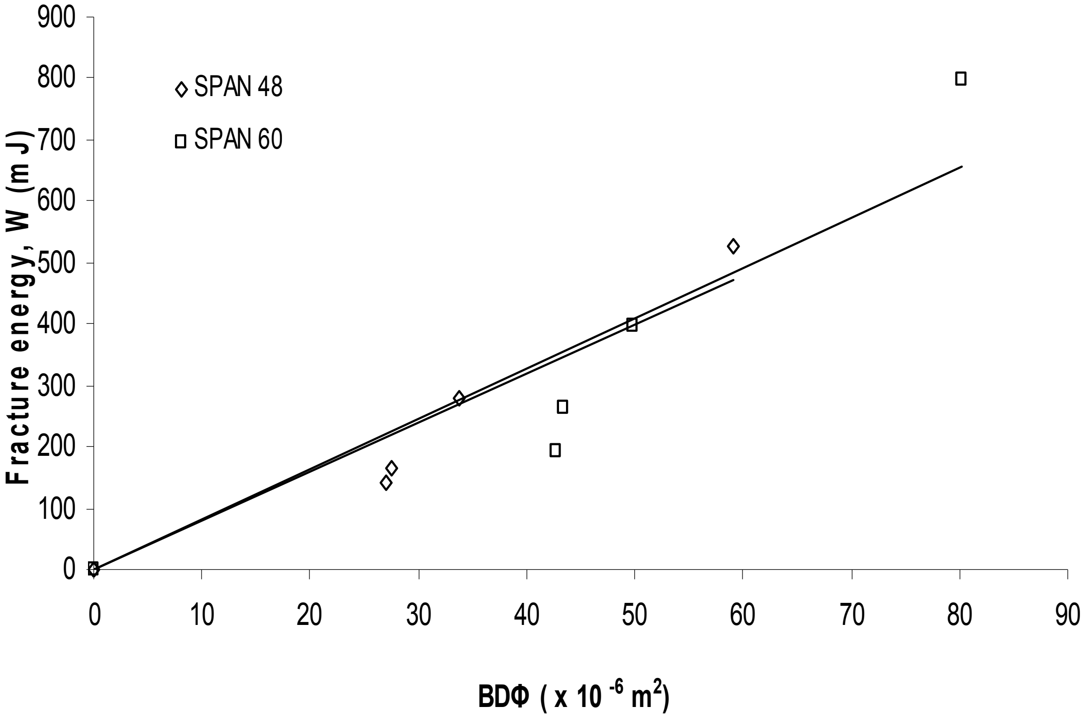

Figure 4.54: Fracture energy against BDΦ of neat PA6 subjected to different support span.

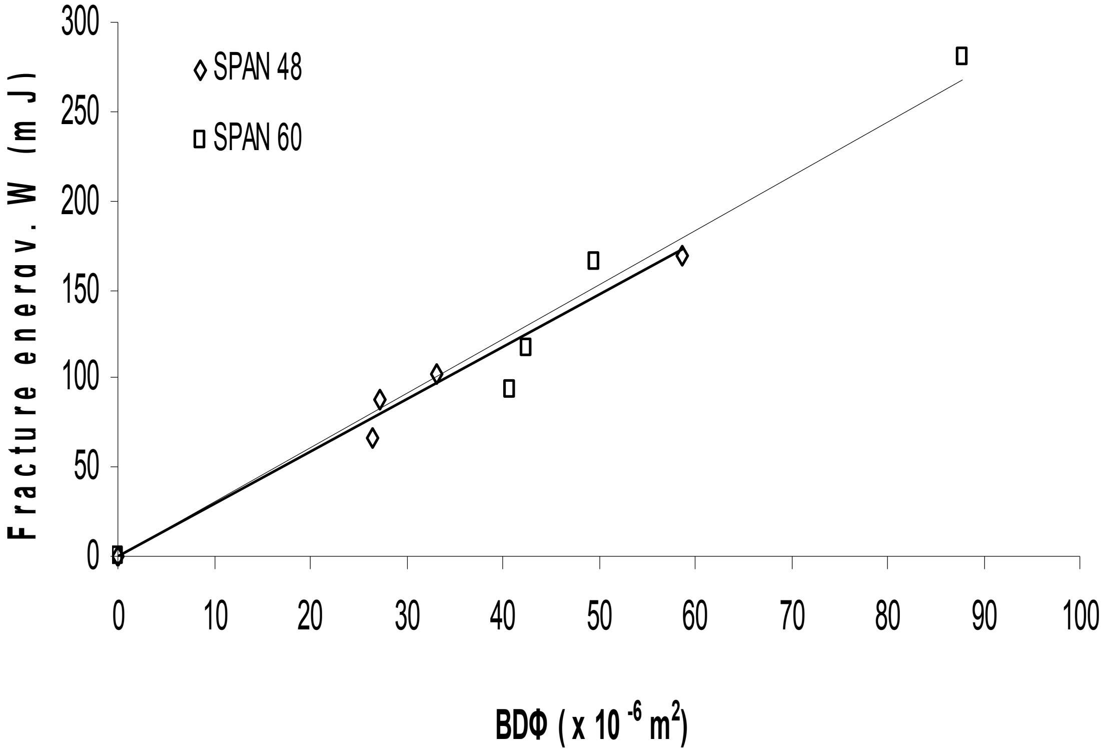

Figure 4.55: Fracture energy against BDΦ of injection moulded 2% V_f SGF/PA6 composites subjected to different support span.

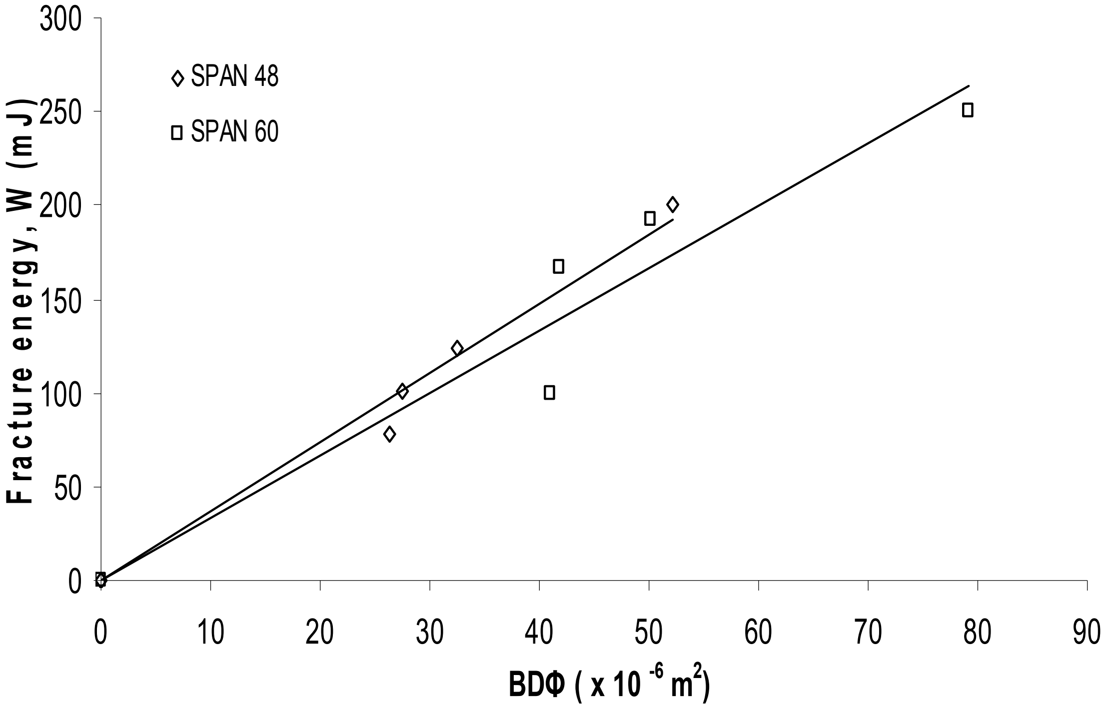

Figure 4.56: Fracture energy against BDΦ of injection moulded 5% V_f SGF/PA6 composites subjected to different support span.

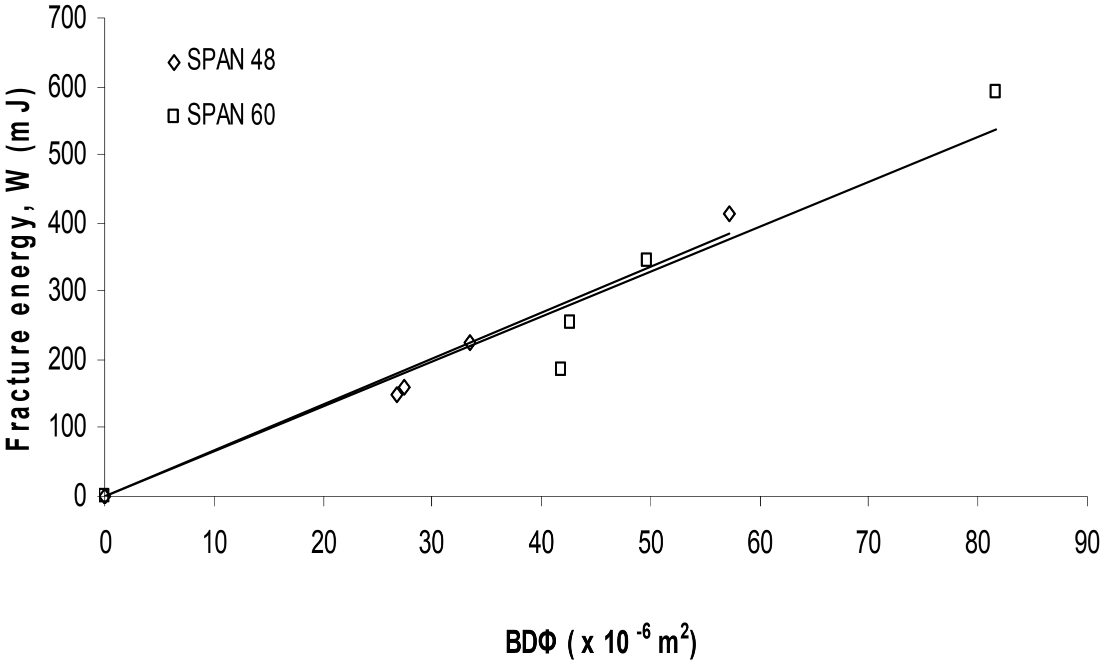

Figure 4.57: Fracture energy against BDΦ of injection moulded 10% V_f SGF/PA6 composites subjected to different support span.

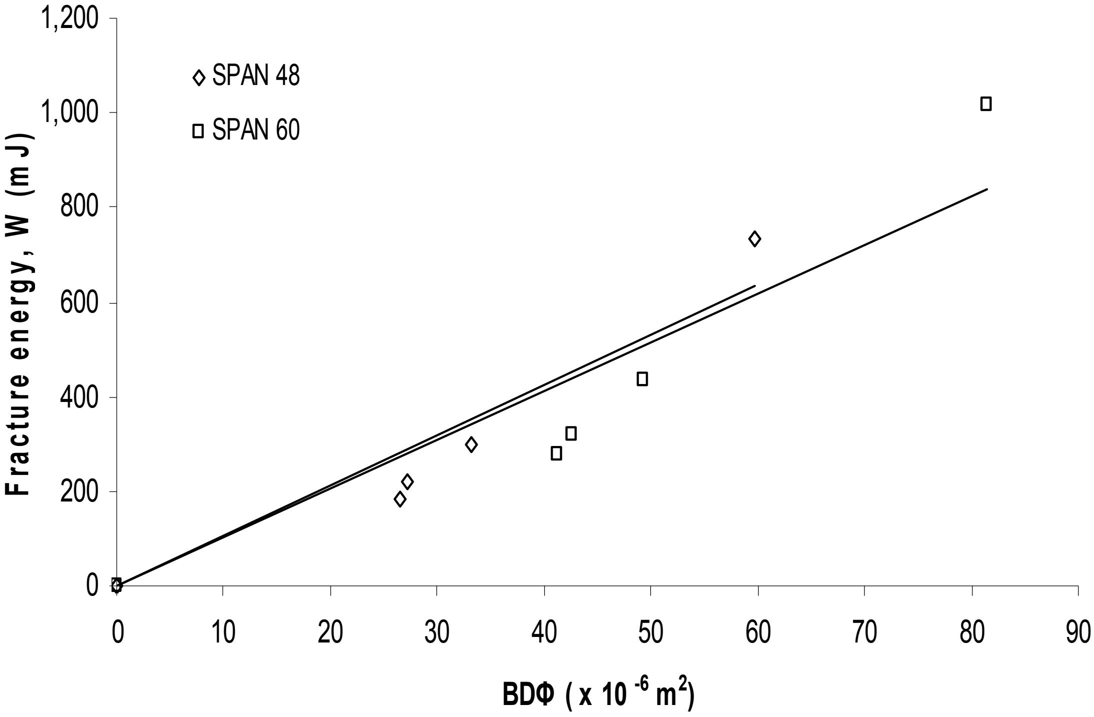

Figure 4.58: Fracture energy against BDΦ of injection moulded 16% V_f SGF/PA6 composites subjected to different support span.

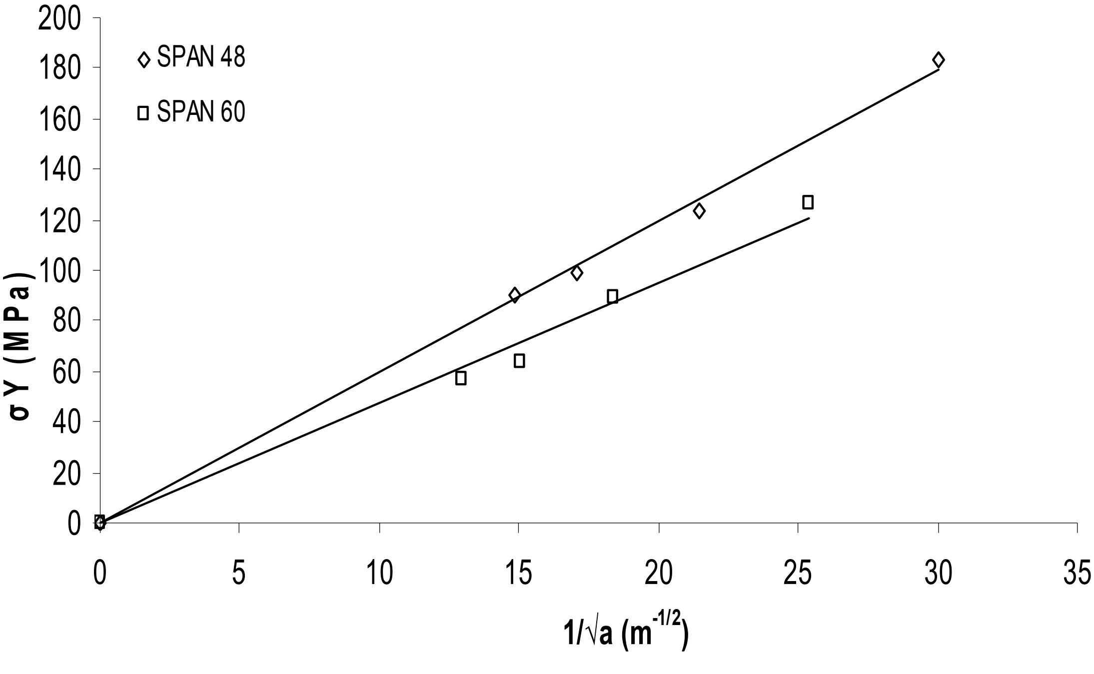

Figure 4.59: Variation of σY against 1/√a of neat PA6 subjected to different support span.

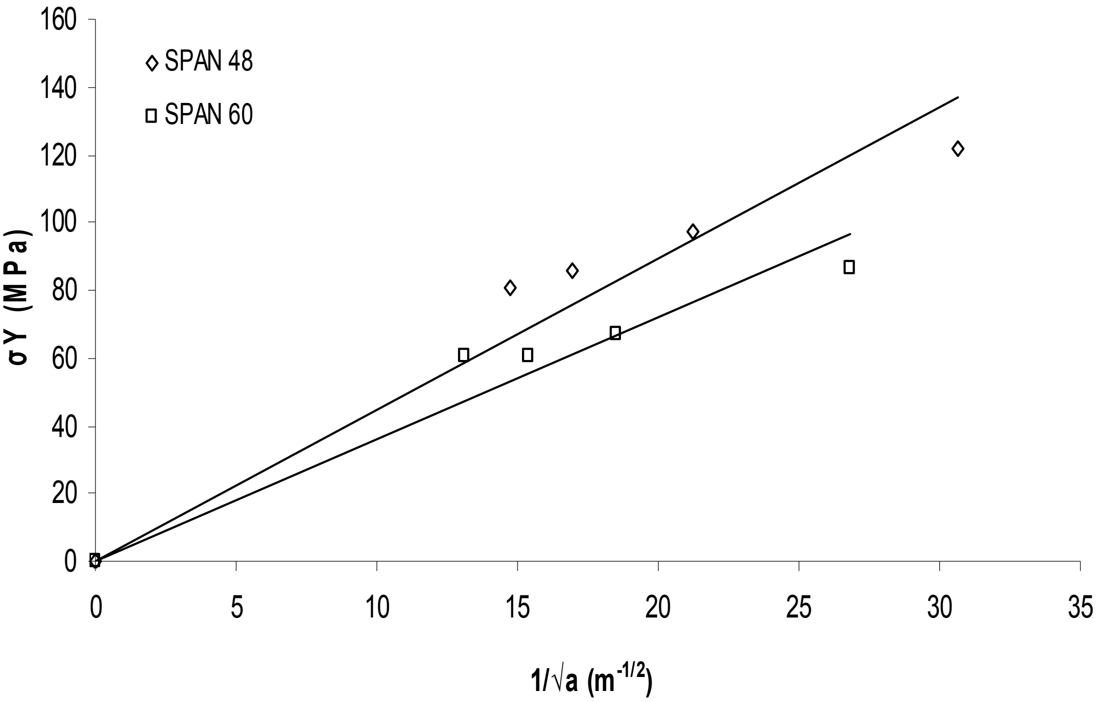

Figure 4.60: Variation of σY against 1/√a of injection moulded 2% V_f SGF/PA6 composites subjected to different support span.

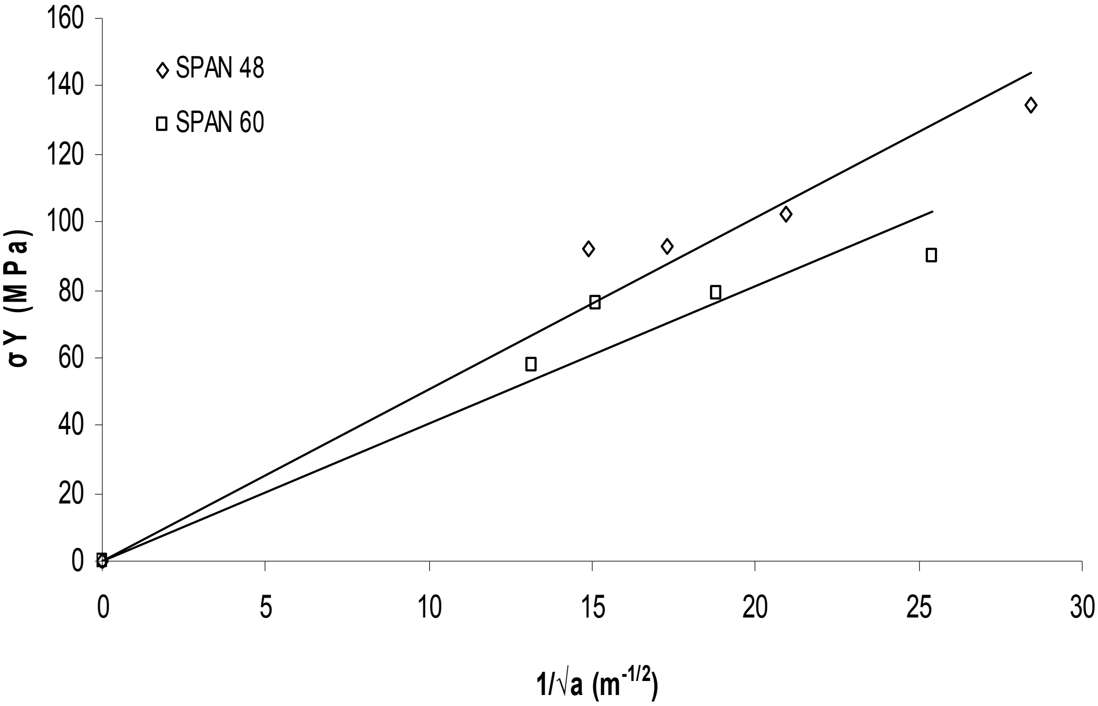

Figure 4.61: Variation of σY against 1/√a of injection moulded 5% V_f of SGF/PA6 composites subjected to different support span.

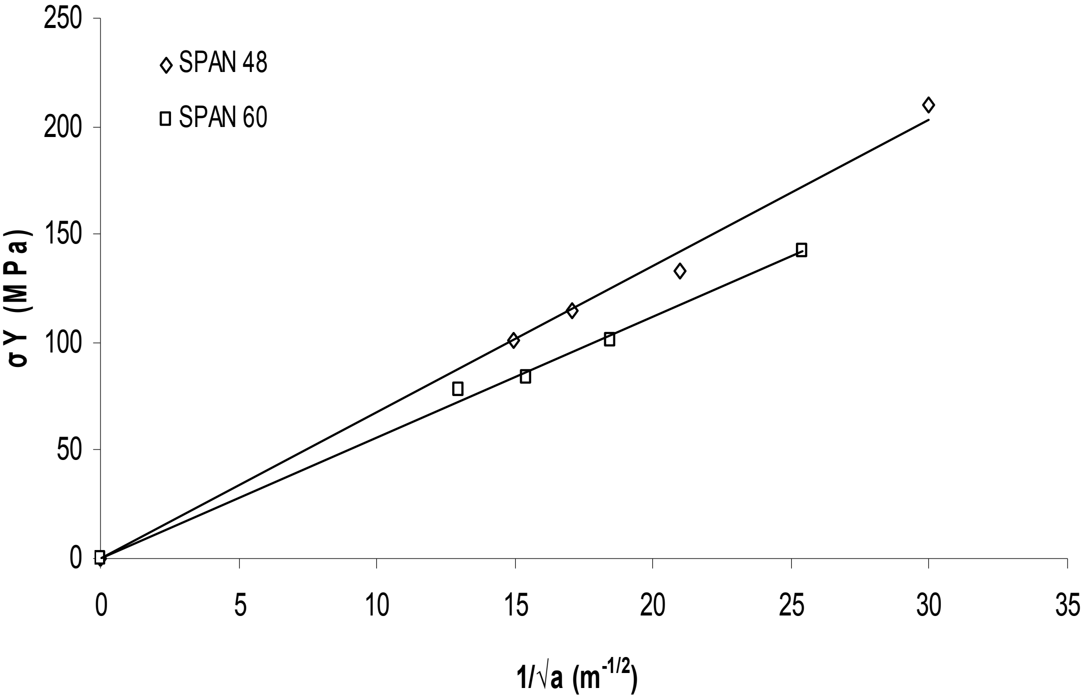

Figure 4.62: Variation of σY against 1/√a of injection moulded 10% V_f SGF/PA6 composites subjected to different support span.

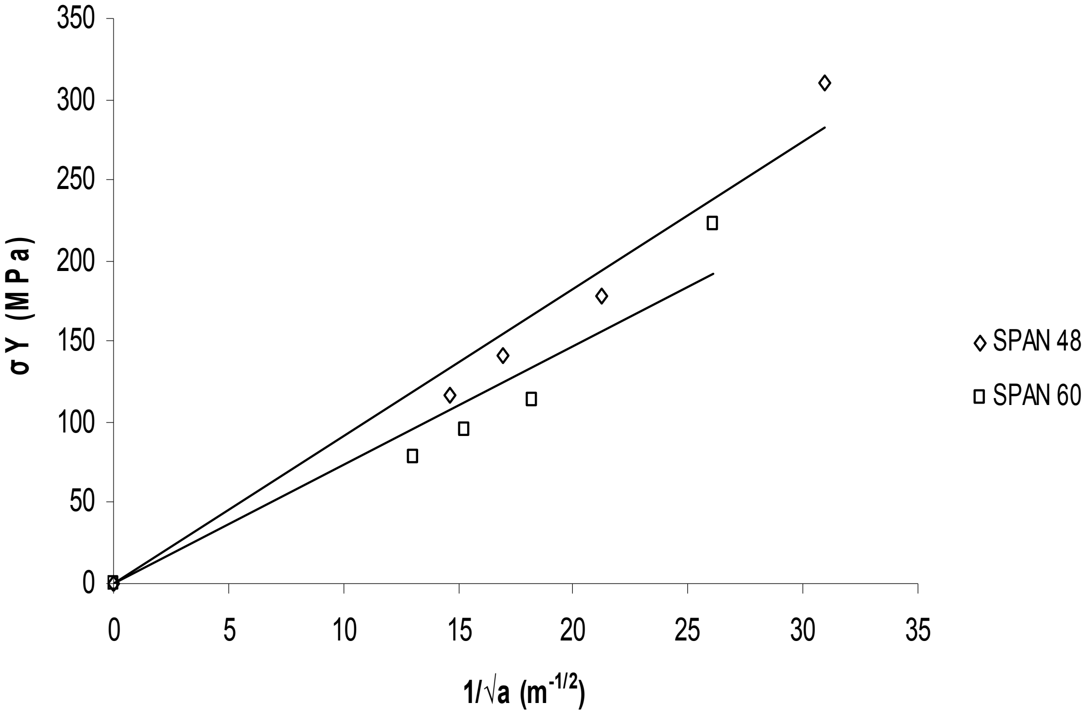

Figure 4.63: Variation of σY against 1/√a of injection moulded 16% V_f SGF/PA6 composites subjected to different support span.

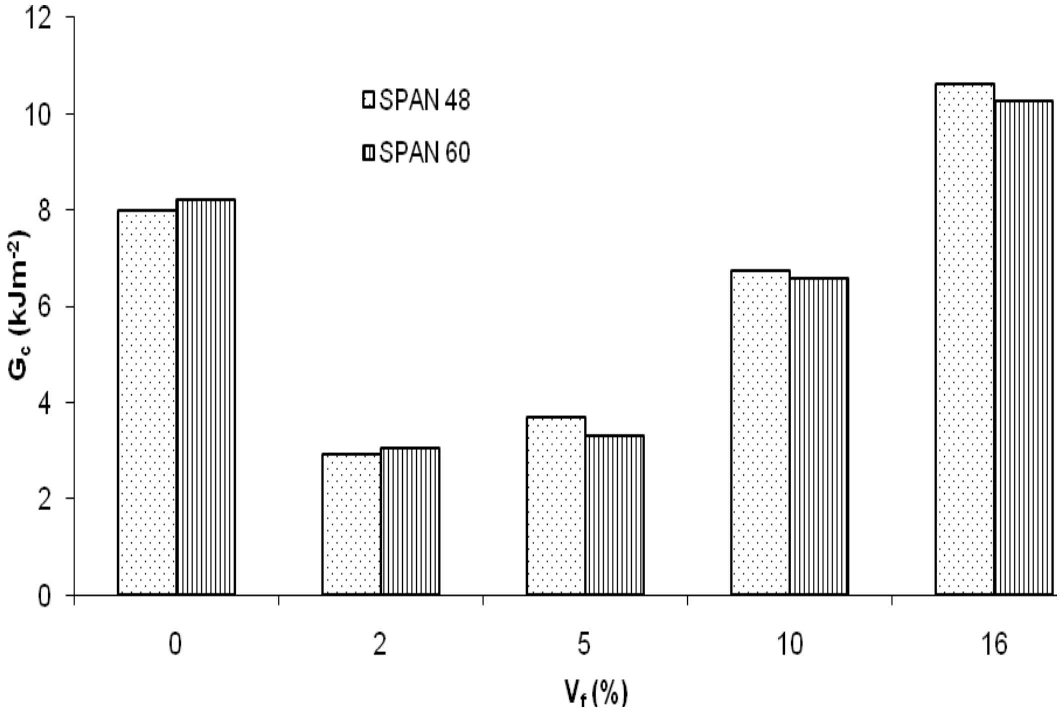

Figure 4.64: Critical strain energy release rate, G_c values of injection moulded SGF/PA6 composites subjected to different support span.

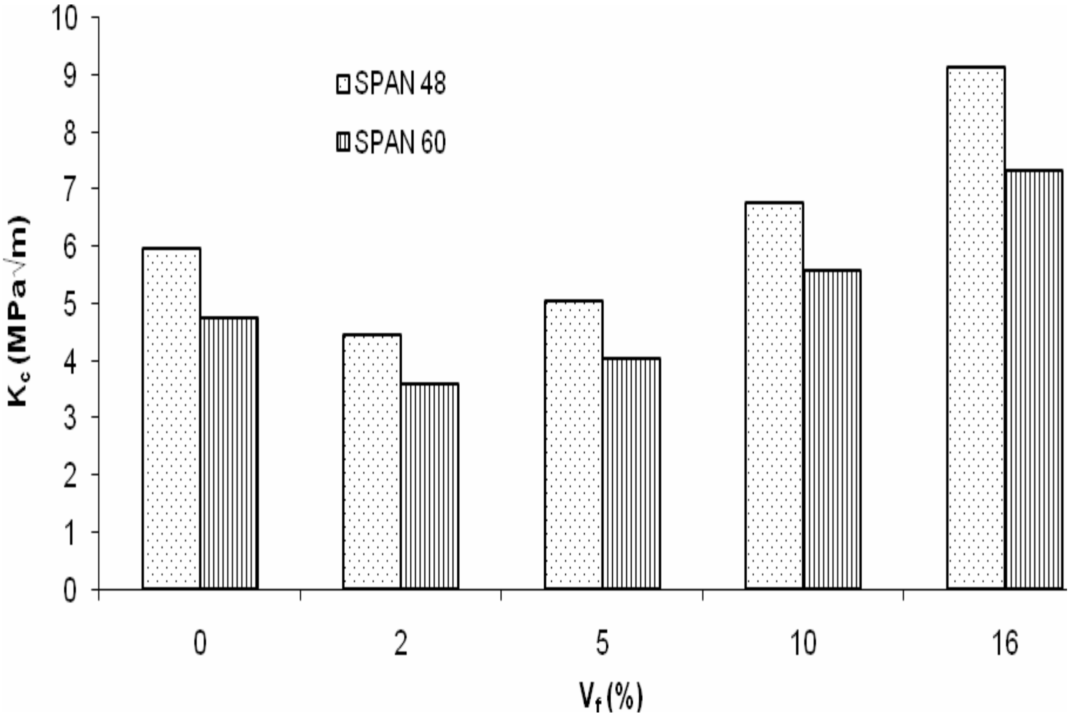

Figure 4.65: Critical stress intensity factor, K_c values of injection moulded SGF/PA6 composites subjected to different support span.

4.6 Impact Properties

In this study, the effects of impact properties were studied in four different aspects. There are the effect of support span, test velocity, test load and test temperature.

4.6.1 The Effect of Support Span

Specimen thickness can affect the toughness of thermoplastic polymers significantly in the presence of glass fibres. This thickness effect is related to the contribution of multiple cracking and fibre bridging which results in higher values being obtained on thicker specimens. In this study, a comparison between two composite geometries has been carried out, which are support span 48 mm and 60 mm with the ratio of span (S) to depth (D) was set and maintain at 4. It was found that fracture energy, W and peak load, P of SGF/PA6 composite for all V_f increased with specimen support span (Figures 4.52 and 4.53). This is correlation with specimen dimension where high stress is required to break thicker specimen. Leach and Moore [130] in their study reported that, the thicker the specimen, the higher the energy absorbed by the material leading to higher energy to fracture.

Figure 4.64 shows that support span of 60 mm show higher G_c value at low glass fibre content (0% and 2% V_f). This is due to the fact that high energy is required to break the specimen at low fibre loading as majority of stress is transferred through matrix. The ability of the specimen to absorb more impact energy increases with specimen support span as a result of the greater rebound energy or residual kinetic energy [131]. As the dimensions increase, its capacity to store elastic energy will also increase. Furthermore, Tai *et al.* [132] in their study reveals that, thicker laminate has a higher stiffness than the thinner one because thicker laminate has a greater moment of inertia, which results in less global bending during impact. They also added that, thicker laminate results in high penetration energy and peak load.

Change in specimen's span-to-depth ratio or composite thickness has slight influence on impact properties. Naven *et al.* [133] found that the thicker the composite, the smaller is the damage area at specific impact velocity due to the lesser displacement on the thicker composites. In the specimen under impact, the larger the width of the rectangular specimen, the higher will be the peak force. Nevertheless, the thickness of the composite is most dominant parameter in the specimens that governs the dynamic response and damage mode of the impact events of strain absorbing.

However, when subjected to high fibre loading (V_f of 5%, 10% and 16%) the trend is slightly reversed where support span of 48 mm showed high G_c values compared to specimens with support span 60 mm. The same behaviour was also observed in K_c value (Figure 4.65). This implies that, when glass fibres are employed, this thickness effect may be enhanced by the decrease in fibre orientation resulting from the thicker specimens. Laura *et al.* [32] found that as the specimen become thicker, the fibre orientation decreased leading to reduction of fracture energy in the thicker specimen. Additionally, as the thickness of specimen is reduced, more energy will be dissipated as a result of plastic deformation near the specimen surface [134]. Khalid [135] in his study observed a decrement in impact strength when increasing the specimens span to depth ratio above 6. This phenomenon was found for both of the steel and composite specimens tested at room temperature.

The impact properties of neat PA6 and SGF/PA6 composites as a function of fibre volume fraction are depicted in Figures 4.52, 4.53, 4.64 and 4.65 respectively. Generally, G_c, K_c, W and P are increasing with fibre content. It is evident that the impact strength of the SGF/PA6 composites increases progressively with the incorporation of glass fibre. This is due to contribution of high stiffness of glass fibre that results in high strength of composites. This indicate that glass fibre reinforcement increases for all the parameters investigated without significantly decreasing specimen deformation relative to neat PA6, which is brittle under impact condition used here. This leads to higher fracture energies for the fibre reinforced materials [136]. In addition, the presence of the fibres tended to reduce resistance to crack initiation, while reducing crack propagation through the matrix by forcing crack lines around the fibre ends [137].

However, G_c, and K_c, values of 2% and 5% V_f showed slightly lower compared to neat PA6. This suggests that at low fibre content, the fibre tends to give notching effect rather than reinforcing the composites. The highest value of neat PA6 in G_c, and K_c, is due to ductility behaviour of neat PA6. It is well known that PA6 matrix is relatively high strength, tough thermoplastic resin and it is notch sensitive material. Therefore this impact behaviour indicates that the resin has a great resistance to crack initiation and much less resistance to crack propagation [137].

For all the parameters discussed above, shows a reduction values with increasing in notch to depth (a/D) ratio due to reduction in fracture area. The used of single-edge-notched specimens with varying notch depth, have found that the deeper the notch, the greater the control of fracture, and lower the measured work of fracture.

Extensive research has been carried out concerning the impact behaviour of composite materials. Bader and Ellis [138] investigated the impact behaviour of carbon fibre epoxy composite materials using the Charpy impact test of V-notched specimens. They found that the notch had a negligible effect, while the span to depth ratio was an important parameter for the impact test of composite materials. On the other hand, experimental studies on low velocity impact developed by Liu *et al.* [139] showed that the thickness has a greater influence on impact perforation resistance than on the in-plane dimensions. In addition, Nakamura *et al.* [140] found that, both K_c and G_c values increased with particle thickness. This result suggests that, at the same particle content, the addition of thicker spherical silica particles increased the toughness of the cured epoxy resin.

The fracture toughness as measured by K_c or G_c is essentially a measure of the extent of plastic deformation associated with crack extension. The quantity of plastic flow would be expected to scale linearly with the specimen depth, since reducing the depth by half could naturally cut the volume of plastically deformed material approximately in half. The toughness therefore increases linearly with the specimen depth. Nevertheless, the toughness is observed to go through a maximum and fall thereafter to a lower value. This loss of toughness beyond a certain critical depth is extremely important in design against fracture, since using too thin a specimen in measuring toughness will yield an unrealistically optimistic value for G_c [141].

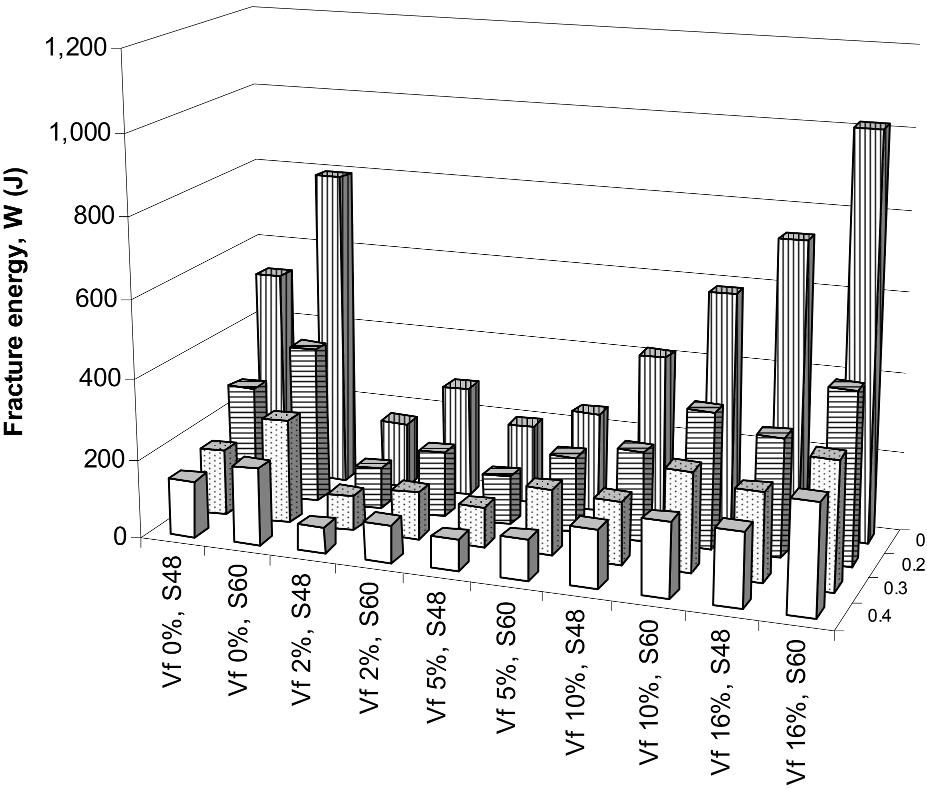

Figure 4.52: Fracture energy, W values of injection moulded SGF/PA6 composites subjected to different support span.

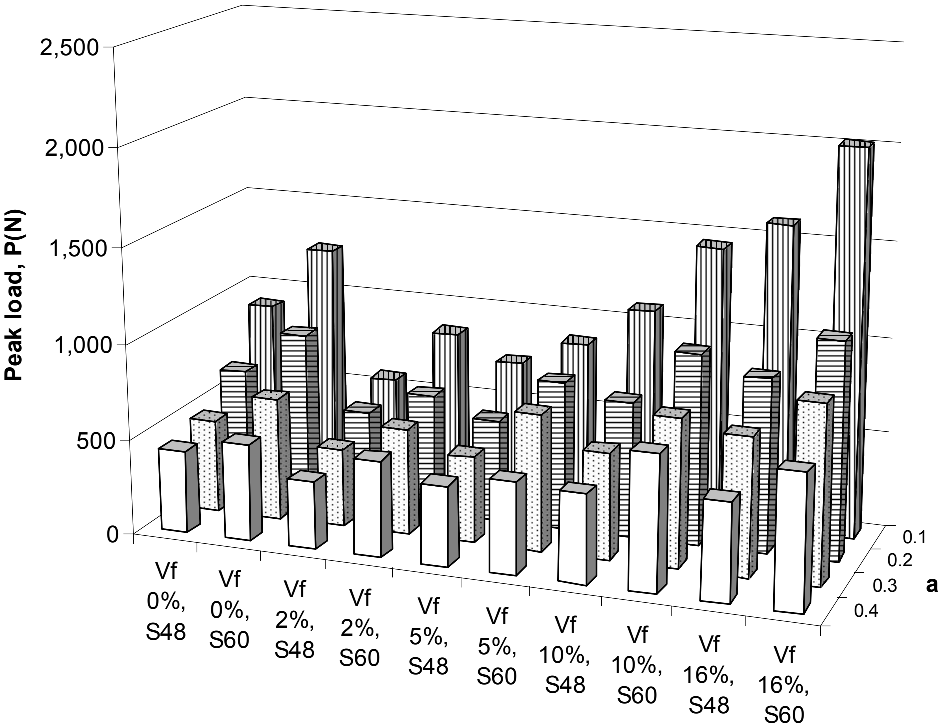

Figure 4.53: Peak load values of injection moulded SGF/PA6 composites subjected to different support span.

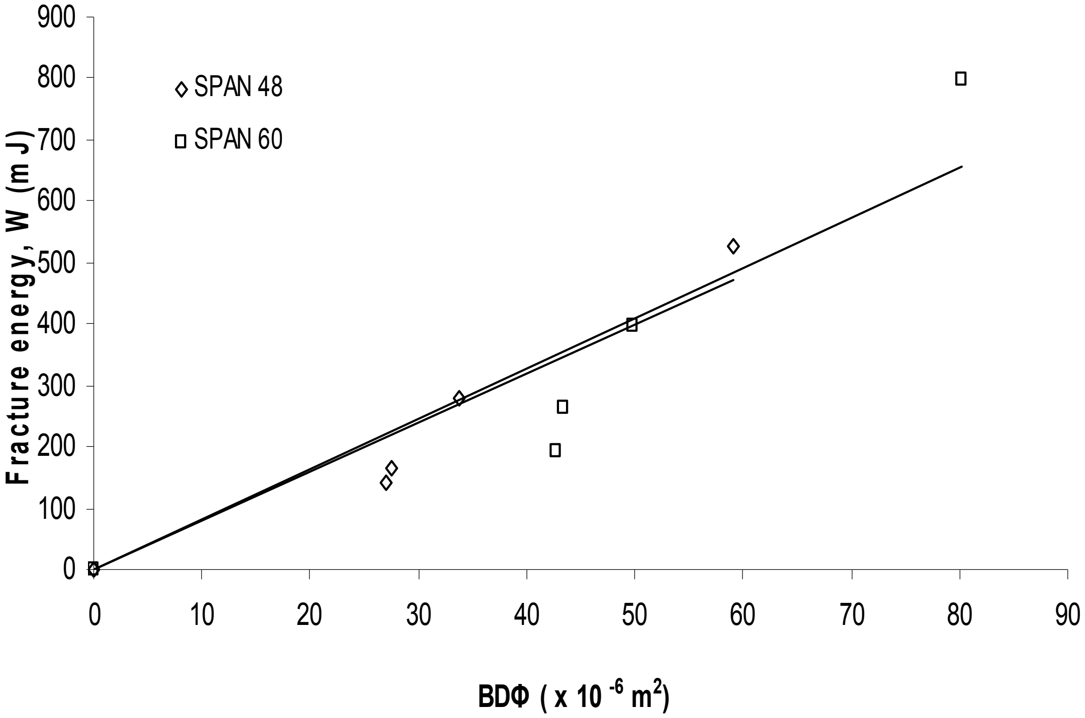

Figure 4.54: Fracture energy against BDΦ of neat PA6 subjected to different support span.

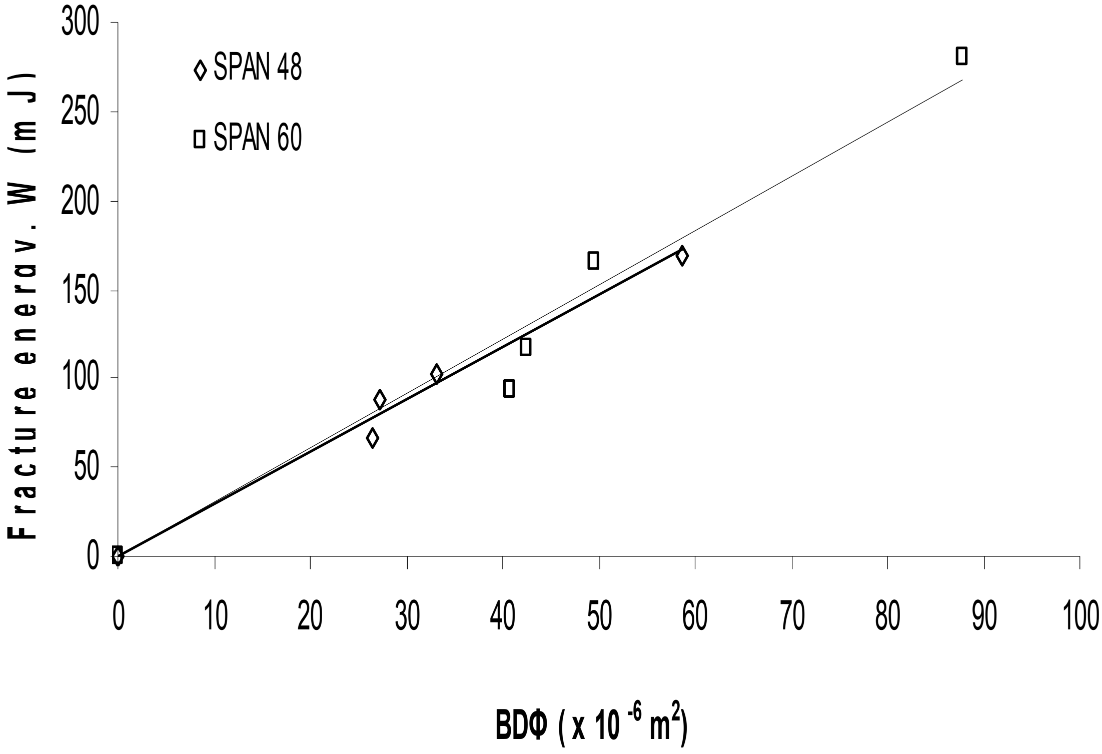

Figure 4.55: Fracture energy against BDΦ of injection moulded 2% V_f SGF/PA6 composites subjected to different support span.

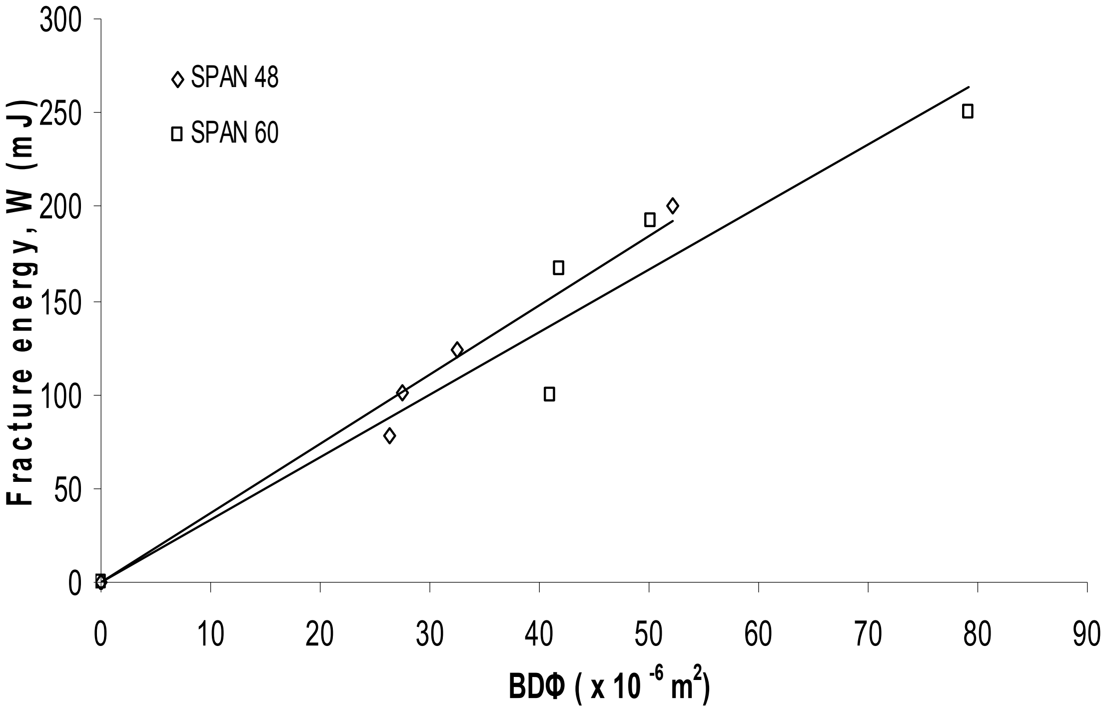

Figure 4.56: Fracture energy against BDΦ of injection moulded 5% V_f SGF/PA6 composites subjected to different support span.

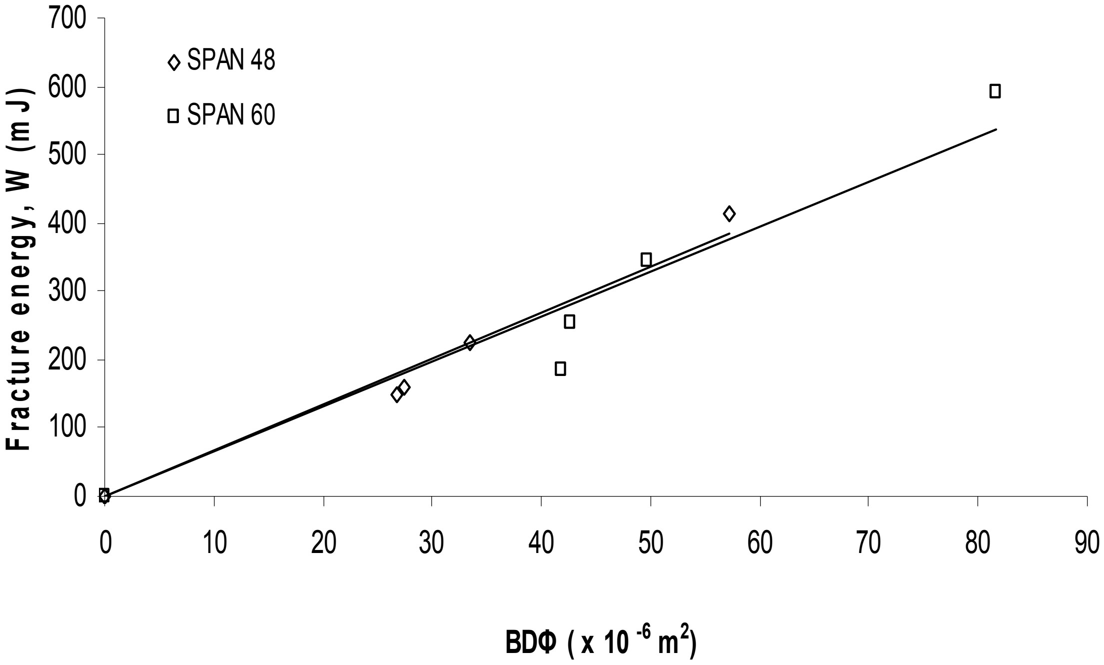

Figure 4.57: Fracture energy against BDΦ of injection moulded 10% V_f SGF/PA6 composites subjected to different support span.

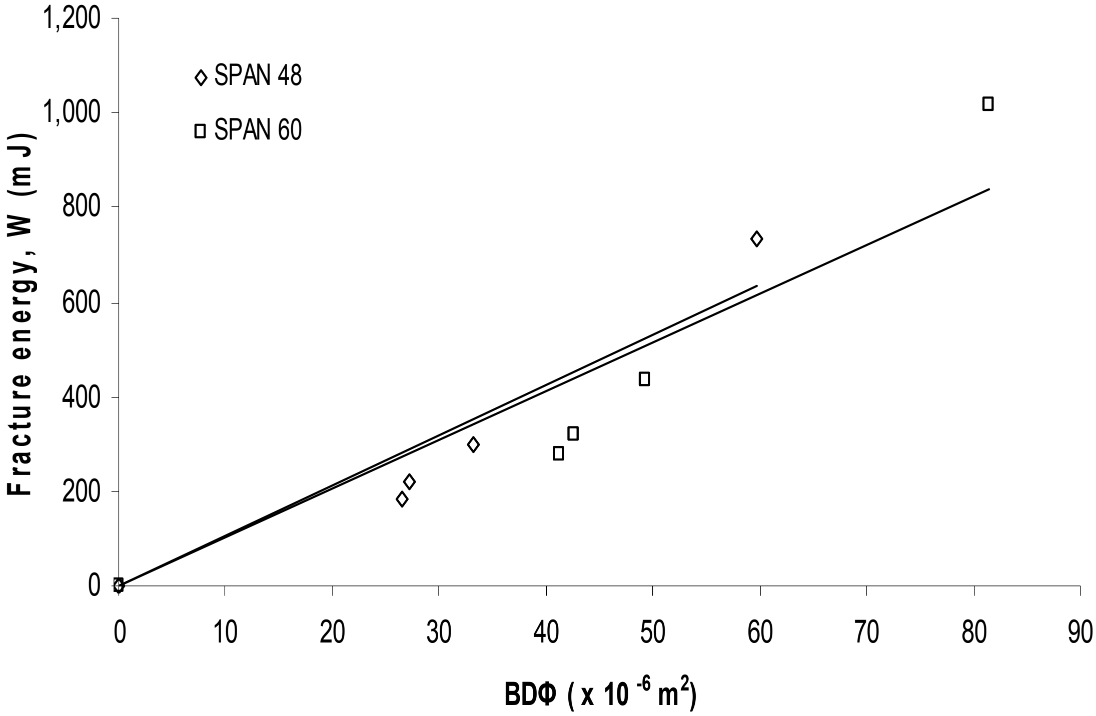

Figure 4.58: Fracture energy against BDΦ of injection moulded 16% V_f SGF/PA6 composites subjected to different support span.

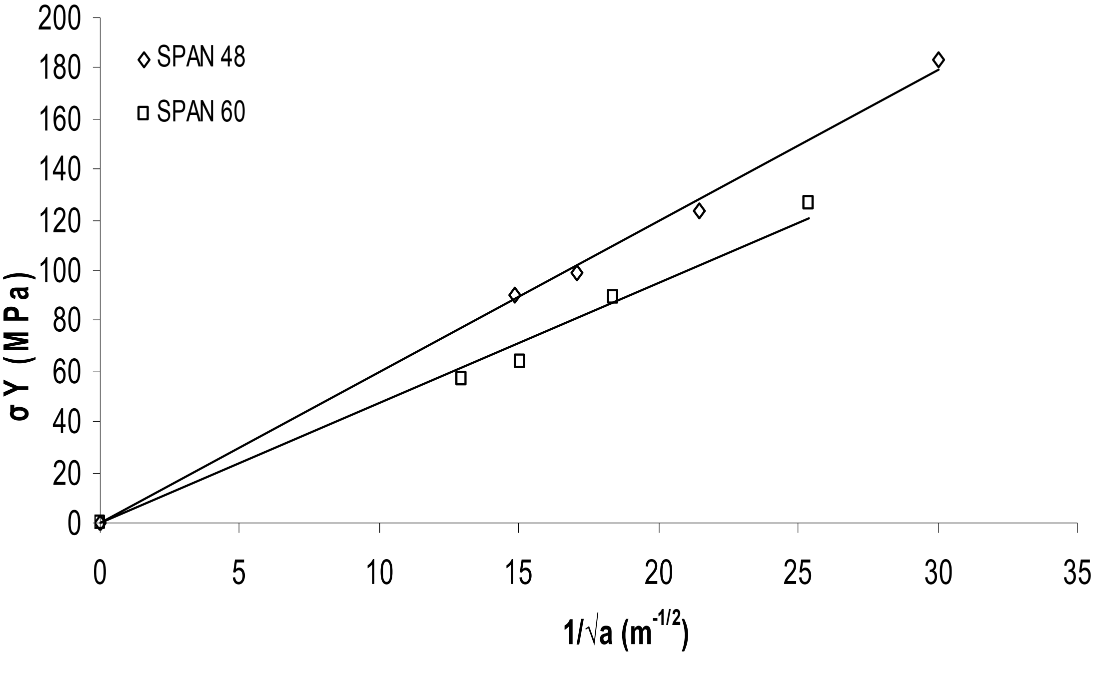

Figure 4.59: Variation of σY against 1/√a of neat PA6 subjected to different support span.

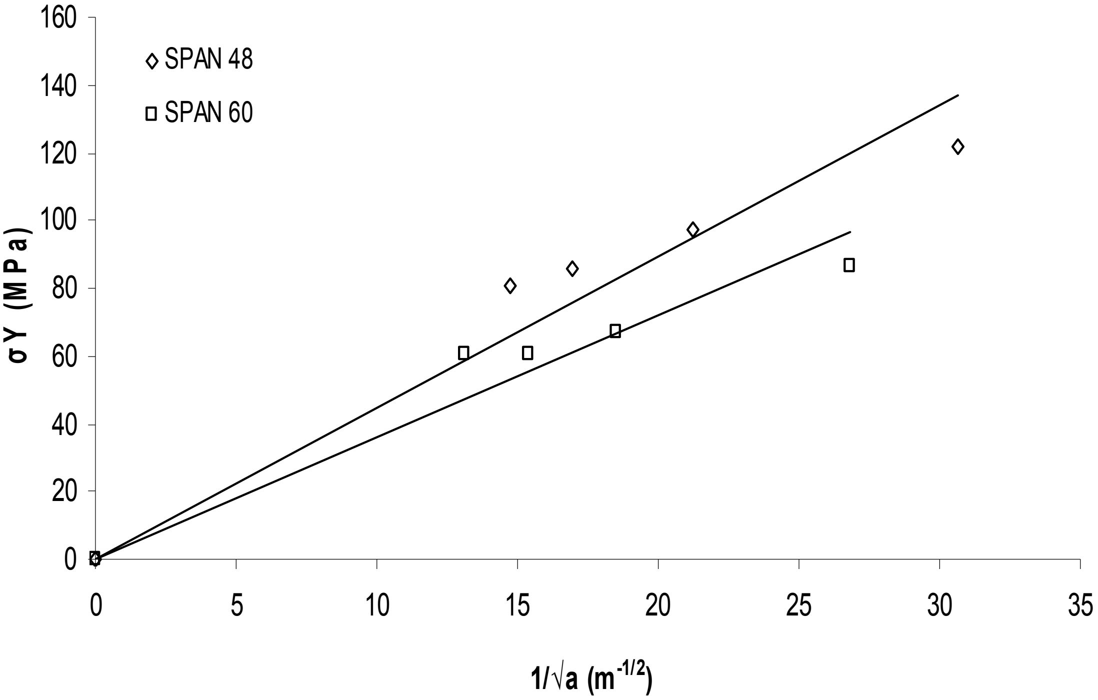

Figure 4.60: Variation of σY against 1/√a of injection moulded 2% V_f SGF/PA6 composites subjected to different support span.

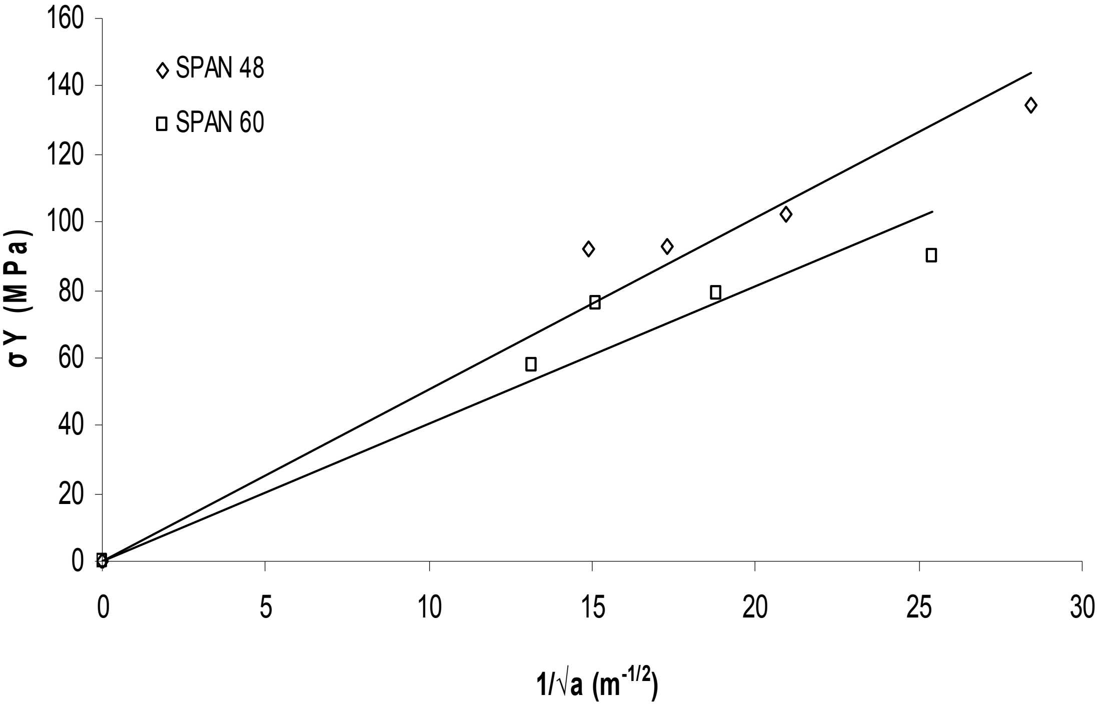

Figure 4.61: Variation of σY against 1/√a of injection moulded 5% V_f of SGF/PA6 composites subjected to different support span.

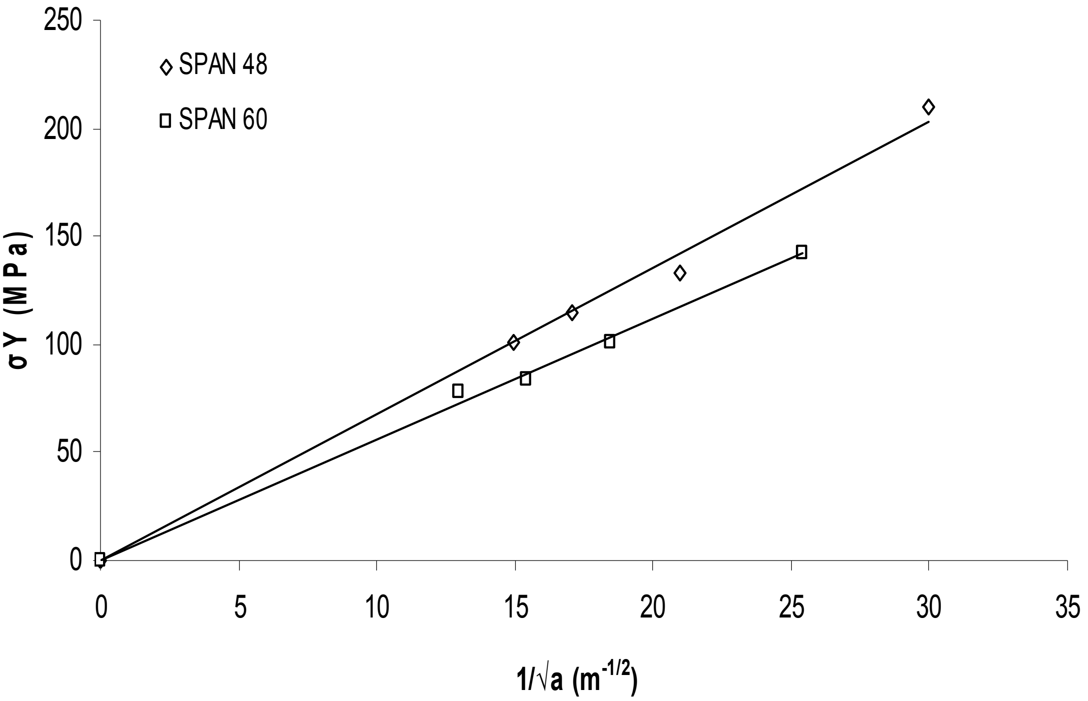

Figure 4.62: Variation of σY against 1/√a of injection moulded 10% V_f SGF/PA6 composites subjected to different support span.

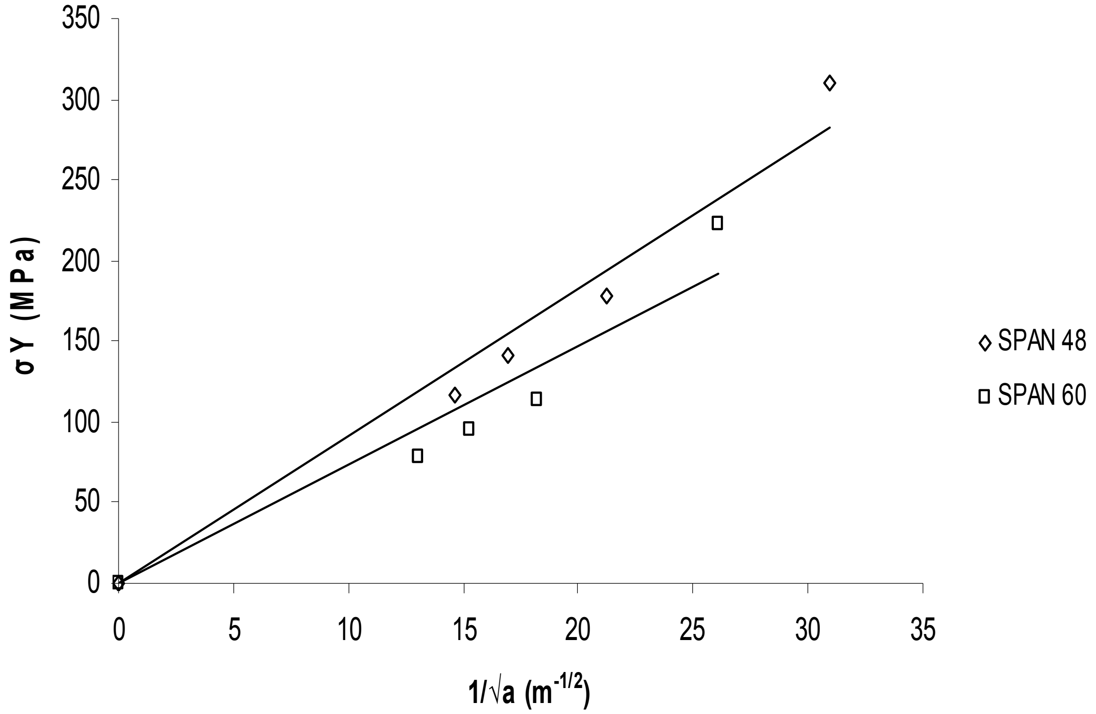

Figure 4.63: Variation of σY against 1/√a of injection moulded 16% V_f SGF/PA6 composites subjected to different support span.

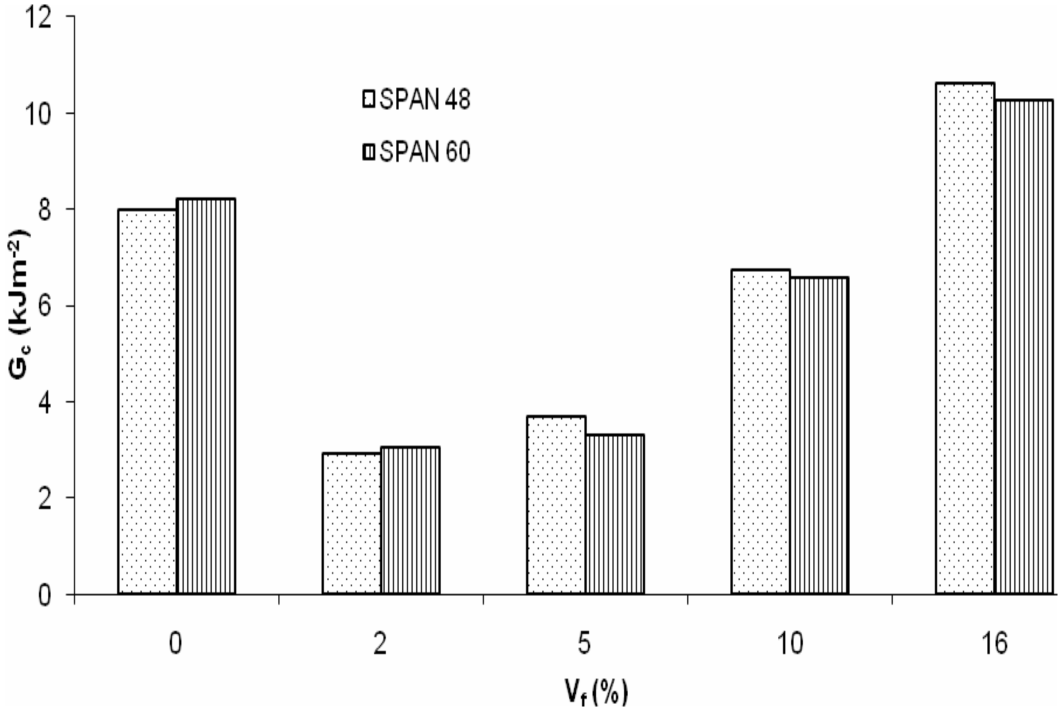

Figure 4.64: Critical strain energy release rate, G_c values of injection moulded SGF/PA6 composites subjected to different support span.

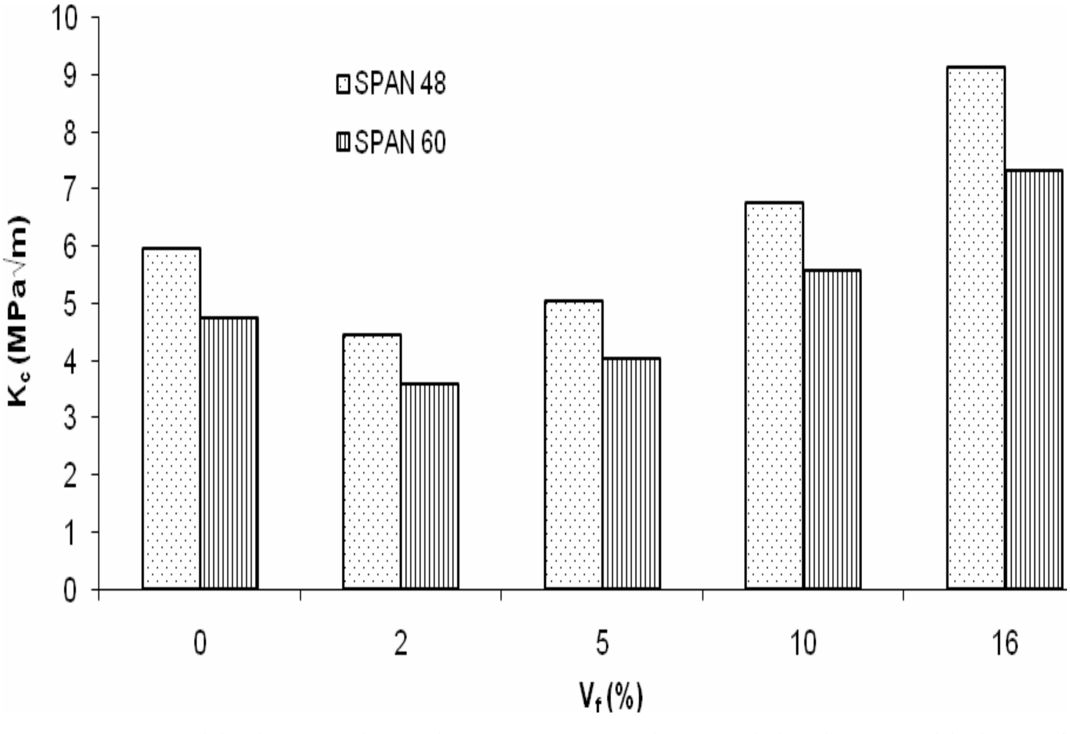

Figure 4.65: Critical stress intensity factor, K_c values of injection moulded SGF/PA6 composites subjected to different support span.

4.5.2 The Effect of Test Velocity

The original position of the load from the point of impact onto the target specimen determined the velocity of the tup and the initial impact energy of the test according to the kinetic energy equation as follows:

$$V = \sqrt{2gh} \tag{4.11}$$

Where v is the velocity, g is a gravitational acceleration and h is a free fall distance to the point of impact [142].

Three batches of material used in this study, there were the specimen with V_f of 0%, 8% and 16%. Fracture energy, W and G_c (Figures 4.66 and 4.67) shows maximum value at test velocity of specimen 16% V_f followed by 0% and 8% V_f. Explanation for this is, at higher volume fractions (16% V_f) the composite tend to fail in brittle manner results in high fracture energy [143]. On the other hand, neat PA6 exhibit ductile fracture behaviour with corresponding high energy absorption. In between, the specimen of 8% V_f showed both contribution from matrix ductility and stiffness of glass fibre. By contrast, P and K_c, (Figures 4.68 and 4.69) showed increment consistently with fibre volume fraction. The experimental results suggest that, the increase in fibre volume fraction results in an increasing the impact resistance properties. Impact properties are reported to increase initially in the increase in glass content but decrease when the glass fibre content is increased beyond 50% by weight [133].

The trend shows that as the fibre volume fraction increases, the absorbed energy also increases. This trend confirms that the higher the fibre volume fractions, the greater the residual velocity, hence the higher the impact energy dissipation by the impacted specimens. Razi and Raman [142] also confirm that low velocity impact properties of wood-polymer composites vary with the concentration and size of the wood chips in the composites. Fibres ability to store energy elastically is the fundamental parameter influencing the low velocity impact response of the composite [133].

For all the parameters discussed above, shows a value reduction with increasing in notch to depth (a/D) ratio due to, a notch acts as a stress concentrator which causes a dramatic decrease in strength. Hence, in case where an object must be able to sustain tensile loads, it is important that the material have a low sensitivity to notches [48].

The summarised impact testing results at different test velocities are shown in Figures 4.66-4.75. Fracture energy, W, peak load, P, G_c and K_c increased linearly with increasing test velocity except some indication in specimen with V_f of 16% where G_c show a significant reduction. Onal and Adanur [144] in their study, claim that mechanical properties of composite were better under low velocity impact, as the glass fibre content increased. The explanation for this is, as glass fibre content increased within the structure, amount of deflection increased as well. Higher strain of glass fibre may lead to this result. This is in line with the study by Kageyama and Kimpara [145] on delamination failures in polymer composites which state that G_c increases with increasing impact velocity and the value at V_0 of 8 ms^{-1} is about 1.8 times higher than the static value. The failure energies tend to increase for the higher velocity impact. This can be related to the strain rate dependent behaviour of the materials and more dissipation of energy at higher velocities due to vibrations [146].

Erickson *et al.* [61] reported that at low impact velocities (lower energies), the striker passed through the material more easily at lower temperatures, thus absorbing less energy compared to equivalent panel at the high temperature. However, at higher impact velocities (higher energies), the striker passed through the material more easily at higher temperatures, thus absorbing less energy than an equivalent panel at the low temperature. At high energy impact (25 J); fibre breakage is the main contributor to energy absorption. This indicates that there is a threshold impact velocity at which the trend of absorbed energy versus temperature reverses, likely due to a change in damage mechanisms at higher impact energies.

On the other hand, Zhang and Richardson [37] have found that peak forces, peak energy, energy at failure and peak deflection increased linearly with increasing striker height composite in pultruded glass fibre reinforced polyester composite materials. The striker height of 250, 350, 450, 550, 650 and 750 mm gives peak energy of 4.75, 6.8, 8.79, 10.95, 12.98 and 15.05 J respectively.

Zhu *et al*. in their study [59] on low velocity flexural impact behaviour of alkali resistance glass fabric reinforced cement composites observed an increment in the maximum flexural stress and absorbed energy of composites with drop height. Their absorbed energy gradually increased up to the drop height of 100 mm. They found that, the impact force increased from 2.076 kN at the drop height of 50 mm to 3.618 kN at the drop height of 100 mm, however there were no significant increases at the drop height of 200 mm. It was also observed that the deflections of all composition of glass fabric reinforced cement composites continuously increased as the drop height increased. In addition, Ochola *et al.* [116] claim that due to the rapid loading, the material tends to a more brittle behaviour resulting in a low strain to failure value.

As further seen, in comparison to carbon fibre reinforced composites, glass fibre reinforced composites fail even under low velocity impacts but tend to collapse seriously in very high velocities, (100 J). This means glass fibre reinforced composites are less strong but they sustain a wide range of impact energy before being seriously collapsed. By contrast, behaviour of carbon fibre reinforced composites is quite different where the plates show good strength under low velocity impacts [59].

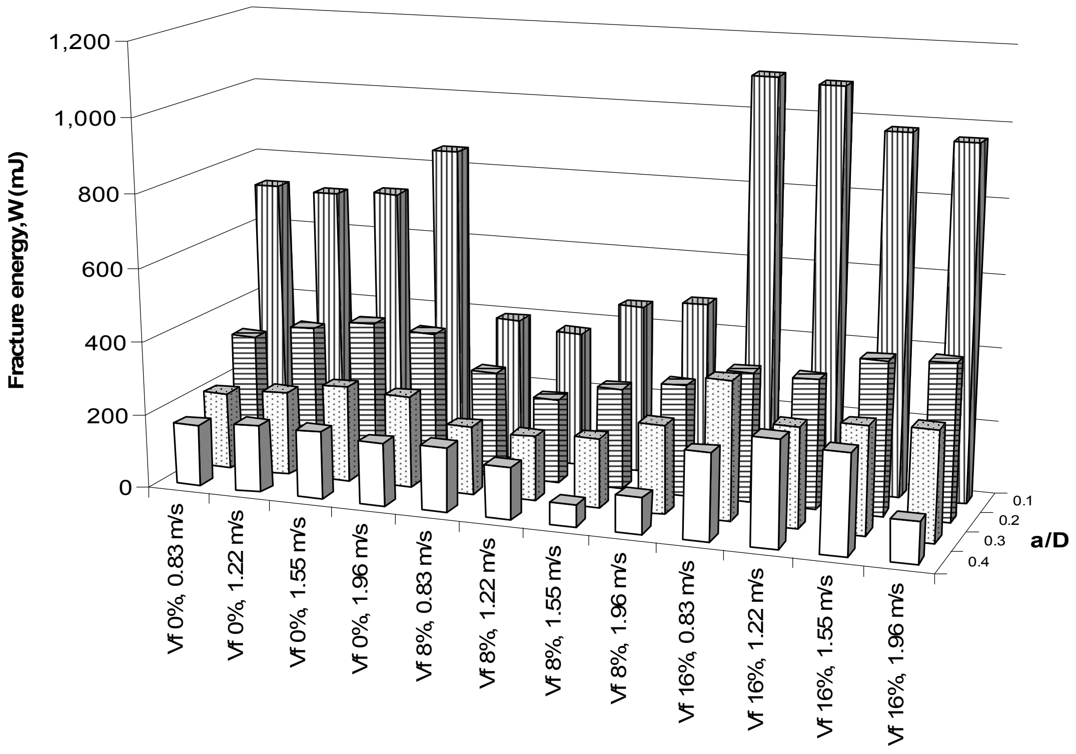

Figure 4.66: Variation of fracture energy, W of injection moulded SGF/PA6 composites subjected to different test velocities.

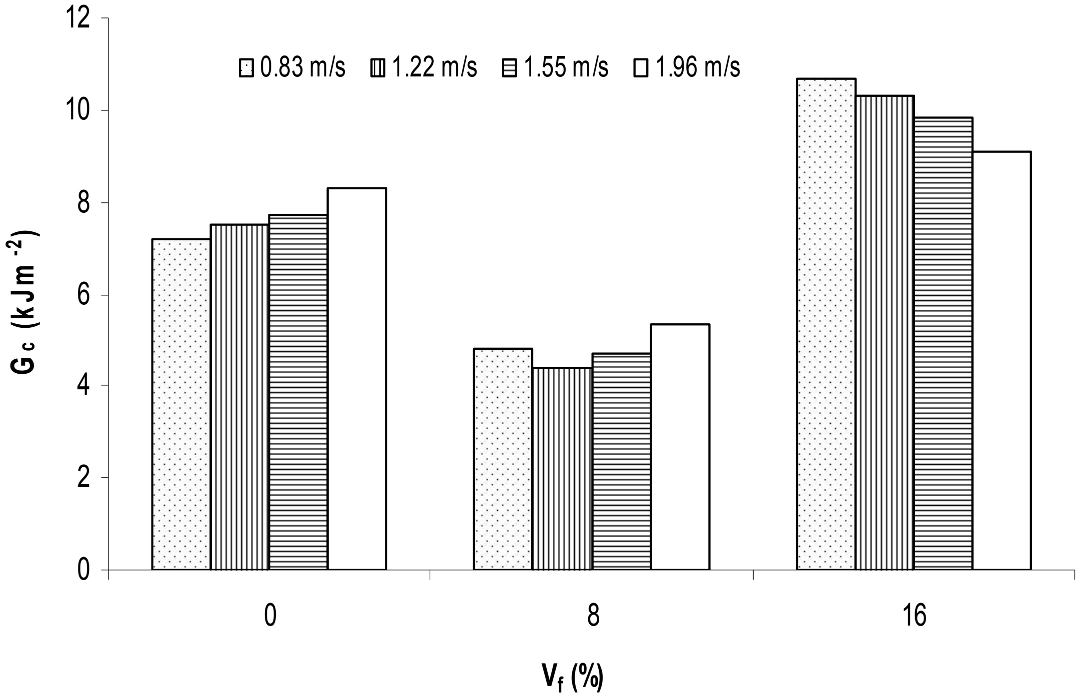

Figure 4.67: Variation of G_c values of injection moulded SGF/PA6 composites subjected to different test velocities.

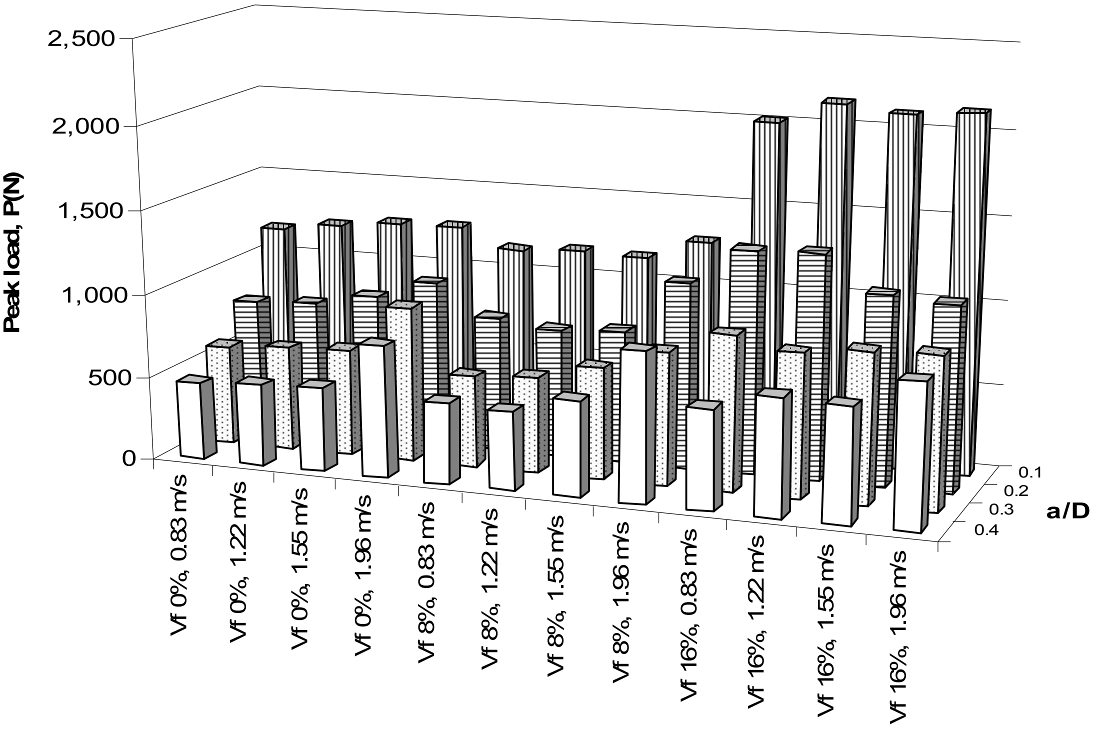

Figure 4.68: Variation of peak load values of injection moulded SGF/PA6 composites subjected to different test velocities.

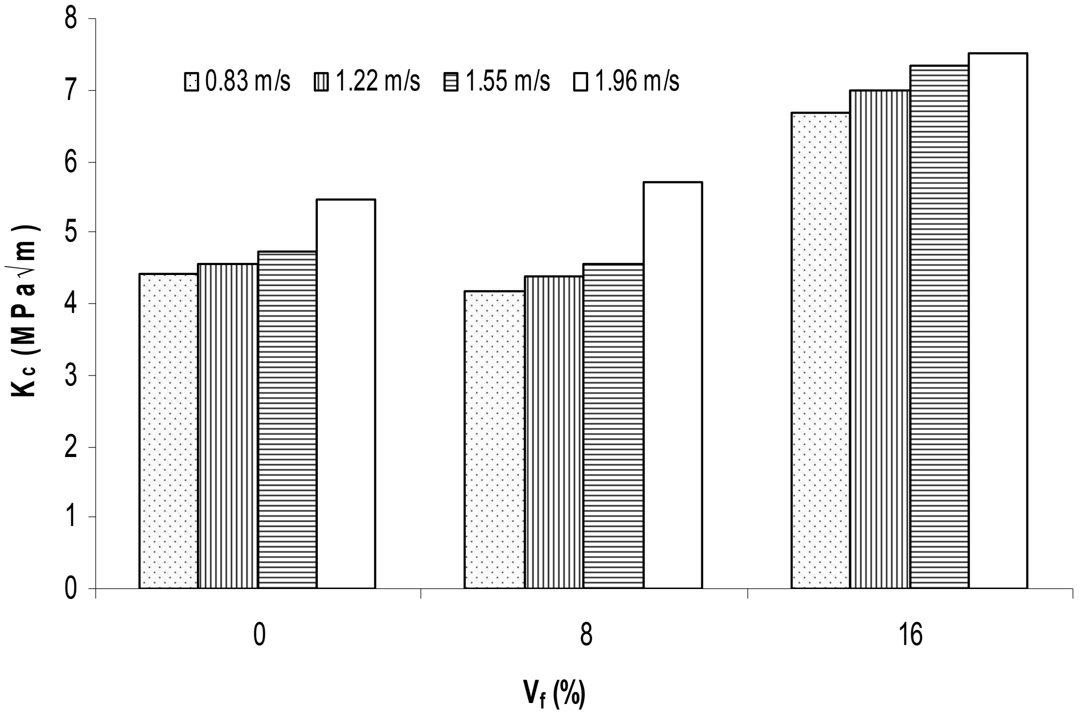

Figure 4.69: Variation of K_c values of injection moulded SGF/PA6 composites subjected to different test velocities.

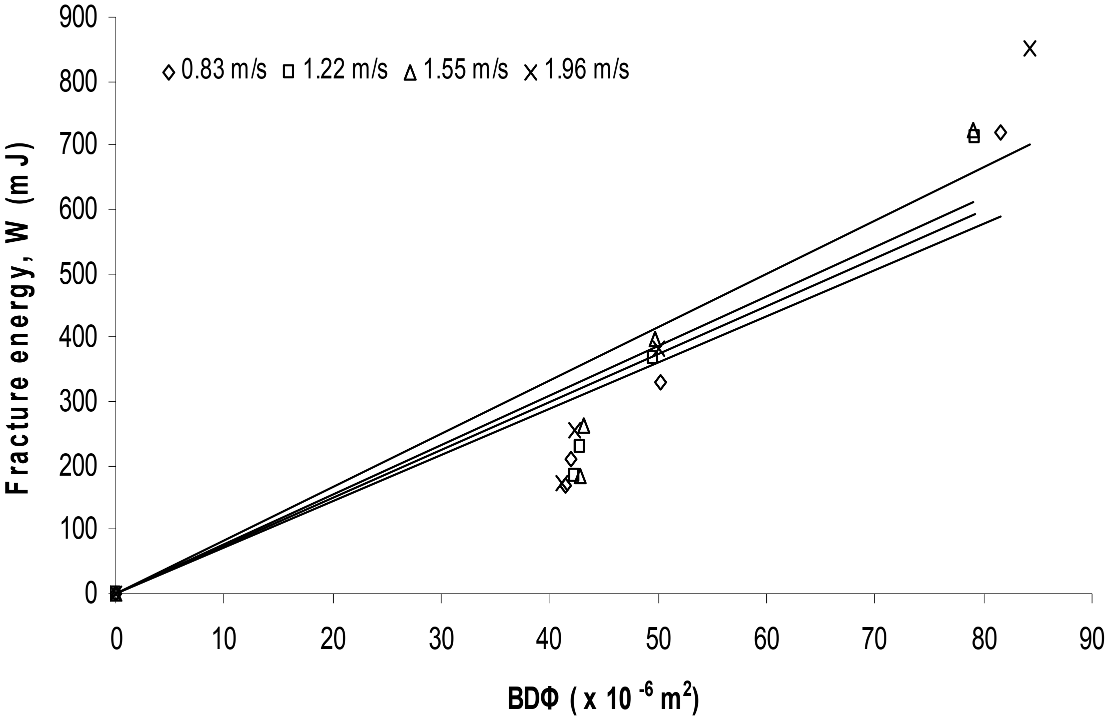

Figure 4.70: Fracture energy, W against BDΦ values of neat PA6 subjected to different test velocities.

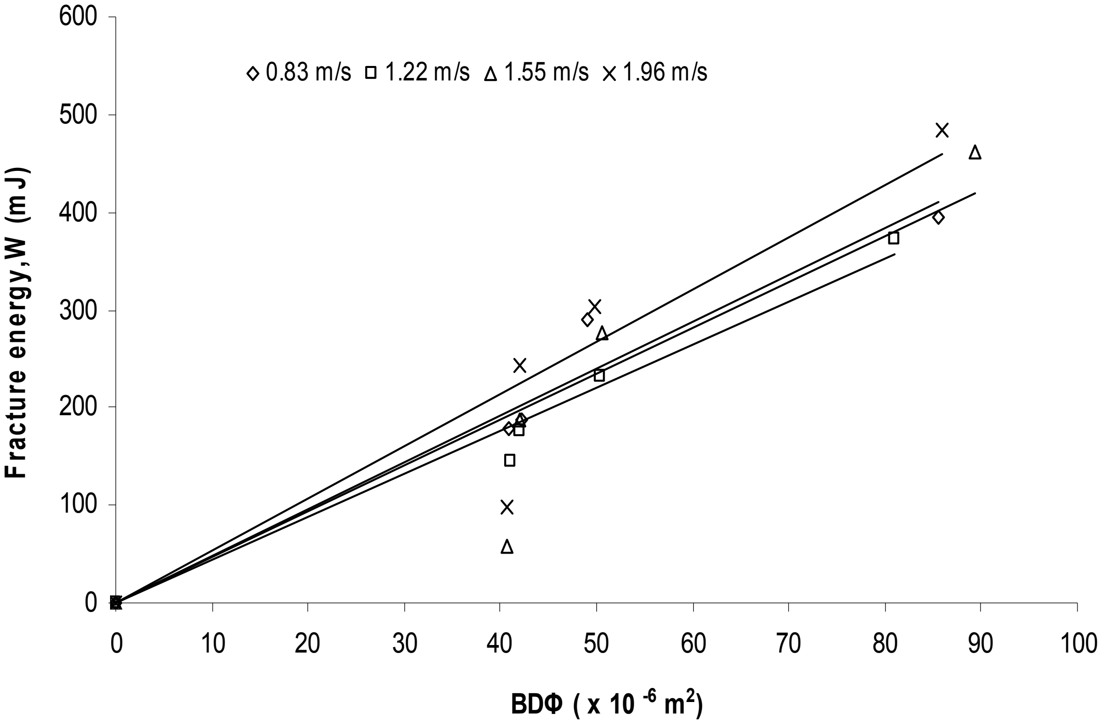

Figure 4.71: Fracture energy, W against BDΦ values of injection moulded 8% V_f SGF/PA6 composites subjected to different test velocities.

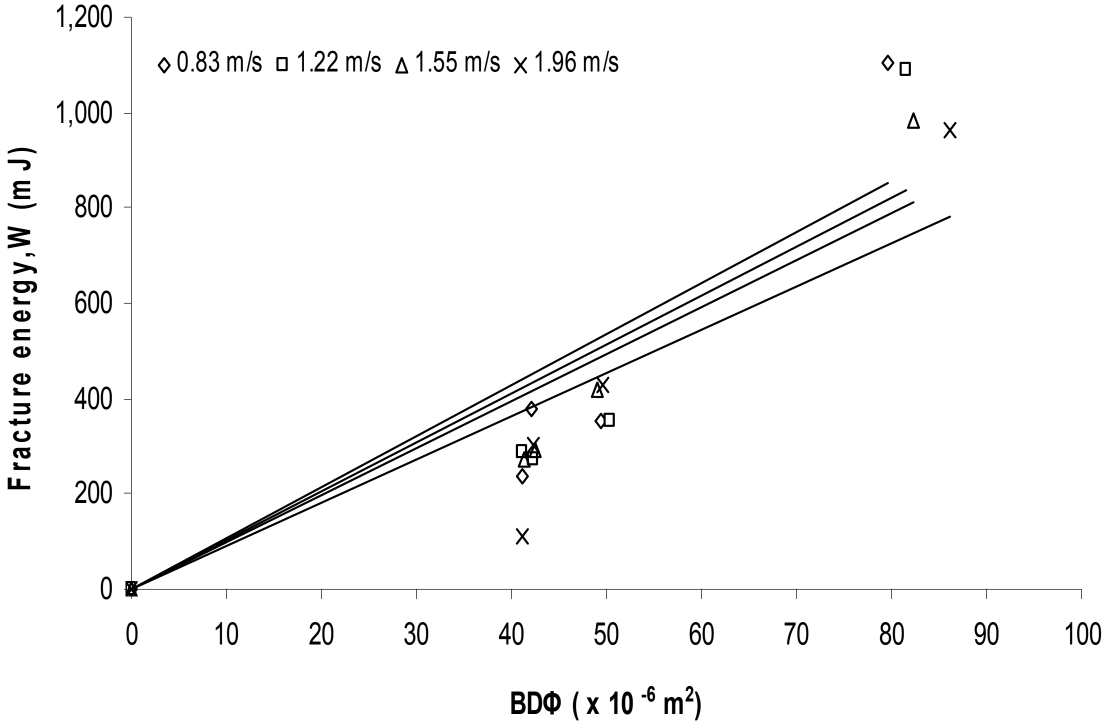

Figure 4.72: Fracture energy, W against BDΦ values of injection moulded 16% V_f SGF/PA6 composites subjected to different test velocities.

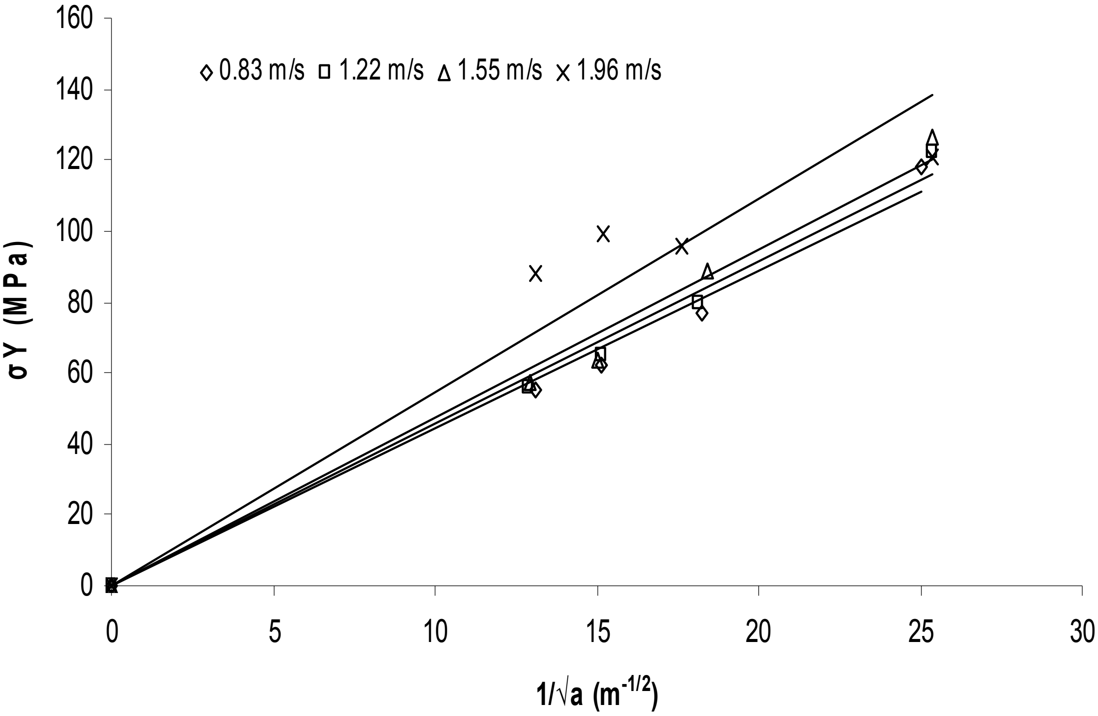

Figure 4.73: Variation of σY against 1/√a of neat PA6 subjected to different test velocities.

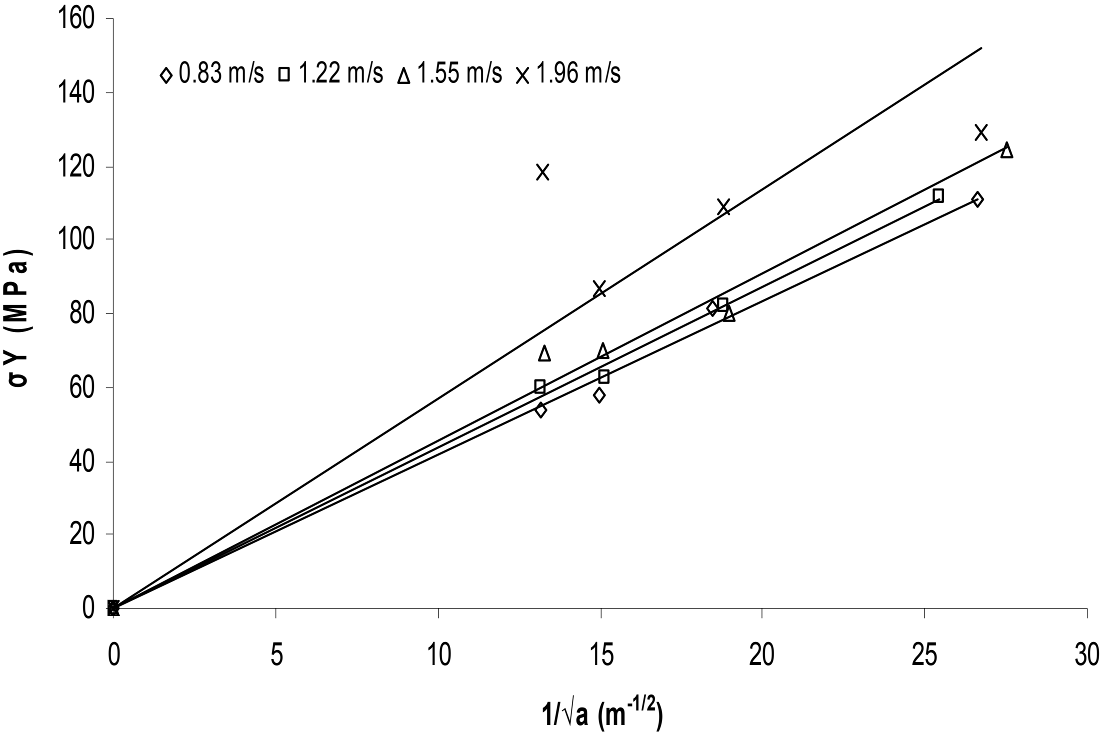

Figure 4.74: Variation of σY against 1/√a of injection moulded 8% V_f SGF/PA6 composites subjected to different test velocities.

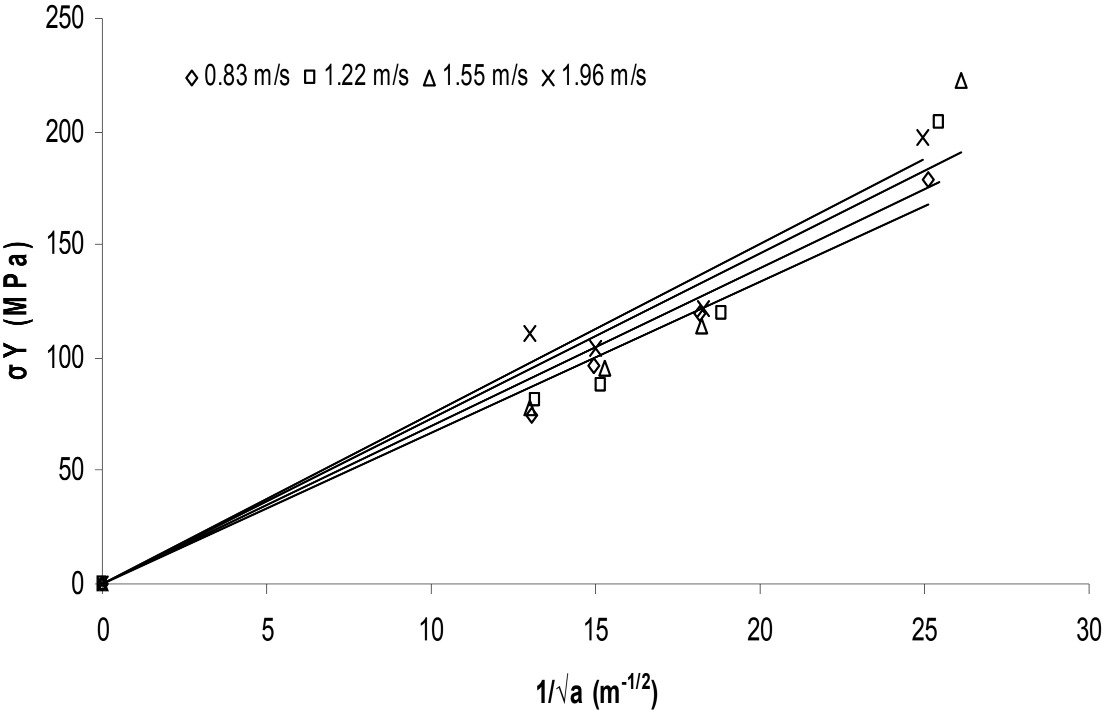

Figure 4.75: Variation of σY against 1/√a of injection moulded 16% V_f SGF/PA6 composites subjected to different test velocities.

4.6.3 The Effect of Test Load

Relationship of energy, E with test load (mass) is given by:

$$E = mgh \tag{4.12}$$

where E is the energy (J), m is the mass of tup (kg), g is the gravity (m/s^2), h is the height (m), [147].

The highest fracture energy, W and peak load, P value (Figures 4.76 and 4.77) shown by composite with V_f of 16%, followed by 0% and 8%. This suggests that energy absorption of composites increased as a function of matrix ductility and as glass percentage increased. The same observation was also reported in G_c (Figure 4.78). On the other hand, 0% and 8% V_f had shown no significant changes in K_c value (Figure 4.79). It is suggested that the incorporation of lower fraction of glass fibre may only give notching effect to the composite. They may introduce a microvoid in the composites and instead of reinforcing the matrix, it weakens the composites. K_c value for 16% V_f showed highest value indicate that high fibre content results in high fracture toughness in composite materials. The results of this evaluation indicate that considerable improvement in impact behaviour is achieved with composites composed of high strength fibre and resins systems with increase toughness. High strength fibres absorb more energy before failure and thus should also yield tougher composites [10].

For all the parameters observed showed, neat PA6 showed slightly higher value compared to specimen with 8% V_f. This is a very interesting behaviour, since PA6 is a semi-crystalline material considered pseudo-ductile, with a strong tendency for unstable propagation. Therefore, the results had to be separated into two groups, according to the fracture behaviour: specimens with ductile and specimens with brittle behaviour. The higher the value, the greater the material’s capacity to absorb strain energy during the fracture process [121].

A reduction in W, P, G_c and K_c values with increasing in notch to depth (a/D) ratio due to reduction in fracture area. This observation can be explained as the crack grows in size, the stiffness decreases, so the force level will decrease. The decrease in force level under the same displacement (strain) level indicates that the elastic strain energy stored in the body is decreasing leading to lower value for all the parameters discussed above.

For the same fibre volume fraction, fracture energy, W, peak load, P and K_c show consistent increment as increasing in impact load. An explanation of this is, as polymer based composite materials were subjected to impact type of loading conditions, energy is absorbed in the process of plastic deformation of matrix material, debonding at matrix/reinforcement interface and in the fracture of reinforcing material. The phenomenon that absorbs least amount of energy for its occurrence becomes prominent and leads to fracture [148]. On the other hand, G_c values only shown a consistent increment at 0% and 16% V_f . 8% V_f does not show any significant different in G_c. This proved that at high fibre loading, material become more sensitive to toughness.

Zhang and Richardson [37] in their study observed an increment in the magnitude and severity of damage with increasing incident impact energies. In addition, increasing the impact energy causes more damage, mainly by allowing defects to propagate easily via the higher stress concentration induced by the impact energy. As a result, impact damage typically appears to be concentrated in a few regions aligned along the centre of impact, depending on defects already present in the material.

Padaki *et al.* [133] in their study found that the work of fracture increases with loading rate due to the rate dependent fracture properties of the reinforced fibres. Increasing the loading rate increases fibre failure stress, thus resulting in larger damage zone during impact.

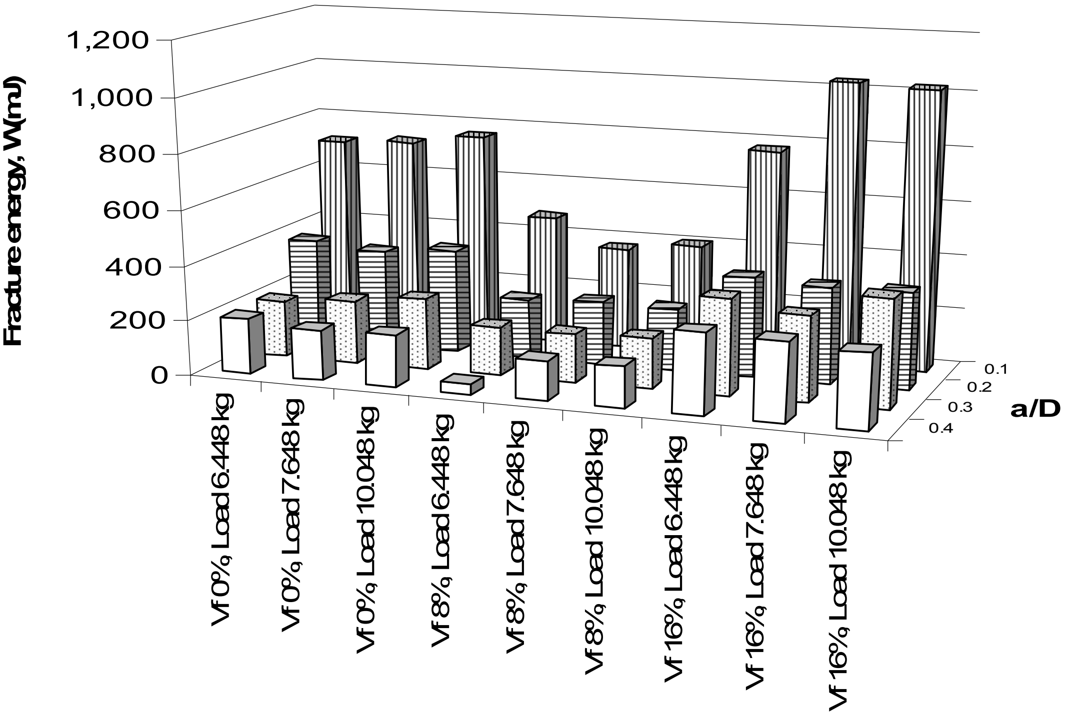

Figure 4.76: Variation of fracture energy, W of injection moulded SGF/PA6 composites subjected to different test load.

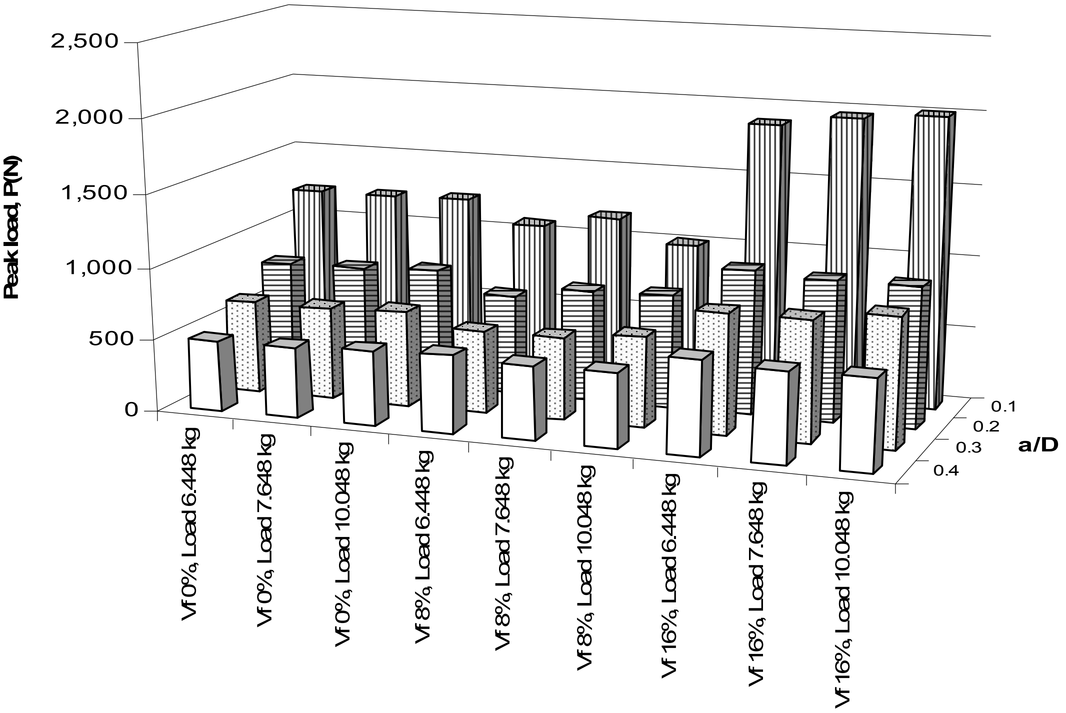

Figure 4.77: Variation of peak load of injection moulded SGF/PA6 composites subjected to different test load.

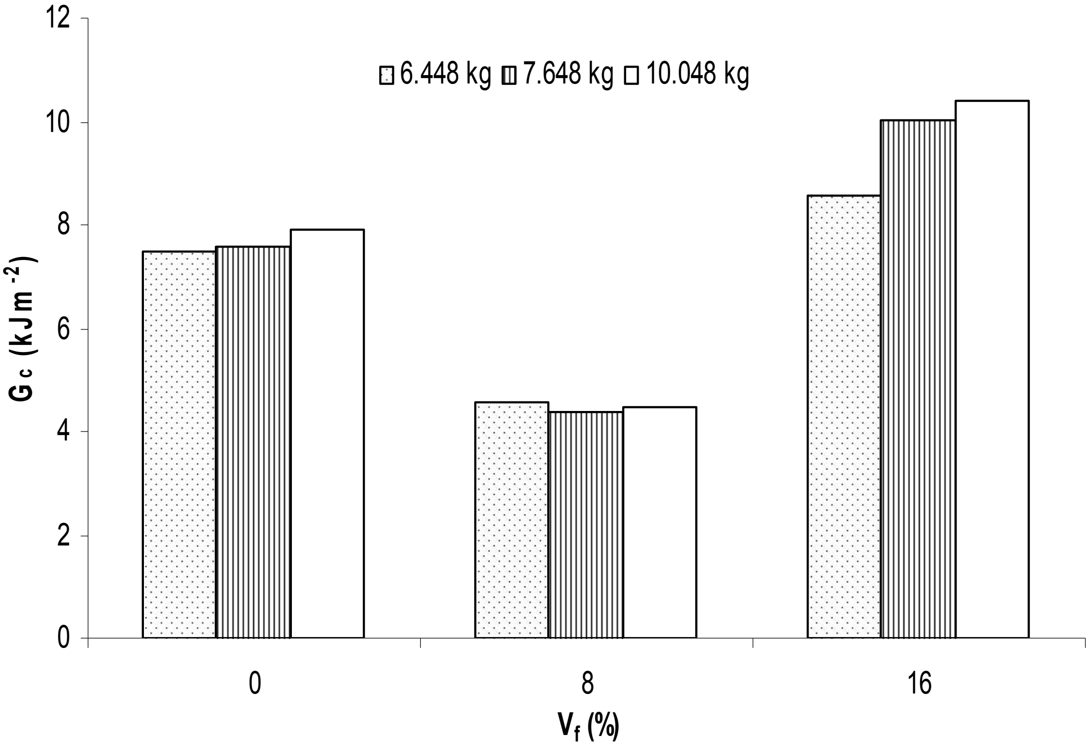

Figure 4.78: Critical strain energy release rate, G_c values of injection moulded SGF/PA6 composites subjected to different test load.

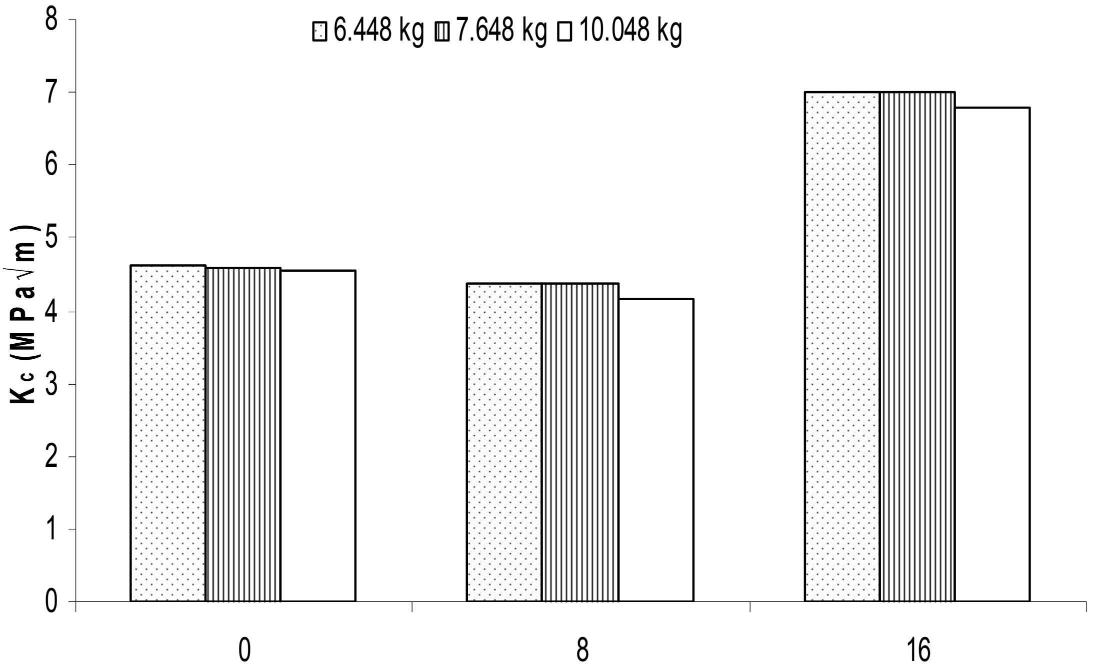

Figure 4.79: Critical stress intensity factor, K_c values of injection moulded SGF/PA6 composites subjected to different test load.

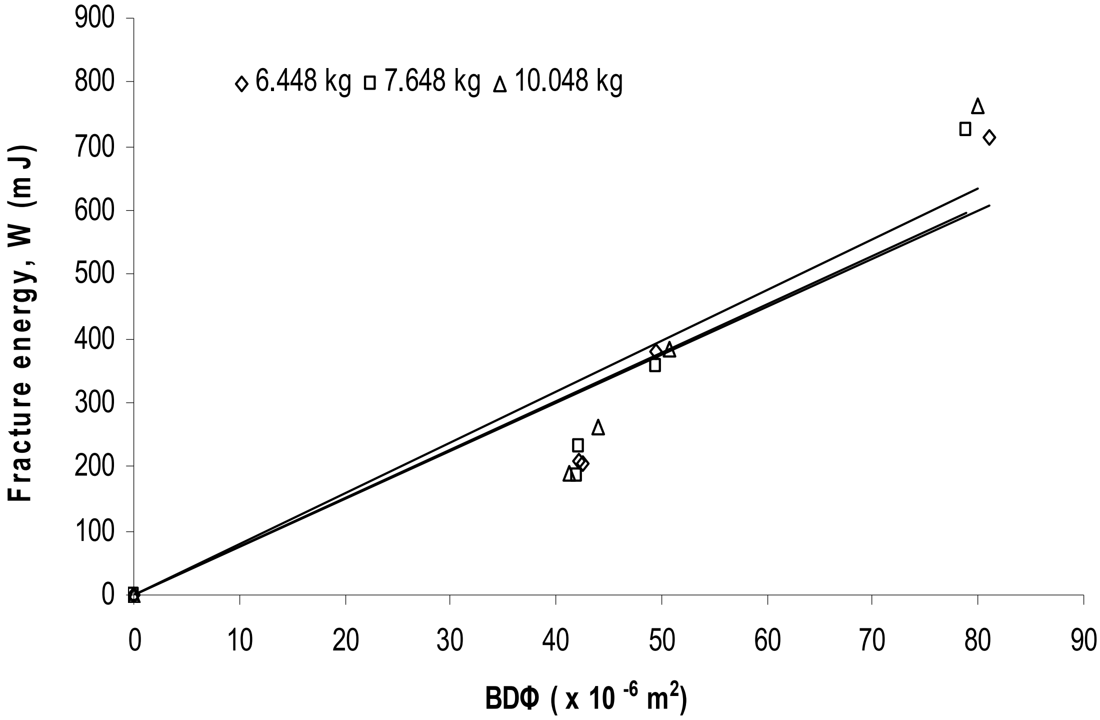

Figure 4.80: Variation of fracture energy against BDΦ of neat PA6 subjected to different test load.

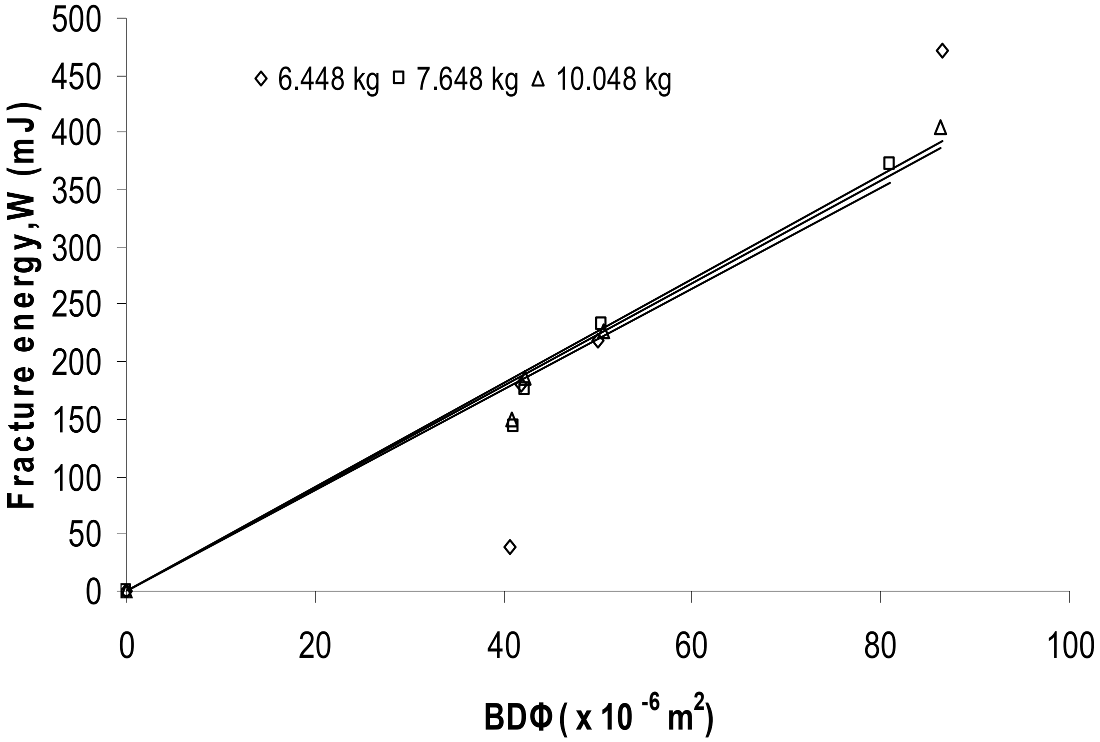

Figure 4.81: Variation of fracture energy against BDΦ of injection moulded 8% V_f SGF/PA6 composites subjected to different test load.

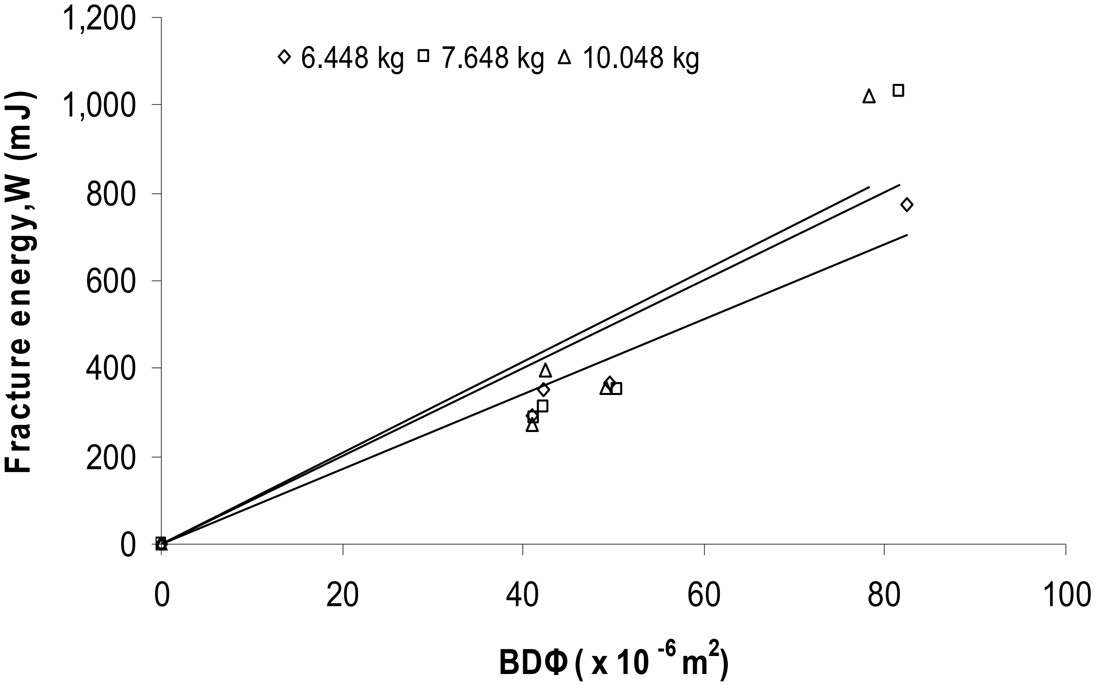

Figure 4.82: Variation of fracture energy against BDΦ of injection moulded 16% V_f SGF/PA6 composites subjected to different test load.

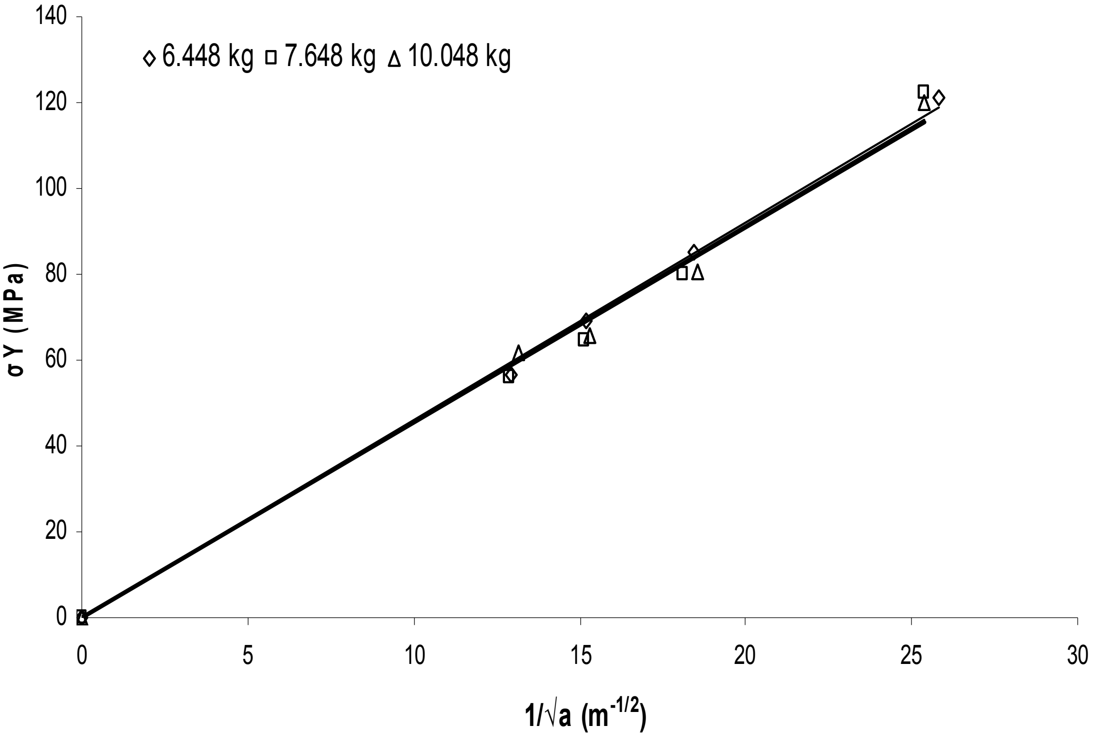

Figure 4.83: Variation of σY against 1/√a of neat PA6 subjected to different test load.

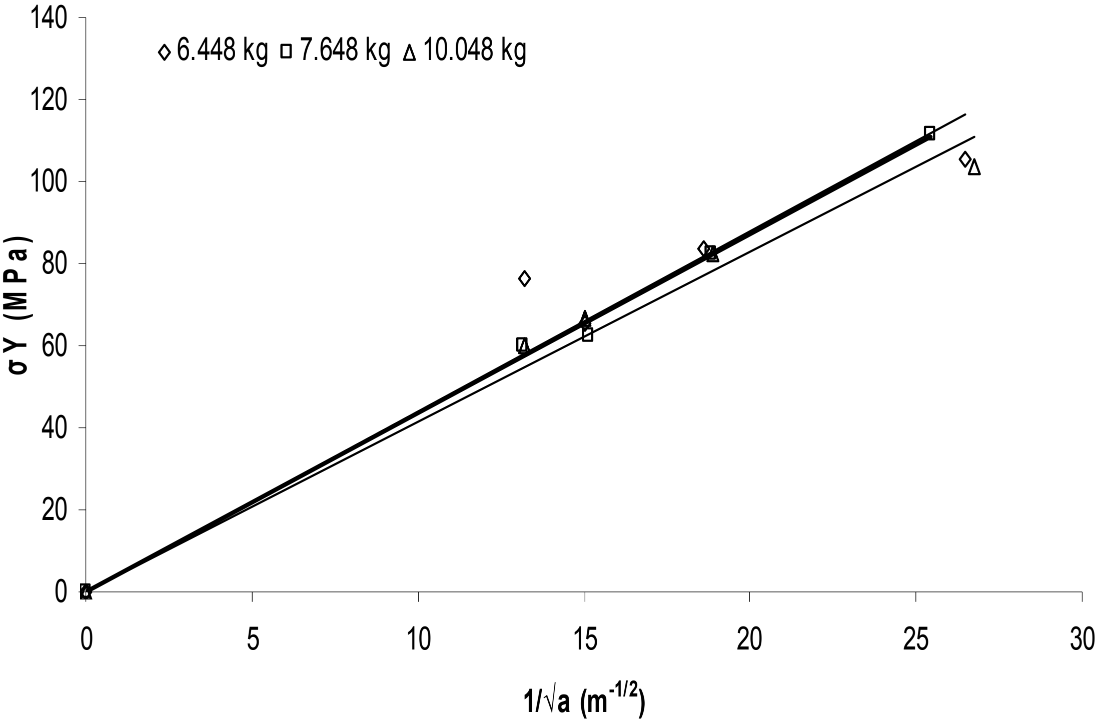

Figure 4.84: Variation of σY against 1/√a of injection moulded 8% V_f SGF/PA6 composites subjected to different test load.

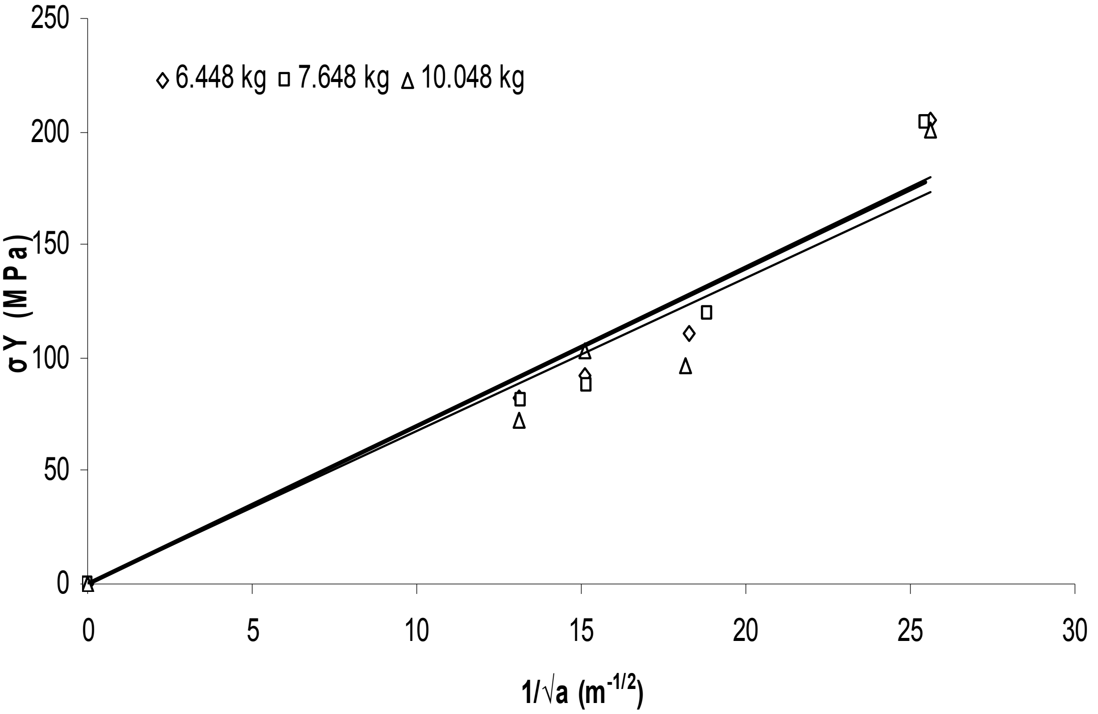

Figure 4.85: Variation of σY against 1/√a of injection moulded 16% V_f SGF/PA6 composites subjected to different test load.

4.5.4 The Effect of Testing Temperature

Thermoplastics and corresponding composites are sensitive to changes in the environment and their mechanical properties may vary considerably with environmental conditions. A combination of humidity and temperature is most detrimental to the material stability under service conditions. This is due to the fact that, the material's functional property is affected by the absorbed moisture. Generally, thermoplastic materials are typically softened by elevated temperatures. As a result, higher temperatures normally reduce the creep modulus of matrix-dominant composites [38]. Thus, mechanical tests are often carried out under various temperatures to determine temperature-dependent properties but it often limited to selected temperature due to high cost and requires time [149].

Figures 4.89-4.93 present variation of temperature influences on impact toughness. Generally, testing temperature show significant effect on fracture energy, W, peak load, P and G_c values. This is however contradicting with the study by Thomason and Vlug [12] where the Charpy impact strength was virtually independent of temperature in the range -50 to 40°C. Gates [150] also observed that the G_c data was independent of sandwich specimen orientation regardless of test temperature and insensitive to changes in crack length. It is significant, however, that G_c increased with a decrease in temperature.

By contrast, K_c shows a significant change with temperature. When the temperature is increased to 60°C, which is close to the T_g, the material is in the transition from the glassy state to the rubbery state. The critical stress intensity factor, K_c then decreases slightly at temperature 70°C. When the temperature is increased further the material is in the rubbery state and this present the weakest point in fracture toughness. This implies that at temperature around and above the T_g the strain rate has a strong effect on impact properties. It is noted that at temperatures below T_g, the elongation increases slowly with increasing temperature. At temperatures around T_g, the elongation increases drastically with increasing temperature. When the testing temperature is increased further, the elongation tends to increase. Therefore, the deformation characteristic and bonding strength of the material at different temperature ranges (i.e., below T_g, around T_g, and above T_g) can be employed to explain the phenomenon observed.

Figures 4.86 - 4.88 show fracture surface of impact specimen at 50, 60 and 70°C. At T_g, 60°C clean fibres are observed as well as a small number of fibres with the matrix still being attached to than those in the brittle region (50°C) which have a lot matrix adhering to them. The condition of the pulled out fibre surfaces is generally considered indicative of the strength of the fibre matrix interfacial bond, clean fibres indicating poor bonding and 'dirty' fibres indicating strong bond. At 70°C failure of the SGF/PA6 composites takes place in a ductile manner. Thus fibre pull-out can occur due to the softened matrix material. In this way, the major contribution to the absorbed energy during the breakdown of the composites should be based on the plastic deformation of the matrix material [17]. It is interesting to note that the matrix around the fibre is very soft. This indicates that the bonding strength at this temperature is very low, thus the material is very weak. This observation is in line with the study done by Shi *et al.* [55]. Their study found that, when the testing temperature is above the T_g, the crack occurred in the matrix and the material around the crack is very soft.

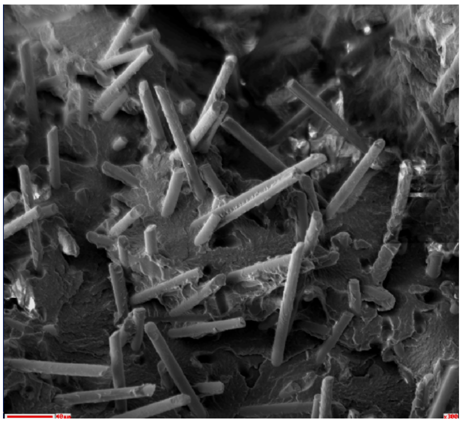

Figure 4.86: Impact specimen fracture surface of injection moulded 16% V_f SGF/PA6 composites at 50˚C.

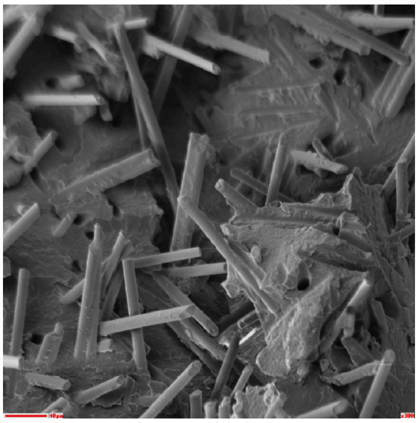

Figure 4.87: Impact specimen fracture surface of injection moulded 16% V_f SGF/PA6 composites at 60˚C.

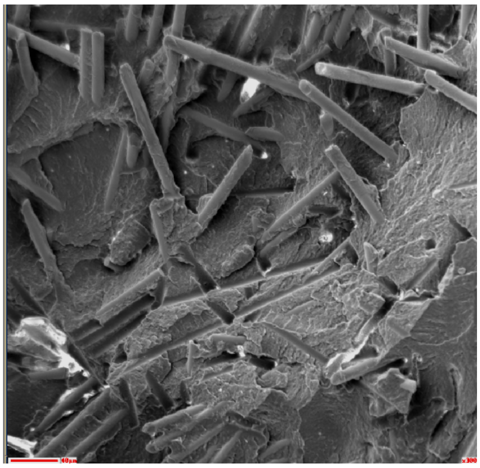

Figure 4.88: Impact specimen fracture surface of injection moulded 16% V_f SGF/PA6 composites at 70˚C.

Fesko [151] in his study state that, the material act as rubber at room temperature but at high temperatures, it can be made to flow. Below the T_g there is limited molecular mobility, while above it higher mobility results in reduced viscosity and potentially greater chemical interaction between components. This explains the general desire to store samples at least 40 °C below their glass transition temperature.

They have been a number of studies upon the effect of testing temperature on G_c and K_c for glassy thermoplastic and in general, it is found that measured values for both parameters decrease as the temperature is increased as long as the failure is brittle. Nevertheless, this statement is contrary with the impact studies on PVC materials where it is generally found that the impact strength increases as the temperature is increased. On the other hand, impact measurements are made at very high rates and the increase in impact strength obtained by raising the test temperature is due to the polymer going through a brittle/ductile transition [42].

It is the resin dominated properties which are seriously affected by the environments, since the resin phase is prone to attack by moisture, heat, or combination. Therefore, when the resin phase is sufficiently degraded by these hygro (moisture) thermal (heat) factors, the fibre-resin interface is easily damaged resulting in the degradation of the resin dominated properties [152]. Masud *et al.* [128] found that high temperature may be responsible for matrix dissociation.

Erickson *et al.* [61] in their study observed temperature increment; leading to increase the absorbed energy. This is an expected result due to the epoxy being more ductile at higher temperatures. More ductility leads to increased plastic deformation; therefore at higher temperatures, there is less elastic strain energy that can be returned to the striker, resulting in greater absorbed energy values. They also claim that the effect of temperature on the impact behaviour is due to a combination of the constituent materials' temperature dependence as well as a change in damage mechanisms observed at different temperatures.

In addition, Amin *et al.* [136] found that, as temperature increased, the back surface cracking and fibre breakage decreased drastically and thus affected the absorbed energy considerably. They also observed as increased temperature the maximum crack length decreased and the maximum delamination length increased considerably. However, at low temperatures, the laminate is rigid leading to a small deflection. With increasing temperature, the laminate becomes less stiff and bending and deflection increase. As a result, increase in the rate of deflection is small at low temperatures and increases as temperature increases.

Ahn and Paul [15] reported, PA6 shows a ductile region at temperatures above 50˚C and a brittle region at temperatures below 50˚C. This ductile-to-brittle transition corresponds to the glass transition of the dry as moulded PA6. However, the addition of clay particles increases the ductile–brittle transition temperature and makes the PA6 slightly more brittle below this transition. The addition of rubber in the absence of clay greatly lowers the ductile–brittle transition temperature and has the effect of increasing toughness for a given temperature like 25˚C.

The effect of temperature on the impact behaviour is likely due to a combination of the constituent materials' temperature dependence as well as a change in damage mechanisms observed at different temperatures. A slight reduction in the stiffness was noted with increasing impact temperature at the highest energy level, but the effect on the strength was mixed. This indicates that, although the ability to absorb the energy from a low-velocity impact is dependent on temperature, the postimpact structural integrity of the composite is somewhat unaffected by the temperature at impact. As expected, a general reduction in residual strength and stiffness was found for increasing levels of impact energy as reported by Erickson *et al.* [61].

On the other hand, Shrivastava & Hussain [152] noticed an oxidative effect on the material as the composite is exposed to higher temperature (60˚C) continuously. This is referred to as 'thermooxidative' degradative mechanism which causes greater strength loss. Epoxy-based composites show rapid dimensional changes at slightly higher temperature which correspond to molecular relaxations in the polymeric chains. Humidity alone at low temperatures however does not cause ill-effects, but in combination with moderate temperatures (up to 50˚C) to high temperatures (60-80˚C), can lead to serious degradative effects such as excessive brittleness, resin cracking and crack formation.

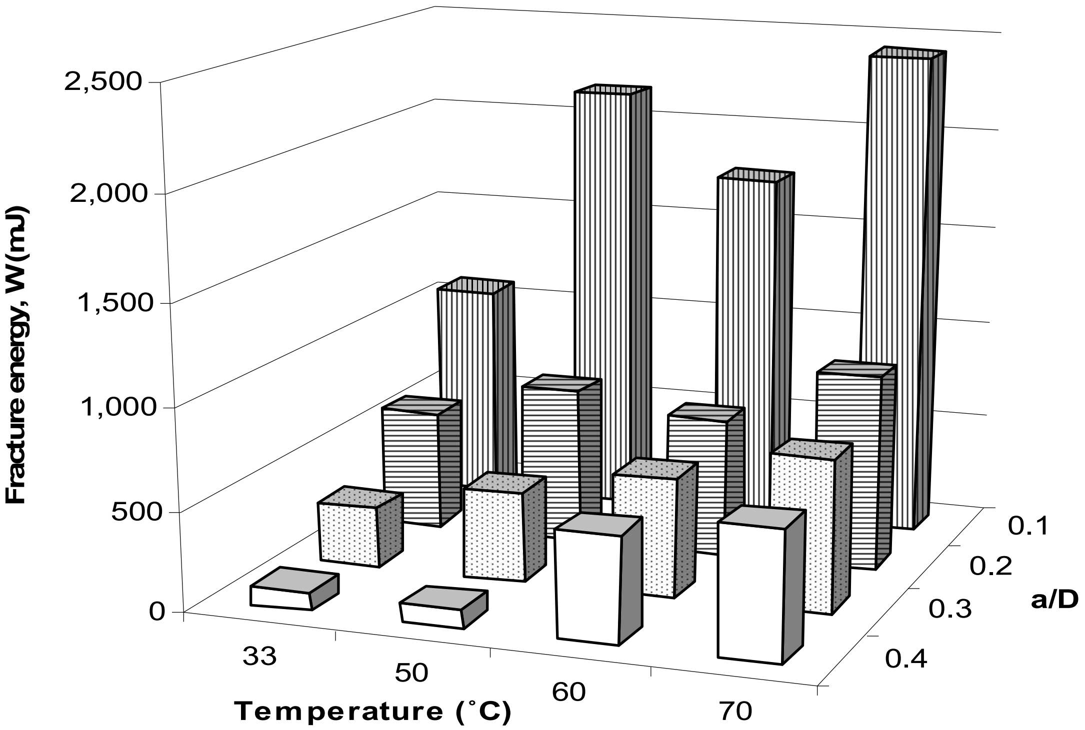

Figure 4.89: Fracture energy, W values of injection moulded 16% V_f SGF/PA6 composites subjected to different temperature.

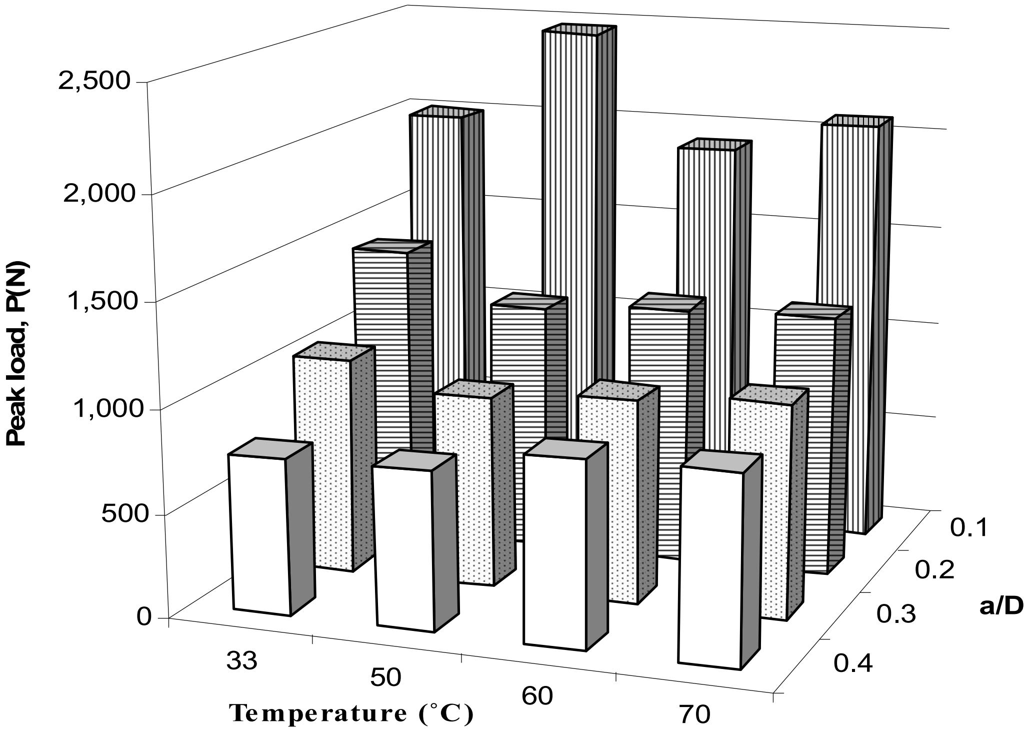

Figure 4.90: Peak load values of injection moulded 16% V_f SGF/PA6 composites subjected to different temperature.

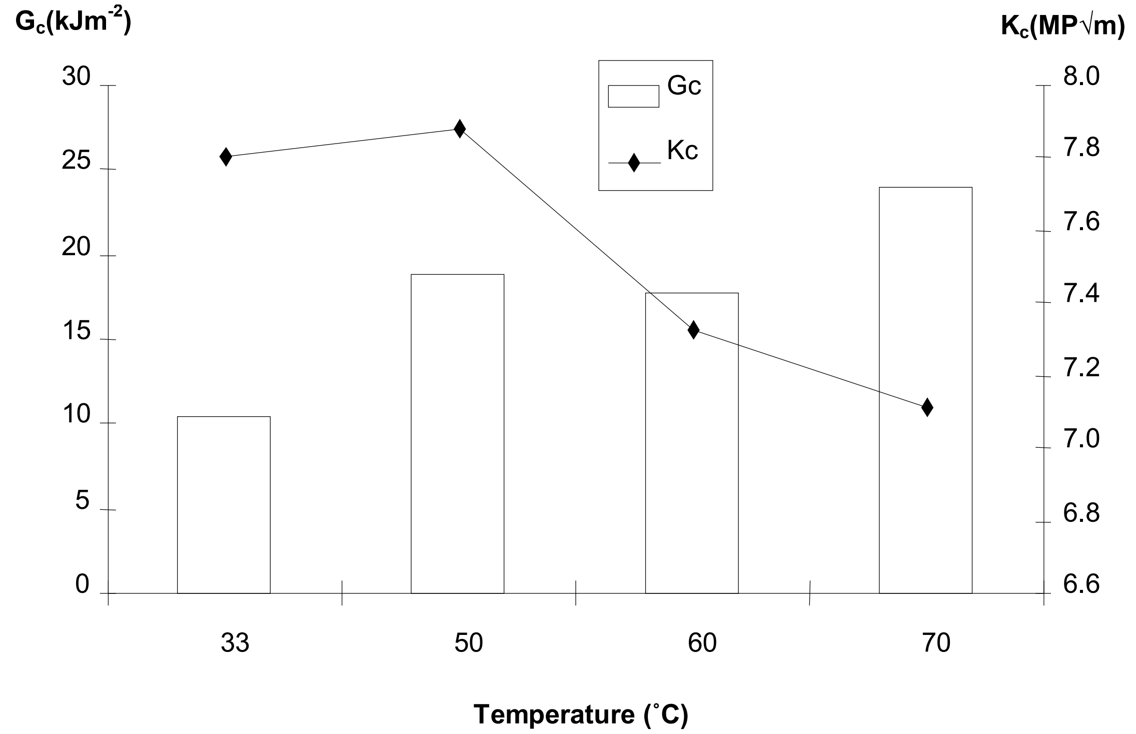

Figure 4.91: Critical strain energy release rate, G_c and critical stress intensity factor, K_c values of injection moulded 16% V_f SGF/PA6 composites.

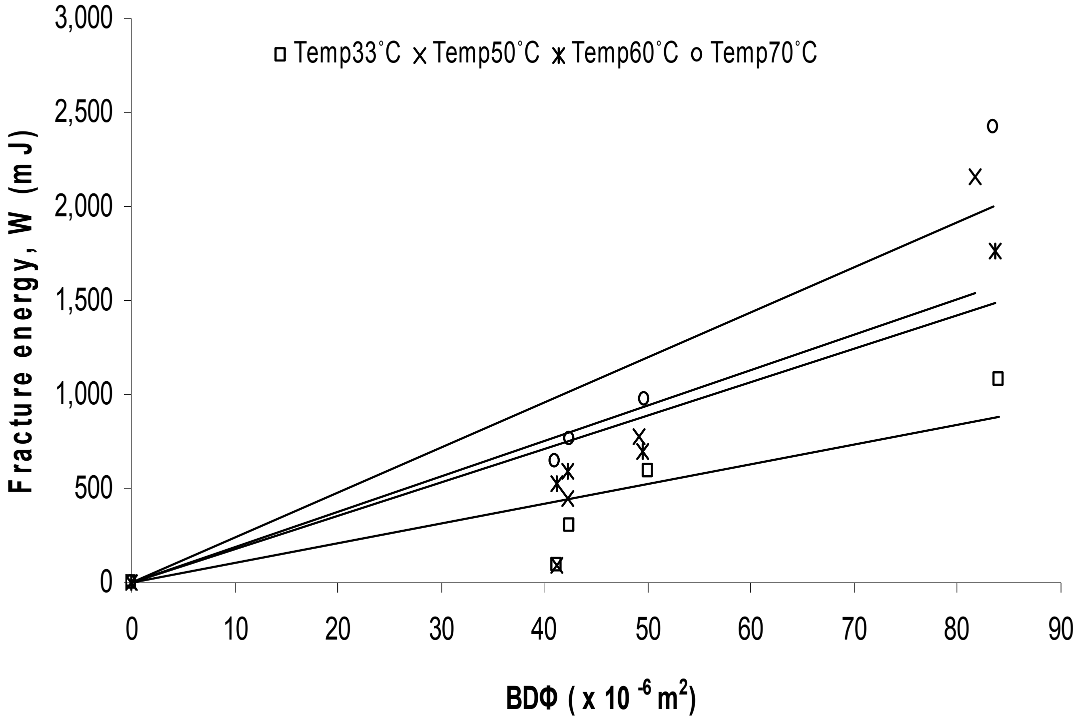

Figure 4.92: Variation of fracture energy against BDΦ of injection moulded 16% V_f SGF/PA6 composites.

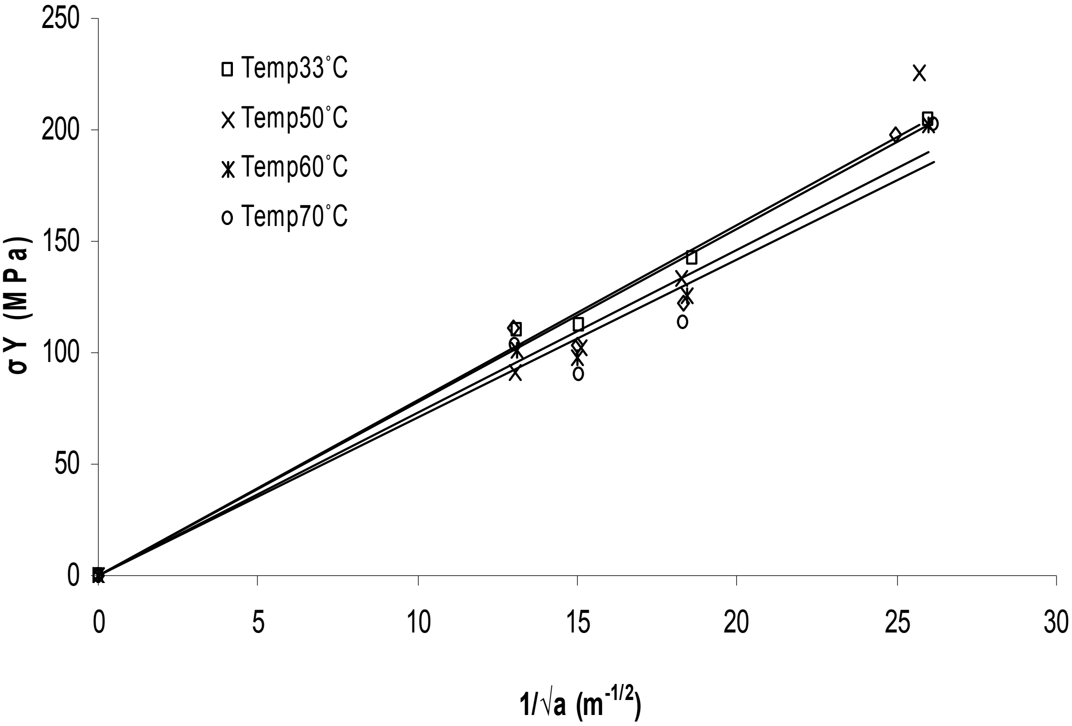

Figure 4.93: Variation of σY against 1/√a of injection moulded 16% V_f SGF/PA6 composites.